MONASH University

Development and Evaluation of a Process for Removing CO_2 from the Atmosphere

Romesh Pramodya Wijesiri

B.Eng. (Chemical Engineering)

A thesis submitted for the degree of *Doctor of Philosophy at*

Monash University in 2019

Department of Chemical Engineering

THIS PAGE HAS INTENTIONALLY BEEN LEFT BLANK

Copyright notice

Abstract

Processes which directly remove CO_2 from atmospheric air, also known as Direct Air Capture (DAC) processes, are an important tool for mitigating the effects of global climate change. The work in this thesis focussed on developing and evaluating such a process utilising a polyethyleneimine loaded mesocellular foam (MCF) silica sorbent with a high amine loading. The research was carried out systematically in three stages.

The first stage aimed to identify how the adsorption temperature and the moisture level affected the adsorption of CO_2 from air by the PEI-MCF sorbent. It was observed that while the large PEI loading resulted in a large uptake of CO_2, it came at the expense of significant resistance to the diffusion of CO_2 which caused slower adsorption kinetics. The highest uptake of CO_2 was observed at 46 °C under both dry and humid conditions. The presence of moisture was observed to enhance the CO_2 uptake by up to 53%. Of the moisture levels studied, the highest uptake was observed for adsorption at 2% mol-H_2O for all temperatures evaluated. At 46°C, this corresponded to a CO_2 uptake of 2.52 mmol/g. It was also noted that the CO_2 uptake was negatively affected at a higher moisture level of 3% mol-H_2O, which suggested that the large amounts of co-adsorbed water may be interfering with the adsorption of CO_2. The results demonstrated that while the sorbent displayed a high CO_2 uptake (>1.2 mmol/g) under a broad range of temperature and moisture levels, it would be better suited for warm climates with a moderate humidity.

The second stage of the research evaluated the performance of the sorbent under steam-assisted temperature vacuum swing adsorption cycle (S-TVSA), where the desorption was carried out by applying a vacuum and heating up the sorbent, while simultaneously purging with steam. It was demonstrated that essentially all the CO_2 can be desorbed under mild vacuum levels (12-56 kPa abs) and temperatures (70-100 °C). It was observed that S-TVSD produced up to 16-fold faster kinetics than TVSD under the same desorption temperature and pressure, demonstrating the superiority of the process. The study also discovered that while moisture improved the CO_2 uptake, the co-adsorbed water caused the desorption performance to deteriorate. It was also demonstrated that PEI-MCF showed minimal degradation (8% loss in capacity after 1500h of processing time) under the process conditions studied.

The final stage of the research focussed on evaluation of the technoeconomic feasibility of a scaled-up DAC process. The minimum cost of capture was identified to be 612 USD/tonne for a process with air entering at 25°C under dry conditions, and 657 USD/tonne for air entering at 22 °C and 39% RH. The higher cost for the humid process was identified to be an effect of the additional energy requirement for desorbing the co-adsorbed water. The largest contributors to the cost of capture were identified

to be the cost of the air-sorbent contactors, and the cost of providing the thermal energy required for the desorption. The study also identified that significant cost reductions could be achieved by utilising waste heat, improving the kinetics of the sorbent and limiting its water uptake.

Publications and Awards During Enrolment

Journal Papers

1. Wijesiri, R.P.; Knowles, G.P.; Yeasmin, H.; Hoadley, A.F.A.; Chaffee, A.L. CO_2 Capture from Air Using Pelletised Polyethyleneimine Impregnated MCF Silica. *Industrial & Engineering Chemistry Research*. **2019**, 58(8), 3293-3303, doi:10.1021/acs.iecr.8b04973.
2. Wijesiri, R.P.; Knowles, G.P.; Yeasmin, H.; Hoadley, A.F.A.; Chaffee, A.L. Desorption Process for Capturing CO_2 from Air with Supported Amine Sorbent. *Industrial & Engineering Chemistry Research*. **2019**, XXXX(XXX), XXX-XXX, doi:10.1021/acs.iecr.9b03140.
3. Wijesiri, R.P.; Knowles, G.P.; Yeasmin, H.; Hoadley, A.F.A.; Chaffee, A.L. Technoeconomic Evaluation of a Process Capturing CO_2 Directly from Air. *Processes.* **2019**, 7(8), 503, doi:10.3390/pr7080503.

Conference Papers

1. Wijesiri, R.P.; Knowles, G.P.; Yeasmin, H.; Hoadley, A.F.A.; Chaffee, A.L., *CO_2 Capture from Air Using Supported Polyethyleneimine Type Sorbent*, in *14th Greenhouse Gas Control Technologies Conference*. 2018: Melbourne, Australia.

Awards

1. Fell Consulting Prize for the best paper presented by a student at the Chemeca 2017 conference.

Thesis Including Published Works Declaration

I hereby declare that this thesis contains no material which has been accepted for the award of any other degree or diploma at any university or equivalent institution and that, to the best of my knowledge and belief, this thesis contains no material previously published or written by another person, except where due reference is made in the text of the thesis.

This thesis includes 3 original paper published in peer reviewed journals. The core theme of the thesis is the adsorption of CO_2 from air by polyethyleneimine impregnated silica. The ideas, development and writing up of all the papers in the thesis were the principal responsibility of myself, the student, working within the Department of Chemical Engineering, Monash University under the supervision of Prof. Andrew Hoadley, Prof. Alan Chaffee, Dr. Gregory Knowles and Dr. Hasina Yeasmin.

The inclusion of co-authors reflects the fact that the work came from active collaboration between researchers and acknowledges input into team-based research.

In the case of Chapters 2-4 my contribution to the work involved the following:

Thesis Chapter	**Publication Title**	**Status** *(published, in press, accepted or returned for revision, submitted)*	**Nature and % of student contribution**	**Co-author name(s) Nature and % of Co-author's contribution***	**Co-author(s), Monash student Y/N***
2	*CO_2 Capture from Air Using Pelletized Polyethyleneimine Impregnated MCF Silica*	*Published*	*80%. conceptualisation, experimental work, analysis of results, writing first draft, writing(editing) subsequent drafts.*	• *Gregory P. Knowles (5%)* • *Hasina Yeasmin (5%)* • *Andrew F.A. Hoadley (5%)* • *Alan L. Chaffee (5%)* *conceptualisation, supervision, funding acquisition, reviewing and editing*	*No* *No* *No* *No*
3	*Desorption Process for Capturing CO_2 from Air with Supported Amine Sorbent*	*Published*	80% *conceptualisation, experimental work, analysis of results, writing first draft, writing(editing) subsequent drafts*	• *Gregory P. Knowles (5%)* • *Hasina Yeasmin (5%)* • *Andrew F.A. Hoadley (5%)* • *Alan L. Chaffee (5%)* *conceptualisation, supervision, funding*	*No* *No* *No* *No*

				acquisition, reviewing and editing	
4	*Technoeconomic Evaluation of a Process Capturing CO_2 Directly from Air*	*Published*	80% *conceptualisation, experimental work, modelling work, analysis of results, writing first draft, writing(editing) subsequent drafts*	• *Gregory P. Knowles (5%)* • *Hasina Yeasmin (5%)* • *Andrew F.A. Hoadley (5%)* • *Alan L. Chaffee (5%)* *conceptualisation, supervision, funding acquisition, reviewing and editing*	*No* *No* *No* *No*

I have not renumbered sections of submitted or published papers in order to generate a consistent presentation within the thesis.

Student name: Romesh Pramodya Wijesiri

Student signature:  **Date:** 28/08/19

I hereby certify that the above declaration correctly reflects the nature and extent of the student's and co-authors' contributions to this work. In instances where I am not the responsible author, I have consulted with the responsible author to agree on the respective contributions of the authors.

Main Supervisor name: Prof. Andrew Hoadley

Main Supervisor signature:  **Date:** 28/08/19

Acknowledgements

First and foremost, I would like to thank my supervisors for their guidance throughout my candidature. Hasina, thank you for the many days and nights you would have spent reviewing my work, and teaching me that I should always aim for perfection in whatever I do. Greg, thank you for teaching me how to approach problems with creativity. I will always be amazed and inspired by the limitless supply of ideas that you can come up with. Alan, thank you for your wisdom and mentorship which was instrumental for shaping what was an amazing research project and an experience for me. Andrew, thank you especially for taking a chance on me and giving me this opportunity. Over the past few years I have learnt so much from you both in the field and outside of it. I will forever be grateful to you for this.

Next, I would like to thank Antonio Benci and David Zuidema from the Monash Instrumentation Development Platform, who always had their doors open to me, whenever I needed their assistance. I will miss walking in to your office to the words “Uh-Oh here comes trouble”.

Dilshan Senaratne, thank you for always having my back and advising me through almost all of my major life decision. Thank you for also being there to help me back on my feet after the ‘occasional’ wrong decisions.

Josheena Naggea, I can’t thank you enough for having been by my side through the good and the bad times, for believing in me on days when even I didn’t, and for teaching me how to be a better me.

I would also like to thank my housemates and friends, who made Melbourne feel like home and made my time here more enjoyable.

Finally, and most importantly, I would like to thank my parents for their never-ending love and support. I know all the sacrifices you had to make to get me to where I am, and I could never fully repay the debt I owe you.

Table of Contents

COPYRIGHT NOTICE I

ABSTRACT II

PUBLICATIONS AND AWARDS DURING ENROLMENT IV

THESIS INCLUDING PUBLISHED WORKS DECLARATION V

ACKNOWLEDGEMENTS VII

LIST OF FIGURES X

LIST OF TABLES XIII

1. INTRODUCTION 1

1.1. MOTIVATION FOR CAPTURING CO_2 FROM AIR 1

1.2. PROCESSES FOR CAPTURING CO_2 FROM AIR 1

1.3. ADSORPTION OF CO_2 FROM AIR WITH POLYETHYLENEIMINE IMPREGNATED SOLID SORBENTS 3

1.4. DESORPTION OF CO_2 FROM SOLID SUPPORTED AMINES 7

1.5. TECHNOECONOMIC FEASIBILITY OF CAPTURING CO_2 FROM AIR WITH SUPPORTED AMINE SORBENTS 10

1.6. KNOWLEDGE GAPS 12

1.7. RESEARCH OBJECTIVES AND THESIS OUTLINE 13

2. CO_2 CAPTURE FROM AIR USING PELLETIZED POLYETHYLENEIMINE IMPREGNATED MCF SILICA 15

3. DESORPTION PROCESS FOR CAPTURING CO_2 FROM AIR WITH SUPPORTED AMINE SORBENT 28

4. TECHNOECONOMIC EVALUATION OF A PROCESS CAPTURING CO_2 DIRECTLY FROM AIR 42

5. CONCLUSIONS AND RECOMMENDATIONS 66

REFERENCES 71

APPENDIX A(I): SUPPORTING INFORMATION FOR "DESORPTION PROCESS FOR CAPTURING CO_2 FROM AIR WITH SUPPORTED AMINE SORBENT" 81

APPENDIX A(II): SUPPORTING INFORMATION FOR "TECHNOECONOMIC EVALUATION OF A PROCESS CAPTURING CO_2 DIRECTLY FROM AIR" 85

APPENDIX B(I): ADDENDUM TO "CO_2 CAPTURE FROM AIR USING PELLETIZED POLYETHYLENEIMINE IMPREGNATED MCF SILICA " 96

APPENDIX B(II): ADDENDUM TO "DESORPTION PROCESS FOR CAPTURING CO_2 FROM AIR WITH SUPPORTED AMINE SORBENT" 97

APPENDIX B(III): ADDENDUM TO "TECHNOECONOMIC EVALUATION OF A PROCESS CAPTURING CO_2 DIRECTLY FROM AIR" 98

APPENDIX C: N_2 SORPTION ISOTHERMS AND PORE SIZE DISTRIBUTION DATA FOR MCFA, MCFB, PEI_80A AND PEI_80B **99**

APPENDIX D: PRELIMINARY STUDY INTO THE EFFECT OF OXYGEN ON THE PERFORMANCE OF PEI IMPREGNATED MCF SILICA FOR ADSORPTION OF CO_2 FROM AIR. **101**

APPENDIX E: CALIBRATION OF THE INSTRUMENTS IN THE EXPERIMENTAL SET-UP **103**

APPENDIX F: LABVIEW PROGRAM USED FOR DATA ACQUISITION **107**

List of Figures

Chapter 1

Figure 1 The influence of the PEI loading on the adsorption of CO_2 from air by PEI impregnated solid sorbents reported in the literature. Adsorption under dry conditions for all data except for Sehaqui et al. [1], which was at 80% RH. The adsorption temperature is given in parentheses in the legend. 4

Figure 2 The influence of the temperature on the adsorption of CO_2 from air by PEI impregnated solid sorbents reported in the literature. The PEI loading is given in parentheses in the legend 5

Figure 3 The influence of the moisture on the adsorption of CO_2 from air by PEI impregnated solid sorbents reported in the literature. The adsorption temperature and the PEI loading are given in parentheses in the legend 6

Figure 4 The energy requirement and cost of capture for DAC processes with SSA reported in the literature. 11

Chapter 2

Figure 1 Experimental set-up for breakthrough analysis of CO_2 19

Figure 2 Breakthrough curves (**a**) and capacity curves (**b**) for the adsorption of CO_2 by PEI_80a at different temperatures. Error bars included for the 46 °C data are based on duplicate runs (Error in breakthrough curve: 0.008 ± 0.008; Error in capacity curve: 0.002 ± 0.003 mmol/g). The error is assumed to be similar for the other data sets 21

Figure 3 Comparison of capacities of the sorbents presented in the current study with PEI impregnated solid sorbents reported in literature for CO_2 capture from ultra-dilute gas mixtures (400-420 ppm CO_2) 21

Figure 4 The temperature dependency of the capacity of PEI_80a in comparison to amine impregnated solid sorbents reported in literature 22

Figure 5 Breakthrough curves (on the left hand side) and capacity curves (on the right hand side) for the adsorption of CO_2 by PEI_80b, under dry conditions and different moisture levels, at 33 °C, 46 °C and 58 °C. 23

Figure 6 CO_2 capacity of PEI_80b under dry conditions and different moisture levels for CO_2 adsorption from 420 ppm CO_2 in N_2. The corresponding % RH values at these conditions are listed above the bars, in red coloured text. The % change in capacity from dry condition is annotated inside the bars, in black coloured text 24

Figure 7 The dependency of the capacity of PEI_80b on the moisture content in comparison to literature data. The % RH values given in the literature were converted to % mol-H_2O basis for comparison, assuming that the experiments were carried out at atmospheric pressure 24

Figure 8 Surface plot of CO_2 capacity of PEI_80b as a function of temperature and moisture level for adsorption from 420 ppm CO_2 in N_2 25

Chapter 3

Figure 1 **(a)** Experimental set-up used for studying the adsorption/desorption of CO_2 by PEI_80b, **(b)** steam generator configuration A and (**c**) steam generator configuration B 32

Figure 2 Flow diagram of the experimental procedure used 33

Figure 3 The amounts of CO_2 adsorbed and desorbed, and the residual CO_2 in the sorbent after the experiment, for different desorption pressures and temperatures at a steam flow rate of 6.4 ± 1.2 g/h. The adsorbed amount is represented by the total height of the bar 34

Figure 4 CO_2 desorption (left hand side) and bed temperature (right hand side) for S-TVSD at pressures of 12 kPa abs, 26 kPa abs and 56 kPa abs at a steam flow rate of 6.4 ± 1.2 g/h. The average desorption rate (mmol/g/h) for each run is denoted in text next to the datasets. Error bars included for the 12kPa abs/90°C data are based on duplicate runs. The error is assumed to be similar for the other data sets 35

Figure 5 CO_2 desorption (left hand side) and bed temperature (right hand side) for S-TVSD at 12 kPa abs/100 °C and 26 kPa abs/100 °C under different steam flow rates. The average desorption rate (mmol/g/h) for each run is denoted in text next to the datasets. Error bars included for the 1.5g/h data at 26 kPa abs/100 °C are based on duplicate runs. The error is assumed to be similar for the other data sets 36

Figure 6 The equilibrium amounts of water adsorbed on the sorbent under the various desorption pressures and temperatures. Error bars presented are based on replicated experiments 36

Figure 7 CO_2 desorption (left hand side) and bed temperature (right hand side) for S-TVSD at 26 kPa abs/100 °C with different amounts of pre-adsorbed water. The average desorption rate (mmol/g/h) for each run is denoted in text next to the datasets. Error bars included for the dry data are based on duplicate runs. The error is assumed to be similar for the other data sets 37

Figure 8 Adsorption capacity of PEI_80b from dry 420 ppm CO_2 at 46 °C over 50 cycles of S-TVSD 37

Figure 9 Comparison of CO_2 desorption under S-TVSD with TVSD and with TVSD with N_2 purge. The S-TVSD runs were at a steam flow rate of 6.4 ± 1.2 g/h. The average desorption rates (mmol/g/h) for each run are denoted in text next to the datasets 37

Figure 10 The thermal energy requirement for steam production for desorption at 100 °C at 12 and 26 kPa abs at various steam flow rates 39

Chapter 4

Figure 1 **a)** A schematic of the proposed air-sorbent contactor configuration and **b)** the process flow diagram of the proposed DAC system. 48

Figure 2 **a)** The adsorption/desorption cycle the contactors are subjected to. **b)** The operational sequence of the contactors, with one bed in desorption at all times and the rest in adsorption. S1 to S3 refer to the stages in the adsorption/desorption cycle (adsorption, desorption and cooling) 50

Figure 3 The experimental data and the model predictions for CO_2 and H_2O adsorption from 420 ppm CO_2 in N_2 in the dry and humid cases. 52

Figure 4 The experimental data and the model predictions for CO_2 mass transfer kinetics in the desorption stage. Legend for titles AA_BBB_CCC_DD (AA- desorption pressure (kPa abs), BBB-desorption temperature(°C), CCC- desorption steam flow rate (kg h^{-1} kg-sorbent^{-1}), DD- amount of water adsorbed during adsorption stage (mol kg^{-1})). More results are depicted in **Figure S1** in the **Supplementary Information**. 52

Figure 5 The experimental data and the model predictions for equilibrium H_2O adsorption amount in the desorption stage at desorption pressures of 12 kPa and 26 kPa abs. 53

Figure 6 The experimental data and the model predictions for heat transfer and H_2O mass transfer kinetics in the desorption stage. Legend for titles AA_BBB_CCC_DD (AA- desorption pressure (kPa abs), BBB-desorption temperature (°C), CCC- desorption steam flow rate (kg h^{-1} kg-sorbent^{-1}), DD- amount of water adsorbed during adsorption stage (mol kg^{-1})). More results are depicted in **Figure S2** in the **Supplementary Information**. 53

Figure 7 Pareto plots for the objective functions of the MOO for the dry and the humid cases. 55

Figure 8 Pareto plots for the variables plotted against the capture rate, for the humid and the dry case. The limits for the y-axes are the bounds for each parameter used in the MOO. T_d was not plotted as it was constant at 100 °C across all the data points. 55

Figure 9 The temperature and RH of the inlet air to the process for each of the points in the Pareto plots 56

Figure 10 The contributions of various components to the cost of capture for the lowest cost case for the dry and humid case. The value for the humid case is given inside brackets in the data labels 57

Figure 11 Tornado plot of the sensitivity of the cost of capture of the lowest cost scenarios for ± 10% changes in the model values. 57

Figure 12 Comparison of the cost and energy data from this study to that of previous studies. The data are that of the lowest cost case described in the respective studies. [a]Carbon Engineering refers to an aqueous hydroxide based process for DAC. 60

Figure 13 Results of the case studies for the dry and the humid case. 62

List of Tables

Chapter 1

Table 1 Amines and supports of various SSA evaluated for DAC applications 3

Table 2 A summary of the desorption technologies evaluated for CO_2 capture with SSA. The data presented here are the desorption conditions with highest average desorption rates reported in the respective studies 9

Chapter 2

Table 1 Results of the characterisation of MCF powder and PEI_80a pellets. 20

Chapter 3

Table 1 A summary of the desorption technologies evaluated for CO_2 capture with SSA. 30

Chapter 4

Table 1 Definition of multi-objective optimization problem 51

Table 2 The results of the parameter estimation for the adsorption/desorption model and the constants used 54

Table 3 The process conditions which yield the lowest cost scenarios and the resulting cycle times and energy requirements of the process 56

1. Introduction

1.1. Motivation for Capturing CO_2 from Air

The increased anthropogenic CO_2 emissions have been identified to be a main reason for global climate change. The annual anthropogenic CO_2 emissions were reported to be approximately 40 gigatonnes in 2017 [1] and can be expected to increase with the growth of the global population and the expansion of industry. Carbon capture technologies present themselves to be a solution for reducing these emissions. The captured CO_2 could either be sequestered, or utilised in various industries [2]. Technologies for removing CO_2 directly from the atmosphere, also known as "Direct Air Capture" (DAC), are of particular importance. This is because they can compensate for the effect of CO_2 emitted from diffuse sources such as the transportation sector, houses and offices, which account for close to half of the total anthropogenic CO_2 emissions [3]. Alternatively, attempting to capture all these emissions at the source would require fitting of capture systems to each emitter, which would neither be economical, nor practical.

DAC also has several advantages in comparison to processes which capture CO_2 from large emitters. For example, when CO_2 is captured from large emitters, which may not be located close to suitable storage/utilisation sites, significant and costly infrastructure is needed for the transportation of CO_2. In comparison, DAC processes could be constructed close to the intended storage/utilisation site, thus minimising these costs. Capturing from large sources also requires that the sizes of the capture systems be tailored to match the size of the emitters. For DAC process, there are less restrictions, and the size could be optimised to take advantage of economies of scale and to better suit the availability of resources. Finally, at large enough scales, DAC processes could theoretically compensate for historic CO_2 emissions and reduce the CO_2 in the atmosphere back to pre-industrial levels, whereas capturing for large sources only offer potential for reducing/eliminating our future emissions. It should be noted that while these advantages are presented here for the sake of comparison, these processes are not considered to be competitors, but rather complementary tools in an arsenal aimed at mitigating the effects of global climate change.

1.2. Processes for Capturing CO_2 from Air

Various processes have been evaluated for DAC applications, including absorption with aqueous hydroxide solutions, and adsorption with alkali solids, zeolites, metal organic frameworks, anionic exchange resin and solid supported amines. Detailed reviews of these are presented in Sanz-Pérez et al. [4] and Goeppert et al. [5].

Absorption with aqueous hydroxide solutions such as NaOH[6-9], $Ca(OH)_2$[10,11] and KOH[12-14] was one of the earliest processes evaluated for DAC. The high binding energy of the CO_2 to the hydroxides made these processes effective at selectively capturing CO_2 from dilute gases. However, this also demanded a significant amount of thermal energy and very high temperatures (900-1000 °C) for the regeneration of the sorbent[8,9,13]. Other challenges of this process include the large evaporative losses of water[6,7,13], particularly when operating in relatively dry environments, and the potential health hazard of the solvents escaping into the atmosphere with the exhaust air from the system.

Evaluations of adsorption with basic solid sorbents such as CaO[15-18] and $Ca(OH)_2$[19] reported that they too needed very high temperatures for the regeneration of the sorbent. Additionally, the kinetics of the adsorption of CO_2 was observed to be very slow and required high adsorption temperatures to achieve a reasonable uptake of CO_2[15-17,19]. Hybrid materials where the alkali sorbents are dispersed in porous materials were reported to improve the adsorption performance under low temperatures, although high temperatures (170-850°C) were still required for regeneration[20-24].

Studies on using physisorbents such as zeolites[25-27] and metal organic frameworks (MOFs) [26,28,29] for DAC reported that while they exhibited a reasonable performance under dry conditions, the presence of moisture caused considerable deterioration of the CO_2 uptake.

Lackner[30] proposed the use of a strong-base ion exchange resin for capturing CO_2 from air, due to attributes such as low regeneration energy, and fast kinetics. For these sorbents, it has been reported that the presence of moisture has a negative effect on the uptake of the CO_2[31-35]. An advantage of this is that the sorbent could be regenerated through moisture swing which has been reported to have a lower energy demand[32,33]. However, this would limit the use of such processes to regions with relatively dry climates or necessitate that the inlet air be pre-dried which would carry additional and likely significant costs.

Most of the recent efforts on capturing CO_2 from air have been focussed on adsorption with solid supported amines, due to their high uptake capacity and selectivity, resilience to moisture which is present in air, and the possibility of regeneration under relatively mild conditions[4,5]. Solid supported amines (SSA) encompass a group of sorbents which consist of various amines physically loaded onto or chemically bonded to porous solid supports. Some of the amines and supports of sorbents evaluated for DAC are listed in **Table 1**. Of these, linear and branched polyethyleneimines (PEI) impregnated sorbents have been the most studied due to their low cost, easy availability, good stability and high adsorption capacity.

Table 1. Amines and supports of various SSA evaluated for DAC applications

Amines	Supports
polyethyleneimine[36-52]	silica[25,36-38,41-43,45-47,50-56,61-63,67,71]
polyallylamine[37,46]	carbon[44,49]
diamine[53]	cellulose[47,48,57-59,63]
3-aminopropylsilane[54]	MOF[29,40,64]
poly(l-lysine)[55],	polymeric resin[39]
triaminesilane[56]	porous polymer networks[65]
3-aminopropylmethyldiethoxysilane[57-60]	zeolites[66]
3-aminopropyltrimethoxysilane[61]	polystyrene[68,70,72]
(N-methylaminopropyl)trimethoxysilane[61]	alumina[36,73]
(N,N-dimethylaminopropyl)trimethoxysilane[61]	
N-(3-(trimethoxysilyl)propyl)ethane-1,2-diamine[53]	
ethylenediamine[29]	
3-(aminopropyl)-trimethoxysilane[62]	
2-(2-(3-trimethoxy-silyl-propyl-amino)ethylamino)ethylamine)[62]	
diamine[63]	
N,N-dimethylethylenediamine[64]	
diethylenetriamine[65]	
ethylenediamine[65]	
tris(2-aminoethyl)amine[40]	
polypropyleneimine[51]	
tetraethylenepentamine[66]	
pentaethylenehexamine[67]	
benzylamine[68-70]	

1.3. Adsorption of CO_2 from Air with Polyethyleneimine Impregnated Solid Sorbents

The CO_2 capture performance of PEI impregnated sorbents has been reported to be highly dependent on factors such as the molecular weight of the amine used, the nature of the amine sites and the loading of amine in the sorbent[36,37,40,42,44,49,51,52,73,74]. Goeppert et al.[74] and Darunte et al.[40] attributed to the high stability of PEIs to their higher molecular weights, thus lower volatility. In comparison, sorbents impregnated with low molecular weight amines were observed to suffer from leaching of the amine phase from the solid support [40,74]. This resulted in the loss of adsorption capacity with time and the potential contaminations of downstream units. It has also been reported that PEIs with higher molecular weights showed better stability against leaching, although at the

compromise of a poorer CO_2 uptake [42,74]. This reduced uptake was identified to be due to the higher viscosity of heavier PEIs, which hindered the diffusion of CO_2. Additionally, branched PEIs have been reported to possess higher CO_2 capacities than linear PEIs, owing to the larger proportion of primary amines present[37].

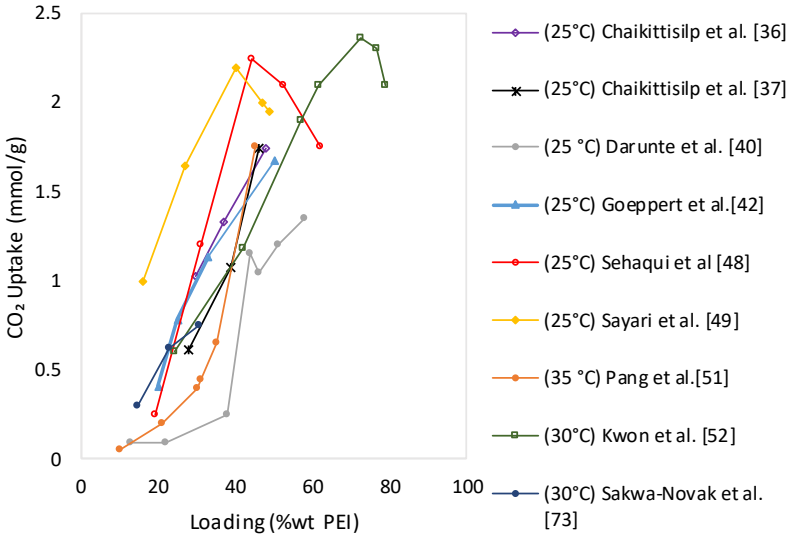

Figure 1: The influence of the PEI loading on the adsorption of CO_2 from air by PEI impregnated solid sorbents reported in the literature. Adsorption under dry conditions for all data except for Sehaqui et al. [48], which was at 80% RH. The adsorption temperature is given in parentheses in the legend.

Investigations into the effect of PEI loading on the CO_2 adsorption showed that higher loadings often resulted in an increased uptake of CO_2 (refer **Figure 1**) [36,37,40,42,51,73]. However, some of these studies[40,42] reported that it also resulted in slower CO_2 adsorption kinetics. The authors attributed this to the increased diffusional resistance present in highly loaded sorbents. Other studies[44,49,52] reported that increasing the PEI loading yielded improved capacities only up to a certain PEI loading, after which further increases deteriorated the CO_2 uptake. In these cases, the increase in diffusional resistance at higher loadings was believed to have become strong enough to have made a portion of the amine sites inaccessible to the CO_2.

The PEI loading has also been reported to have an effect on how the adsorption of CO_2 is influenced by the air temperature (refer **Figure 2**). Sorbents with low PEI loadings have displayed a reduction in the CO_2 uptake as the adsorption temperature is increased[42,47]. This is consistent with the thermodynamics of the exothermic nature of the reaction between the amine sites and the CO_2. However, in sorbents with high PEI loadings, increasing the adsorption temperature has been reported to increase the CO_2 uptake up until a certain critical temperature is reached[42,44,52]. Following this, further increases in temperature yielded reductions in the CO_2 uptake. This could be explained using the findings of Wang and Song[75] who identified that sorbents with higher PEI loadings had higher

proportions of the total amine sites in inner layers which have reduced accessibility due to diffusional limitations. As a result, higher temperatures are required for the CO_2 to overcome diffusional limitations and access these amine sites. However, at temperatures higher than a certain critical temperature, the negative effect on the thermodynamics of the reaction between the CO_2 and the amines outweighs the positive effect on the diffusion, resulting in a reduced CO_2 uptake.

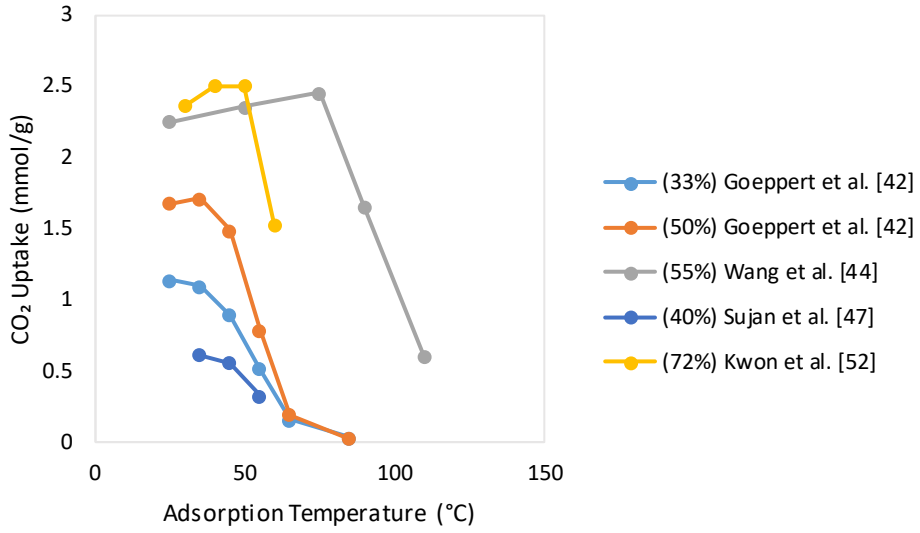

Figure 2: The influence of the temperature on the adsorption of CO_2 from air by PEI impregnated solid sorbents reported in the literature. The PEI loading is given in parentheses in the legend.

A unique advantage of these sorbents for use for DAC applications is their resilience to the moisture that is typically present in air. As seen in **Figure 3**, some studies[41,44,47-49,52] have reported that PEI impregnated sorbents displayed enhanced CO_2 uptake under humid conditions. Depending on the adsorption conditions and the sorbent used, CO_2 uptake has been reported to increase by as much as five-fold [48].

Most of the aforementioned studies[44,48,49,52] attributed the enhancements to the difference in reaction pathways, via which CO_2 reacts with the amine sites, under dry and humid conditions. The studies suggested that under dry conditions, two amine sites react with one CO_2 molecule, forming carbamates (**Reaction 1**), while in the presence of moisture, one CO_2 molecule reacts with one amine site to form bicarbonates (**Reaction 2**).

Under dry conditions: $CO_2 + 2R_1R_2NH \leftrightarrow R_1R_2NH^+ + R_1R_2NHCOO^-$ (**Reaction 1**)

Under wet conditions: $CO_2 + R_1R_2NH + H_2O \leftrightarrow R_1R_2NH_2^+HCO_3^-$ (**Reaction 2**)

However, it should be noted that the formation of bicarbonates alone could only provide a maximum enhancement of 2-fold and cannot fully explain the larger increase in capacity observed by

Sehaqui et al.[48]. It is also worthwhile mentioning that while carbamates and bicarbonates are the two most predominantly discussed reaction products, there have been reports of CO_2 uptake via the formation of carbamic acid under dry conditions[76,77], and via the formation of carbonates in the presence of moisture[76].

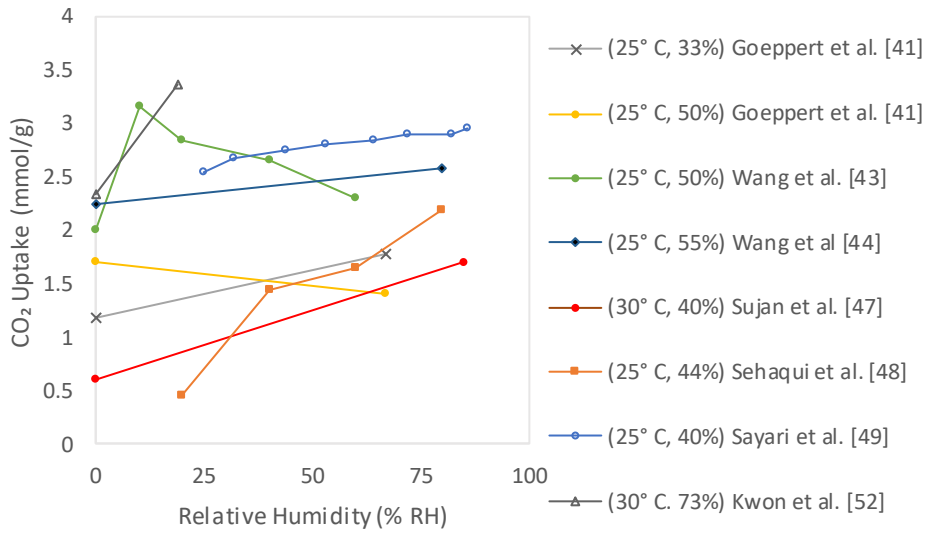

Figure 3: The influence of the moisture on the adsorption of CO_2 from air by PEI impregnated solid sorbents reported in the literature. The adsorption temperature and the PEI loading are given in parentheses in the legend.

Other studies[46,78] on solid supported amines have attributed the enhancement in CO_2 capacity to improved diffusion of CO_2 in the PEI phase of the sorbent. Mebane et al.[78] proposed that water enhanced the formation of diffusive intermediates which in turn aided the transport of CO_2 in the amine phase. Zerze et al.[46] proposed that amine polymers may be existing as thick films on the surface of the sorbents, and that water vapour may loosen the polymer network thereby enhancing the transport of CO_2.

The promoting effect of water on CO_2 adsorption has not been universally observed for DAC with SSA. Wang et al.[43] observed that at 10% RH, a higher uptake than under dry conditions was achieved. Yet, further increases in humidity were detrimental to the uptake of CO_2, which was attributed to competitive adsorption between H_2O and CO_2 at high humidity levels. Alternatively Liu et al.[79] suggested that this may be explained by increased mass transfer resistances due to the formation of a water film on the adsorbent, or due to capillary condensation of water leading to blockages in the micropores. Goeppert et al.[41] observed that much like the effect of temperature, that of moisture too was dependent on the PEI loading of the sorbent. It was reported that while a 33% wt PEI sorbent showed an increase in the CO_2 uptake when the RH was increased from 0 to 67%, a 50% wt PEI sorbent

displayed a decrease in the uptake under the same conditions. This reduced uptake was attributed to the co-adsorbed water hindering the diffusion of CO_2 within the sorbent

1.4. Desorption of CO_2 from Solid Supported Amines

Desorption of CO_2 from SSA can be achieved via applying a partial pressure driving force in the form of a vacuum or a purge gas, applying a temperature driving force by heating up the sorbent, or a combination of these. Various desorption technologies have been evaluated for CO_2 capture applications with SSA, although most of these have not been done in the context of DAC applications. These studies have been undertaken with a variety of sorbents and different desorption conditions. To facilitate comparison, the process conditions of several studies have been summarised in **Table 2**, where the CO_2 purity and the average desorption rate achieved are noted.

Temperature concentration swing desorption (TCSD) [42-44,63,64,71,80-82] has been the most widely studied desorption technology. For TCSD, the sorbent is heated while purging with an inert gas to lower the partial pressure of CO_2 surrounding the sorbent. While fast desorption can be achieved, the desorbed CO_2 is produced in a dilute form due to the purge gas [42-44]. Alternatively, TCSD with a CO_2 purge can be used to desorb CO_2 as a high purity product, at the expense of a slower average desorption rate [64,80]. This poor desorption rate exhibited with the CO_2 purge has been attributed to the significantly higher partial pressure of CO_2 around the sorbent, and hence the smaller driving force for desorption [80]. In addition to the slower kinetics of this approach, SSAs reportedly undergo degradation when exposed to high CO_2 concentration atmospheres at elevated temperatures. This has been attributed to the formation of urea linkages [69,83-87]. However, it has been reported that this type of degradation can be inhibited[58,85,87,88] or even reversed[84] in the presence of moisture.

Another technology that can be used to desorb CO_2 is vacuum swing desorption (VSD). In this process, the desorption is achieved by applying a vacuum on the sorbent, after the adsorption stage and at the same temperature. This would likely be unsuitable for DAC, as the CO_2 is adsorbed from air, at a partial pressure of about 0.04 kPa abs. To achieve desorption, the sorbent would need to be evacuated to below this pressure, requiring very large vacuum pumps, and, hence, relatively large capital costs for equipment and high energy requirements.

Alternatively, temperature vacuum swing desorption (TVSD) can be used to avoid the need for high vacuum levels (<0.04 kPa abs) for DAC application. In this type of process, desorption is achieved by applying milder vacuum levels and simultaneously heating the sorbent [47,60,63,70,81,82,89]. As no inert gas purge is used, the product gas mainly consists of the adsorbed species (typically CO_2 and

H_2O), and the desorbed CO_2 could be obtained at higher concentration. However, while desorption of high purity CO_2 is made possible with TVSD, it has been reported to produce slower desorption than TCSD with an inert purge gas [63,81,82]. Wurzbacher et al.[60,63] compared the desorption performance under TVSD when the CO_2 was adsorbed from humid air (20-80 % RH), and observed that while the presence of moisture enhanced the uptake of CO_2, it also resulted in a disproportionately higher uptake of H_2O. The study suggested that this additional uptake of water would in turn result in a higher thermal energy requirement during the regeneration of the sorbent. In contrast, Bos et al. [70] reported that the presence of moisture reduced the energy requirement of the process. The study reported that the increase in the CO_2 uptake by the sorbent, in the presence of moisture, compensated for the added thermal energy demand for desorption of water. It was further suggested that the desorption of water may lower the partial pressure of CO_2 around the sorbent and promote the desorption of CO_2.

As another approach for desorbing high purity CO_2, TCSD with steam as a purge gas, also known as steam stripping, has been evaluated [90-92]. As the water in the desorbed product can easily be condensed, CO_2 could be obtained at high purity. In comparison to TCSD with inert gas, steam stripping showed faster desorption kinetics [90,92]. The authors suggested that this accelerated desorption was a result of the water molecules interacting with the amine sites and displacing the CO_2 adsorbed on these sites. Sandhu et al. [90] reported that the adsorption of water by the sorbent, during steam stripping, released a significant amount of heat, which increased the sorbent temperature by as much as 12 °C [90]. It is possible that this heat generation helped to accelerate the process by increasing the amount of energy available to be utilised for CO_2 desorption, which is endothermic in nature.

As an added advantage of steam stripping, the presence of moisture could be expected to stabilise the sorbent from CO_2 induced degradation [58,84,88]. Indeed, Sandhu et al. [90] reported that steam stripping resulted in a 2% loss in the cyclic capacity for a PEI impregnated silica, in comparison to the 6% loss observed with a N_2 purge. Hammache et al. [92] reported no degradation of the amines, negligible leaching and minimal changes to the structure of the silica sorbent, for desorption with steam stripping at 105 °C, for a PEI functionalised silica sorbent. In contrast, Chaikittisilp et al. [36] reported an 81% reduction in capacity for a PEI loaded SBA-15 sorbent, after steam exposure at 105 °C. It was suggested that this was likely caused by the collapse of the mesostructure. An alumina support, evaluated in the same study showed better stability, losing only 25% of its capacity.

Table 2. A summary of the desorption technologies evaluated for CO_2 capture with SSA. The data presented here are the desorption conditions with highest average desorption rates reported in the respective studies.

Ref	Type	Sorbent[a]	Adsorption from	Desorption conditions			Average desorption rate[d] (mmol/g/h)	Purity (% mol)
				T (°C)	P (kPa abs)[b]	Purge gas[c]		
[42]	TCSD	amine/silica (3 g)	air (400-420 ppm CO_2)	100	-	335 (N_2)	5.01	10
[43]	TCSD	amine/HP2MGL resin (1 g)	5000 ppm CO_2 in N_2	100	-	50 (N_2)	3.99	19
[44]	TCSD	amine/carbon (0.5 g)	5000 ppm CO_2 in N_2	110	-	50 (N_2)	5.89	22
[47]	TVSD	amine/cellulose-silica (unspecified)	380 ppm CO_2/397 ppm He in N_2	90	0.06-0.7	-	1.86	98
[60]	TVSD	amine/cellulose (10 g)	air (400-510 ppm CO_2 at 80% RH)	95	5	-	0.65	94-97
[63]	TCSD	amine/silica (23 g)	air (400-440 ppm CO_2)	90	-	800 (Ar)	0.20	unspecified
	TVSD	amine/silica (23 g)	air (400-440 ppm CO_2)	90	1	-	0.15	96
[64]	TCSD	amine/MOF (0.09 g)	15% CO_2 in N_2	120	-	25 (N_2)	10.08	unspecified
	TCSD- CO_2 purge	amine/MOF (0.09 g)	15% CO_2 in N_2	150	-	25 (CO_2)	4.32	unspecified
[70]	S-TVSD	amine/polystyrene (30.4)	5000 ppm CO_2 in N_2	116	50	2000(steam)	2.88	unspecified
[71]	TCSD	amine/silica (1000 g)	air (394 ppm CO_2)	130	-	8000 (9% H_2O/N_2)	0.83	6
[81]	TCSD	amine/polystyrene (19 g)	45% CO_2 in N_2	100	-	226 (N_2)	5.00	unspecified
	TVSD	amine/polystyrene (19 g)	45% CO_2 in N_2	100	10	-	4.20	unspecified
[82]	TCSD	amine/silica (1 g)	5% CO_2 in N_2	150	-	50 (N_2)	0.97	unspecified
	TVSD	amine/silica (1 g)	5% CO_2 in N_2	150	10	-	0.96	unspecified
	TVSD- inert gas purge	amine/silica (1 g)	5% CO_2 in N_2	150	10	50 (N_2)	0.98	unspecified
[89]	S-TVSD	unspecified SSA (40 g)	air (40% RH)	100	20	2.5 (steam)	1.35	unspecified
	TVSD	unspecified SSA (40 g)	air (40% RH)	100	20	-	0.41	unspecified
[90]	Steam Stripping	amine/silica (1 g)	10% CO_2 in N_2	110	-	unspecified (90% H_2O/N_2)	13.86	75
[91]	Steam Stripping	amine/silica (2 g)	CO_2 in N_2 (unspecified concentration)	103	-	72 (steam)	12.47	unspecified
[92]	Steam Stripping	amine/silica (1 g)	10% CO_2 in He	105	-	unspecified (90% H_2O/He)	17.45	75

[a] *sample mass studied is indicated within parentheses.* [b] *desorption pressure for cases where a vacuum was used.* [c] *purge gas flow rate in g/h for steam and in ml/min for the rest. The gas used is indicated within parentheses.* [d] *average desorption rate calculated as the total desorbed amount divided by the total desorption time.*

Steam-assisted temperature vacuum swing desorption (S-TVSD) is a hybrid approach [70,89]. In addition to applying a vacuum and heating the sorbent, a steam purge is used to sweep the desorbed CO_2 from the atmosphere surrounding the sorbent. The sweeping effect lowers the partial pressure of CO_2 below that which could be achieved with pure TVSD, providing a larger driving force for desorption. Additionally, as the process operates under a vacuum, the steam could be produced at lower temperatures (<100 °C). We note that since the steam can be produced at low temperatures, solar thermal energy or waste heat might be used to supply this. The benefit of having a purge gas during TVSD has been demonstrated by Serna-Guerrero et al. [82], where using a N_2 purge improved the average desorption rate at 70 °C by about a factor of 3. Similarly, Fujiki et al. [93] demonstrated that the use of a steam purge resulted in about a 2-fold faster desorption rates for a VSD process.

Similarly, Gebald et al. [89] demonstrated that S-TVSD produced approximately 3 times faster kinetics than TVSD under DAC conditions. They observed that lower pressures combined with higher temperatures yielded higher desorption rates. Gebald et al. [89] also pointed out that while higher steam flow rates led to faster desorption times, it would also negatively affect the economics of the process. The preferred steam rate was suggested to be less than 0.1-0.2 kg/h per kg of sorbent. The patent [89] also presented the results of cyclic testing which showed a 13% loss in capacity after 200 cycles of adsorption/desorption. It was further reported that S-TVSD had a lower energy requirement than both TVSD and steam stripping type processes. In contrast, Bos et al. [70] reported that while S-TVSD yielded faster desorption of CO_2, it may have a larger energy demand than TVSD, due to the thermal energy needed for steam generation. It was also observed[70] that the enhancing effect on the desorption kinetics by the steam purge was less significant when adsorption was carried out in the presence of moisture, in comparison to that under dry conditions.

1.5. Technoeconomic Feasibility of Capturing CO_2 from Air with Supported Amine Sorbents

There are a few reports [60,71,89,94-96,98] on the energy requirement and the cost of capture of DAC processes with SSA (refer **Figure 4**). In two of the early studies, Kulkarni and Sholl [96] and Zhang et al. [71] carried out an economic analysis based on only the operating cost of the processes. They reported costs of 43-494 [96] and 91-227 [71] USD/tonne of CO_2 captured. Krekel et al. [95] expanded on the work carried out by Zhang et al. [71], and reported that once the capital expenses are included, the cost of capture would be increased significantly to 792-1200 USD/tonne. Moreover, these costs of capture for Zhang et al. [71] and Krekel et al. [95] did not include the CO_2 emissions from energy generation. Once these emissions were considered, the cost was reported to increase to 152-425[71] and 824-1333[95] USD/tonne, respectively. These results highlighted the importance of using low

carbon energy sources for supplying energy to DAC processes. Sinha et al. [94] estimated a cost of capture of 60-190 USD/tonne, without including the emissions from energy generation. Subsequently. Sinha and Realff [98] carried out a parametric study which estimated the cost to be 14 USD/tonne for a 'best-case scenario' and 1065 USD/tonne for a 'worst-case scenario'. The study[98] proposed the 'mid-range' cost estimate to be 86-221 USD/tonne. While the emissions from energy generation were not included in these calculated costs, the study suggested that the use of solar or wind power would produce the least amount of emissions.

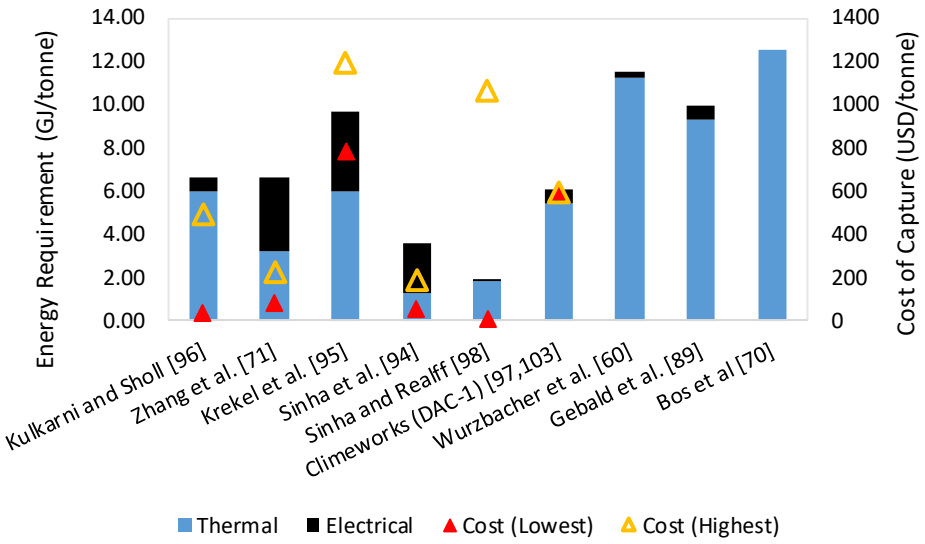

Figure 4: The energy requirement and cost of capture for DAC processes with SSA reported in the literature. The energy requirement in the figure corresponds to that of the lowest cost scenario in the respective studies.

DAC has been the focus of several commercial projects including Climeworks [99], Global Thermostat [100], Carbon Engineering [101] and Infinitree [102]. Of these, Climeworks [99] and Global Thermostat [100] utilise SSA based processes. The cost of capture reported for the operations of first-generation DAC system by Climeworks was estimated to be 600 USD/tonne[103]. This is an important benchmark, as it is based on a commercially operating system, as opposed to results of studies which are sensitive to the scope and assumptions used. Climeworks has further expressed their confidence in reducing this cost down to 200 USD/tonne by 2021, and down to 100 USD/tonne by 2030 [103]. Similarly, Global Thermostat expects a cost of capture of 100 USD/tonne for their first commercial DAC process [103].

In comparison, removing CO_2 from air via afforestation and forest management has a cost of capture of 15-50 USD/tonne[104]. However, this approach carries a large land requirement, which would compete with the land available for food production. Moreover, the land available also enforces an upper limit on the scale at which CO_2 can be removed. In comparison, CO_2 removal by DAC faces less

stringent limitations on the degree of possible scaling. However, it is important to stress that DAC is not envisioned to be an alternative for good forest management practices, but rather as a technology to supplement the rate of CO_2 removal by the natural carbon cycle.

The minimum energy requirements of the DAC processes with SSA, reported in the literature, are in the range of 3.6 [94] to 12.5 [70] GJ/tonne of CO_2 captured. This is largely accounted for by the thermal energy required for the desorption process. This mainly consists of the sensible heat required to heat up the sorbent to the desorption temperature, and the large heat of desorption for CO_2. When adsorption is considered under humid conditions, the heat of desorption of water, which gets co-adsorbed on SSA, adds to the thermal energy demand [60,70]. It was reported [60,70] that the energy for desorbing the water could account for >30% of the total thermal energy demand of the process. However, the economic evaluations to date [71,94-96] do not appear to have considered the desorption of this co-adsorbed water in their analysis. While Sinha and Realff [98] considered the co-adsorption of water by the sorbent, it was assumed that the adsorbed water would not be released during the desorption stage. Another big contributor to the energy consumption is that needed for pushing air through the air-sorbent contactors. Due to the low concentration of CO_2 in air, large amounts of air need to be processed to capture the CO_2. This results in large energy requirements, even for low pressure drop contactor configurations as are described in some studies [94,96].

1.6. Knowledge Gaps

The knowledge gaps identified from the review of the literature, which this thesis aims to address are as follows

1. At the time of carrying out this research, only a few studies[42,44] had evaluated the effect of the adsorption temperature on the CO_2 adsorption performance by PEI impregnated solid sorbents, under DAC conditions. While more studies[41,43,44,48,49] had evaluated the effect of different moisture levels, no study had evaluated the effect of moisture at a series of different temperatures. This information would be critical for identifying the suitability of the sorbents for DAC applications, depending on the climate of the intended location for the process. Moreover, at the time of carrying out this research, there was no information available on how highly loaded (>55% wt PEI) sorbents behave under different temperatures and moisture levels, under DAC conditions.
2. The majority of the research on SSA for DAC applications have focussed on the development of sorbents with a large CO_2 uptake. Limited focus has been placed on identifying suitable desorption methods[47,60,63,70,89], which are also critical for the successful deployment of DAC systems. While some more studies [42,44,64,71] evaluated desorption under TCSD

processes, these would be unsuitable for practical DAC applications, as the CO_2 is desorbed in dilute form as a mixture with other inert gases.

Furthermore, the literature review identified S-TVSD to be a promising technology for desorption, due to the fast desorption kinetics produced under mild vacuum levels, the possibility of desorbing the CO_2 at high purity, and the improved stability of the sorbent in wet atmospheres. However, at the time of carrying out the research, S-TVSD for DAC applications had been described only in a single patent [89], which disclosed minimal information of the desorption kinetics.

3. DAC processes with SSA need to be economically feasible if their deployment is to be successful. However, at the time of carrying out the research there were only a few reports[71,94-96,98] which had addressed this, and there was a significant discrepancy in their results. Furthermore, these studies[71,94-96] did not attempt to optimise the process conditions to minimise the cost of capture, and no evaluation had been done on the effect of co-adsorbed water on the economics of the process.

1.7. Research Objectives and Thesis Outline

The research in this thesis was carried out with the aim of developing a process for capturing CO_2 from atmospheric air using a pelletised PEI loaded mesocellular foam (MCF) silica sorbent with a high amine loading. This sorbent was chosen as it was previously found to be highly promising for post combustion capture[85] and preliminary thermogravimetry studies had indicated its suitability for direct air capture applications[105,106]. The specific research aims, as tailored to address the knowledge gaps identified in **Section 1.6**., are as follows:

1. **Identification of the effect of adsorption temperature and moisture on the CO_2 uptake by PEI impregnated silica sorbent:** The research uses a laboratory-scale breakthrough analysis set-up to characterise the adsorption performance of the sorbent, under a series of different temperatures and moisture levels, under DAC conditions.

2. **Identification of a suitable desorption technology for a DAC process with SSA:** The research uses a custom-built laboratory-scale experimental set-up to carry out a rigorous investigation on how the process conditions (temperature, pressure, steam flow rate, co-adsorbed moisture) affect the desorption performance of the sorbent, and determine its potential for DAC applications.

3. **Evaluating the technoeconomic feasibility of a DAC process**: The results of laboratory scale experimental data are used to develop a process model to evaluate the economics of a scaled-up DAC process. This model is then subjected to a multi-objective optimisation to determine the process conditions which yield the minimum cost of capture of the process.

This thesis addresses these aims in three chapters presented in the form of publications. **Chapter 2** addresses the first research aim and has been published in *Industrial & Engineering Chemistry Research*. **Chapter 3** addresses the second research aim and has been published in *Industrial & Engineering Chemistry Research*. **Chapter 4** addresses the third research aim and has been published in *Processes.* Finally**, Chapter 5** presents the overall conclusions of the work and recommendations for future work.

2. CO_2 Capture from Air Using Pelletized Polyethyleneimine Impregnated MCF Silica

This chapter focusses on the first research objective of the thesis: identifying the effect of temperature and moisture on the adsorption performance of PEI impregnated solid sorbents. The development of a PEI supported MCF silica sorbent with a high PEI loading, and the characterisation of its adsorption performance under a series of different temperatures and moisture levels is described here.

It was observed that although the high amine loading allowed for a large CO_2 uptake capacity, it also resulted in slower adsorption kinetics. The study identified that while low temperatures were better for the thermodynamics of the reaction between the CO_2 and amine sites, the uptake of CO_2 was limited by diffusional resistances in the sorbent. In contrast, higher temperatures allowed for better diffusion of CO_2, but the thermodynamics were less favoured. The amount of CO_2 adsorbed by the sorbent was determined by the combined effect of these two factors. Due to the large diffusional resistances of the sorbent studied, the highest uptake was achieved under relatively warm conditions (46 °C). While, the presence of moisture (0.5 and 2% mol-H_2O in feed gas) yielded up to 53% enhancement in capacity, higher moisture levels (3% mol-H_2O) appeared to be detrimental to the CO_2 uptake. This suggested that at high moisture levels, the large amounts of co-adsorbed water may be interfering with the adsorption of CO_2.

The study also compared the performance of two PEI-MCF silica sorbents, PEI_80a and PEI_80b, prepared under slightly different synthesis methods. PEI_80a had previously demonstrated promising CO_2 adsorption performance under preliminary thermogravimetry studies [105,106]. In the synthesis of PEI_80b, an additional sonication step was used during the impregnation step of PEI into the MCF silica. This was hypothesised to improve the CO_2 adsorption by the sorbent, owing to better infiltration and dispersion of the amine polymers into the pores of the silica support. Elemental analysis of the two sorbents confirmed that the two methods resulted in a similar loading of PEI (66% and 63% wt, for PEI_80a and PEI_80b, respectively). Despite this, PEI_80b displayed up to 55% higher CO_2 uptake than PEI_80a, under the same adsorption conditions, which confirmed the positive effect of the sonication step on the adsorption performance of the sorbent.

Finally, the study also highlighted that at an adsorption temperature of 81 °C there was negligible CO_2 uptake, which gave a preliminary indication that desorption could be carried out under mild temperatures.

The content of this chapter has been published in *Ind. Eng. Chem. Res.*

The N_2 sorption isotherm data and the pore size distributions for the materials discussed in this chapter are presented in **Appendix C**. The calibration plots for the instruments used for the experimental work in **Chapter 2** are presented in **Appendix E**. The LabVIEW program used for data acquisition is presented in **Appendix F.**

I&EC research
Industrial & Engineering Chemistry Research

Article

Cite This: *Ind. Eng. Chem. Res.* 2019, 58, 3293−3303

pubs.acs.org/IECR

CO_2 Capture from Air Using Pelletized Polyethylenimine Impregnated MCF Silica

Romesh P. Wijesiri,[†,‡] Gregory P. Knowles,[‡] Hasina Yeasmin,[†] Andrew F. A. Hoadley,*[,†] and Alan L. Chaffee*[,‡]

[†]Department of Chemical Engineering and [‡]School of Chemistry, Monash University, Wellington Road, Clayton, VIC 3800, Australia

ABSTRACT: Two polyethylenimine impregnated mesocellular foam silica sorbents (PEI_80a and PEI_80b) were evaluated for capturing CO_2 from 420 ppm of CO_2 in N_2 under both dry and humid conditions. A fixed bed adsorption setup was used to evaluate the CO_2 uptake under isothermal conditions between 33 and 81 °C with a gas flow of 200 mL/min. Under dry conditions, the highest capacity was observed at 46 and 52 °C for PEI_80a (1.29 mmol/g) and at 46 °C for PEI_80b (1.94 mmol/g). There was negligible uptake of CO_2 at 81 °C, indicating possible regeneration at relatively low temperatures. For PEI_80b, the introduction of moisture (0.5 and 2% mol-H_2O in feed gas) yielded up to 53% enhancement in capacity. Higher moisture levels (3% mol-H_2O) appeared to be detrimental to the CO_2 uptake. The highest capacity of 2.52 mmol/g was achieved at a temperature of 46 °C and a moisture level of 2% mol-H_2O.

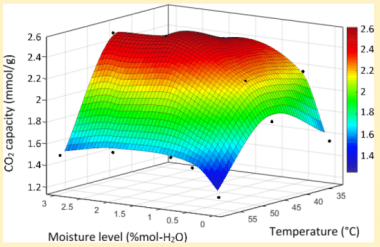

1. INTRODUCTION

Capturing CO_2 directly from the atmosphere and its subsequent sequestration or utilization are recognized as an important solution for combatting global climate change. This is because capturing CO_2 from air, also referred to as direct air capture (DAC), can compensate for diffuse CO_2 emissions which amount to close to half of all anthropogenic CO_2 released.[1] It offers some advantages in comparison to capturing CO_2 from large point sources, such as being less restricted with the choice of location and the size of the facility.[2] Moreover, the conversion of the captured CO_2 to synthetic fuels[3,4] with the use of renewable energy to power the process would offer the possibility of setting up an artificial carbon cycle. The captured CO_2 could alternatively be used for the production of chemical intermediates[5] or for use in greenhouses.[6]

The initial studies on air capture were often focused on the absorption of CO_2 into aqueous hydroxide solutions such as NaOH,[7,8] $Ca(OH)_2$,[9] and KOH.[10] Material and energy balances done by Baciocchi et al.[11] and Zeman[12] determined that while the high binding energy of CO_2 to metal hydroxide made them favorable in the absorption step, this also resulted in a significant energy requirement for regeneration. A few studies[13−15] were also conducted on the use of zeolites for the capture of CO_2 from air. Although they exhibited a reasonable performance under dry conditions, the introduction of moisture was reported to cause considerable deterioration to the uptake of CO_2.[15] Lackner[16] proposed the use of a strong base ion-exchange resin for capturing CO_2 from air, due to attributes such as low regeneration energy and fast kinetics. For these sorbents, it has been reported that the presence of moisture has a negative effect on the uptake of the CO_2, allowing for desorption to be carried out through moisture swing.[17,18] However, much like in the case of the zeolites, this necessitates that the air be dried prior to coming into contact with the sorbent.

Most recent efforts on capturing CO_2 from air are focused on the use of solid supported amines. These encompass a group of sorbents which consist of various amines physically loaded onto or chemically bonded to porous solid supports such as silica,[19−24] alumina,[25,26] metal organic frameworks,[27,28] and cellulose.[29,30] Such sorbents had previously been evaluated for CO_2 capture from closed cabin breathing environments such as submarines.[31] Linear and branched polyethylenimines (PEI) of various molecular weights are among the most studied amines for the preparation of solid supported amine type sorbents due to their low cost, easy availability, and high adsorption capacity.[20−23,25−27,32−34] Apart from this, other amines such as polyallylamine,[19,24] diethanolamine,[35] tetraethylenepentamine,[35] and ethylenediamine[36] have also been evaluated for air capture applications. A detailed review of direct air capture technologies is presented in Sanz-Pérez et al.[37]

The CO_2 capture performance of solid supported amine sorbents has been reported to be highly dependent on factors such as the type of amine used, the nature of the amine sites, and the loading of amine in the sorbent. Goeppert et al.[35] evaluated a series of different amines loaded onto silica, and

Received: October 9, 2018
Revised: December 22, 2018
Accepted: February 5, 2019
Published: February 5, 2019

determined that low molecular weight amines such as monoethanolamine (MEA) and diethanolamine (DEA) presented significant leaching problems during regeneration under vacuum (0.1−0.5 mmHg) at 80−100 °C. The leaching was attributed to the low boiling point and thus the high volatility of the low molecular weight amines. This resulted in the loss of adsorption capacity with time and the potential contaminations of downstream units. In contrast, PEIs displayed improved stabilities and higher uptake capacities. Additionally, linear PEIs were seen to possess higher capacities than branched PEIs, although at the compromise of greater leaching. The higher capacities were attributed to the larger proportion of primary amines in comparison to secondary/tertiary amines present in the linear PEI.

Similar leaching problems were reported by Darunte et al.[27] for a tris(2-aminoethyl)amine (TREN) impregnated MIL-101(Cr) adsorbent. Despite having an initial capacity of 2.8 mmol/g at 25 °C, the capacity was reported to drop down to 2.5 mmol/g after three 6 h cycles of adsorption. A series of PEI impregnated MIL-101(Cr) at different PEI loadings was also evaluated by Darunte et al.[27] who reported increased uptake capacities as PEI loading was increased from 13 to 58 wt % PEI. However, the time taken to reach adsorption equilibrium was seen to significantly increase as the PEI loading was increased. The 58 wt % PEI loaded sorbent took 340 min to reach saturation in comparison to the 240 min taken by the 44 wt % PEI loaded sorbent. The authors attributed this to the increased diffusional resistance present in highly loaded sorbents. Similar trends of increasing capacity were reported by Goeppert et al.[21] when the PEI loading was increased from 20 to 50 wt % for PEI impregnated fumed silica and Pang et al.[22] when the PEI loading was increased from 10 to 45 wt % PEI for a PEI impregnated SBA-15.

In contrast, Sayari et al.[23] and Wang et al.[38] reported that increases in PEI loading yield improved capacities only up to a certain PEI loading, after which the CO_2 capacity was negatively affected. For the PEI impregnated mesoporous carbon studied by Wang et al.,[38] the maximum loading was at 60 wt % PEI while it occurred at 40 wt % PEI for the MCM-41 supported PEI sorbent studied by Sayari et al.[23] In both cases, the increase in diffusional resistance at higher loadings was believed to have become strong enough to have reduced the CO_2 uptake.

A unique advantage of solid supported amines is their resilience to the moisture typically present in air. In fact, some studies[23,29,38,39] have reported enhancements of the capture performance under humid conditions. Goeppert et al.[39] reported a 50% increase in capacity when the relative humidity was increased from 0% to 67% for a 33 wt % PEI loaded fumed silica sorbent at 25 °C. In other studies, a 40 wt % PEI loaded MCM-41 silica sorbent showed a 34% increase in capacity when relative humidity was increased from 0% to 86% at 25 °C,[23] and a 55 wt % PEI loaded mesoporous carbon sorbent showed a 14% increase in uptake capacity when relative humidity was increased from 0% to 80% at 25 °C.[38] The highest enhancement in capacity was reported for a 44 wt % PEI loaded nanofibrillated cellulose (NFC) sorbent[29] which showed nearly a fivefold increase in capacity when the RH was increased from 20% to 80% at 25 °C.

Most of the aforementioned studies[23,29,38] attributed the enhancements to the difference in reaction pathways, via which CO_2 reacts with the amine sites, under dry and humid conditions. The studies suggested that in the presence of moisture, one CO_2 molecule reacts with one amine site to form bicarbonates (Reaction 2), while under dry conditions, two amine sites are required to react with one CO_2 molecule, forming carbamates (Reaction 1).

$$\text{Under dry conditions: } CO_2 + 2R_1R_2NH \leftrightarrow R_1R_2NH^+ + R_1R_2NHCOO^- \quad (1)$$

$$\text{Under wet conditions: } CO_2 + R_1R_2NH + H_2O \leftrightarrow \cancel{R_1R_2NH^+HCO_2^-}\ R_1R_2NH^+HCO_3^- \quad (2)$$

However, it should be noted that the formation of bicarbonates alone could only provide a maximum enhancement of twofold and cannot fully explain the 4.9-fold increase in capacity observed by Sehaqui et al.[29] It is also worthwhile mentioning that while carbamates and bicarbonates are the two most predominantly discussed reaction products, there have been reports of CO_2 uptake via the formation of carbamic acid under dry conditions[40,41] and via the formation of carbonates in the presence of moisture.[40]

Other studies[24,42] on solid supported amines have attributed the enhancement in CO_2 capacity to improved diffusion of CO_2 in the PEI phase of the sorbent. Mebane et al.[42] proposed that water enhanced the formation of diffusive intermediates which in turn aided the transport of CO_2 in the amine phase. Zerze et al.[24] proposed that amine polymers may be existing as thick films on the surface of the sorbents and that water vapor may loosen the polymer network thereby enhancing the transport of CO_2.

The promoting effect of water on CO_2 adsorption has not been universally observed for solid supported amines. Wang et al.[34] observed that for a 50 wt % PEI loaded HP2MGL resin sorbent, increasing the moisture content to a RH of 10% delivered a 58% improvement in capacity in comparison to dry conditions, yet further increases in humidity were detrimental to the uptake of CO_2. Goeppert et al.[39] observed a 17% decrease in capacity of a 50 wt % PEI loaded fumed silica when the relative humidity was increased from 0% to 67% at 25 °C. It has been suggested that this deterioration of capacity at high moisture contents may be due to competitive adsorption between H_2O and CO_2.[34,43] Alternatively Liu et al.[44] suggested that this may be explained by increased mass transfer resistances due to the formation of a water film on the adsorbent or due to capillary condensation of water leading to blockages in the micropores.

These reports suggest that the PEI content of the sorbents determines how the performance of the sorbent is affected by the presence of moisture and that high levels of moisture may be detrimental to highly loaded sorbents. It is also evident that there is a scarcity, in the studies available, on the effect of moisture on direct air capture applications. Furthermore, most available literatures only evaluate the effect of moisture at a set temperature of 25 °C, while in practical air capture applications, the operating temperature may vary from subzero temperatures to ∼55 °C depending on the location and preferred process condition. A similar argument can be made for investigations into the performance of sorbents under dry conditions. While more data are available for dry conditions than for humid conditions, there are only a limited number of studies[21,24,38,45] that have studied the capture performance of these sorbents over a range of temperatures. As such, the assessment of the suitability of these sorbents for direct air

DOI: 10.1021/acs.iecr.8b04973
Ind. Eng. Chem. Res. 2019, 58, 3293−3303

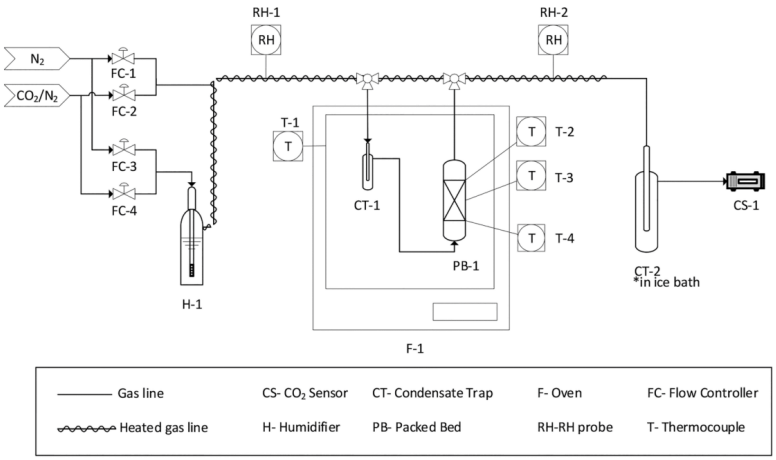

Figure 1. Experimental setup for breakthrough analysis of CO_2.

capture applications calls for further investigations into how their performance varies over a broader range of adsorption conditions.

Given the interest in sorbents with a high loading of PEI, the present study considers the potential of shaped mesocellular foam silica loaded with an 80% pore volume equivalent of 1200 MW branched PEI for CO_2 capture from air. This sorbent was previously found to be highly prospective for postcombustion capture,[46] and preliminary thermogravimetry studies indicated its suitability for direct air capture applications.[47,48] MCF silica was chosen as the support for the sorbent due to the large pore volumes inherent in this material. This makes it ideal for loading of large proportions of amines within the spherical cells which are interconnected to form a three-dimensional pore system.[49,50] It was previously demonstrated that sonication of the bulk solution of PEI and mesoporous silica during the impregnation step promoted good infiltration and dispersion of the amine polymers into the pores of this support.[51] To evaluate the effect of the sonication on the CO_2 capture performance of the sorbent, two different sorbents were synthesized, with and without the sonication step. This paper details the results of the investigation into how the adsorption temperature and the moisture content of the feed gas affect the CO_2 capture performance of the sorbent.

2. EXPERIMENTAL SECTION

2.1. Material Synthesis. Two samples of PEI loaded MCF silica pellets were prepared. In both samples, branched PEI (average molecular weight 1200 MW) acquired from Sigma-Aldrich was used to impregnate 80% of the pore volume in mesocellular foam (MCF) silica. PEI_80a was prepared according to the method described in Knowles et al.[46] Fourier transform infrared studies previously done by our group[49] confirmed that PEI can effectively be incorporated into the MCF via this method. PEI_80b was prepared using the same method, except the bulk solution of MCF and PEI was sonicated using a Soniclean 250HT on "Degas" setting for 3 h upon mixing and prior to the mechanical stirring. The samples in powder form were degassed at 110 °C under vacuum for 24 h and thereafter purged with pure CO_2 at 60 °C for 24 h. The carbonated powder was then made into 4 mm diameter cylindrical pellets using a TDP-6T single punch tablet press. Finally, each pellet was cut into quadrants with an approximate Sauter mean diameter of 1.8 mm.

2.2. Material Characterization. N_2 adsorption at 77 K data of the two samples in pellet form and the MCF silica was collected using a Micromeritics TriStar 3020 equipment or a Micromeritics ASAP 2020. These data were used to estimate the specific surface area and the mesopore volume using the BET method[52] and the BJH method,[53] respectively. The true densities of the materials were determined via helium pycnometry using a Micromeritics Accupyc 1340. Elemental analysis was carried out, using a PerkinElmer 2400 Series II CHNS/O Elemental Analyzer, to determine the C, H, and N content of the PEI-silica samples. The results were used to verify the amine loading of the sorbent. The samples being analyzed were degassed at 105 °C under vacuum for 12 h prior to each characterization experiment.

2.3. Fixed Bed CO_2 Adsorption Experimental Setup. The experimental setup used for the analysis of the CO_2 adsorption performance of the MCF-PEI pellets is represented in Figure 1. The adsorbent (4 g of PEI_80a or 3.4 g of PEI_80b) was packed in a glass column (120 mm length ×10 mm ID) and contained by 1 cm glass wool plugs at each end and terminated with Swagelok fittings. The void fraction of the bed was calculated to be 0.54 using the densities measured via He pycnometry. To simulate the CO_2 concentration in air, a gas mixture of 420 ppm of CO_2 in N_2 at a flow rate of 200 mL/min was prepared using a series of Bronkhorst mass flow controllers which blend N_2 and a custom gas mix of 1000 ppm of CO_2 in N_2 acquired from Air Liquide. The humidification of the feed gas was achieved by passing a portion of the feed gas through a bubbler filled with deionized water contained in a heated water bath. The gas lines carrying humid gas were spiral wrapped with HTS/Amptek heat tape and heated to 5 °C below the adsorption bed temperature to prevent condensation in the lines. As an additional precaution to prevent the adsorbent from coming into contact with liquid water, a

DOI: 10.1021/acs.iecr.8b04973
Ind. Eng. Chem. Res. 2019, 58, 3293−3303

condensate trap was placed immediately upstream of the column. The feed gas was passed through the adsorption column contained in an oven which was used to maintain the temperature of the adsorbent bed. The exhaust gas was then passed through a second condensate trap, which was placed in an ice bath, to knock out any residual moisture and prevent the condensation in the downstream gas lines. The dry gas was then passed through a Gascard NG nondispersive infrared CO_2 analyzer to measure the CO_2 concentration in the exhaust gas. The humidities of the feed gas and the exhaust gas were measured using two Vaisala HMP110 relative humidity probes which record the relative humidity and the temperature of the gas passing through. The temperatures inside the oven and inside the column were measured using type T thermocouples.

2.4. Experimental Procedure. Prior to each experiment, the MCF-PEI pellets in the bed were regenerated by purging with N_2 at 100 °C until no CO_2 or water was detected in the exhaust gas. Thereafter, the oven temperature was set to the adsorption temperature to be evaluated. The temperatures of the humidifier and the heat tape were set to 10 and 5 °C lower than the adsorption temperature, respectively. The bypass system was used at start-up to validate the CO_2 concentration and moisture content of the feed gas. Once the desired analysis conditions had been achieved, the gas was directed through the adsorption column, and the moisture content and the CO_2 concentration of the exhaust gas were recorded using the exhaust gas humidity sensor (Figure 1) and the CO_2 sensor. The periodic data of the CO_2 concentration recorded from the CO_2 sensor were then used to plot the breakthrough curves for the adsorption of CO_2. The CO_2 uptake capacity curves for the sorbent were calculated by integrating the breakthrough curves according to eq 3 where q_t is adsorption capacity (mmol/g) at time t, $\dot{n}$ is the flow rate of the feed gas (mmol/h), m is the mass of sorbent (g) in the bed, and t is the adsorption time (h). C_0 and C_t are the CO_2 concentrations (mol/mol) in the feed gas and the exhaust gas at time t, respectively.

$$q_t = \int_0^t \frac{\dot{n}(C_0 - C_t)}{m} \mathrm{d}t \tag{3}$$

3. RESULTS AND DISCUSSION

3.1. Material Characterization. Table 1 shows the results of the characterization experiments done on the PEI_80a, PEI_80b, and the respective MCF silica supports. In comparison to the expected % wt PEI loadings, the loadings calculated according to the results of the CHN analysis were ∼5 wt % PEI lower for both samples. This indicates that the impregnation was largely successful except for minor losses of PEI. The pore volume data suggests that virtually all the pores of the MCF support have been filled by the PEI phase, despite only being impregnated with an 80% pore volume equivalent of PEI. To explain this, it is hypothesized that the PEI phase may simply be blocking the pore openings rather than filling the pores completely. This is supported by the investigations of Holewinski et al.[54] which suggested that the pore filling of SBA-15 silica occurs differently in the case of sorbents with low and high PEI loadings. When low amounts of PEI are loaded onto the silica support, the PEI forms a coating on the pore walls. When the PEI content is increased beyond a certain critical value, the polymers agglomerate to form plugs which are the same diameter as the pore but do not extend through the length of the pore.

Table 1. Results of the Characterisation of MCF Powder and PEI_80a Pellets

	true density (g/cm^3)	BET surface area (m^2/g)	mesopore volume (pore diameter 2−50 nm) (cm^3/g)	PEI content (% wt PEI)[a]	PEI content (% wt PEI)[b]
MCFa	2.11	594 ± 6	3.21	–	–
PEI_80a	1.25	3.1 ± 0.1	0.020	71	66.0 ± 0.7
MCFb	2.15	453 ± 3	2.49	–	–
PEI_80b	1.26	3.9 ± 0.1	0.021	68	63.1 ± 1.5

[a]Calculated according to the initial mass of PEI added during sorbent synthesis. [b]Calculated according to the results of CHN analysis.

3.2. Effect of Temperature. The breakthrough curves and the capacity curves plotted for the adsorption of CO_2 from 420 ppm of CO_2 in N_2 by PEI_80a at different isothermal conditions (36, 40, 46, 52, 58, 66, 71, and 81 °C) are presented in Figure 2a and Figure 2b, respectively. The curves demonstrate that apart from the experiments at and above 66 °C, PEI_80a does not reach saturation within 40 h. At adsorption temperatures below 66 °C, the breakthrough curves can be seen to form a drawn-out tail, while still adsorbing approximately 20% of the CO_2 in the feed gas stream. This can also be observed in the capacity curves (Figure 2b) which appear to plateau after about 20 h from the start of adsorption. This suggests that the CO_2 faces increasing mass transfer resistances as the sorbent is progressively saturated with CO_2. The slow kinetics of adsorption observed here are consistent with those reported in Goeppert et al.,[21] for PEI impregnated silica sorbents, measured under similar experimental conditions. A 50 wt % PEI loaded silica was reported to take over 40 h to reach saturation at 25 °C, and like in the cases presented here, a long drawn out tail in the breakthrough curve was observed after ∼15 h of adsorption.

Experiments carried out for over 70 h demonstrated that the majority of the CO_2 uptake takes place in the first 40 h of adsorption. As such, the experiments described in the current paper were limited to 40 h for obtaining the relevant capacity data. It should be noted that in practical DAC systems, it is highly unlikely that the adsorption would be carried out for such extended time frames, owing to the energy consumption of pumping air through the contactor. This study does not aim to address the optimization of cycle times but rather aims to compare the performance of the sorbent under different adsorption conditions.

The capacities for PEI impregnated sorbents reported in literature are plotted in Figure 3, alongside the capacities obtained for PEI_80a and PEI_80b in this study. The capacity data in the literature have been measured either using fixed bed systems,[21,25,38,39] similar to this study, or using thermogravimetric analysis.[19,22,23,26,27,34] As mentioned earlier, most sorbents have been evaluated only at 25 °C making it difficult for direct comparisons to be made with PEI_80a and PEI_80b. The few studies[21,38] which evaluated the sorbent performance at different temperatures have shown that temperature has a significant effect on the CO_2 uptake, allowing preliminary inferences to be made on what adsorption temperatures may be favorable for air capture processes using amine loaded sorbents.

From the comparison of the capacity curves for PEI_80a at different temperatures (see Figure 2b), it is observed that

DOI: 10.1021/acs.iecr.8b04973
Ind. Eng. Chem. Res. 2019, 58, 3293−3303

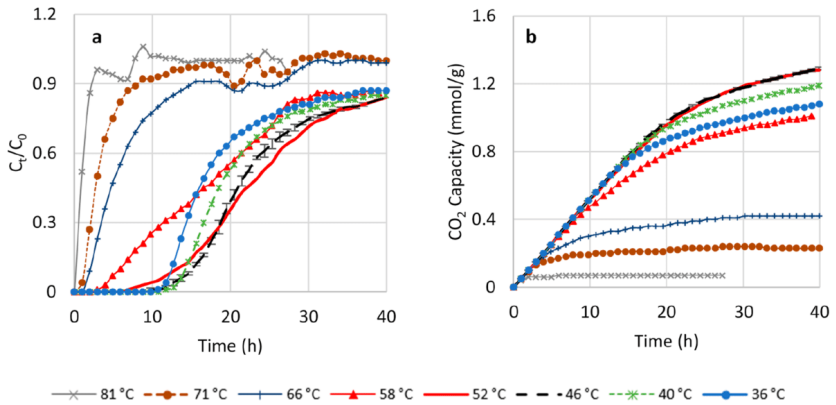

Figure 2. Breakthrough curves (a) and capacity curves (b) for the adsorption of CO_2 by PEI_80a at different temperatures. Error bars included for the 46 °C data are based on duplicate runs (error in breakthrough curve: 0.008 ± 0.008; error in capacity curve: 0.002 ± 0.003 mmol/g). The error is assumed to be similar for the other data sets.

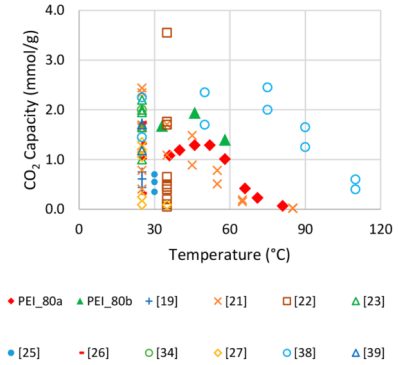

Figure 3. Comparison of capacities of the sorbents presented in the current study with PEI impregnated solid sorbents reported in the literature for CO_2 capture from ultradilute gas mixtures (400−420 ppm of CO_2).

increasing the adsorption temperatures from 36 to 40 °C and from 40 to 46 °C led to progressively higher adsorption of CO_2, reaching 1.29 mmol/g at 46 °C. When the adsorption temperature was further increased from 46 to 52 °C, no further improvements in uptake were seen. Increasing the adsorption temperature from 52 up to 81 °C resulted in a steep decrease in CO_2 capacity reaching 0.07 mmol/g at 81 °C.

The initial increases in adsorption capacity as the adsorption temperature is raised can be attributed to the improvement of the diffusion of CO_2 in the PEI polymer phase of the sorbent. This view is supported by the mechanism put forward by the Song group.[55−57] They proposed that the CO_2 uptake by solid supported amines occurred in two stages: rapid sorption by the amine sites in the exposed outer layers of PEI, followed by the slow diffusion of CO_2 through the PEI polymer phase to the interior amine sites. While the reaction between the CO_2 and the amine sites is favorable at lower temperatures due to its exothermic nature, the majority of the amine sites within the inner PEI layers may not be accessible at these temperatures due to diffusional limitations. As the adsorption temperature is increased, however, the proportion of the inner sites that are accessible to the CO_2 is increased, resulting in improved uptake.

However, as the adsorption temperature is increased beyond a certain critical temperature, the negative effect on the thermodynamics of the (exothermic) reaction becomes more dominant. As a result, the CO_2 uptake by the sorbent is reduced even though the diffusional resistances are lowered and more amine sites are made accessible. In the case of the PEI_80a, the decreases in adsorption capacity as the temperature is increased beyond 52 °C indicate that the critical temperature for this sorbent lies between 46 and 52 °C.

The variation of CO_2 capacity with temperature for PEI_80a is depicted in Figure 4, alongside data available for other amine impregnated sorbents which have been evaluated for air capture. The results of the TGA studies[48] done in tandem by our group on PEI_80a are also plotted on the same figure and show a consistent trend. This comparison makes it evident that different sorbents display different temperatures at which uptake is at its highest.[21,38] This appears to be dependent on factors such as the nature of the support and the amine loading upon it. For example, between two otherwise identical sorbents, the 50 wt % PEI loaded fumed silica had a higher critical temperature (35 °C) in comparison to a 33 wt % PEI loaded sorbent (≤25 °C).[21] This could be explained using the findings of Wang and Song[55] who identified that sorbents with higher PEI loadings had higher proportions of the total amine sites in the inner layers. As a result, higher temperatures are required for the CO_2 to overcome the diffusional limitations and access the amine sites. This also explains why the capacity of PEI_80a (66 wt % PEI) peaked at a higher temperature than the sorbents studied by Goeppert et al.[21] However, it should be noted that the 50 wt % PEI loaded mesoporous carbon[38] displayed a higher critical temperature despite having a lower loading than PEI_80a, which suggests that the nature of the support may also influence the behavior of the sorbent. When considering the 30 wt % polyallylamine (PAA) loaded

DOI: 10.1021/acs.iecr.8b04973
Ind. Eng. Chem. Res. 2019, 58, 3293−3303

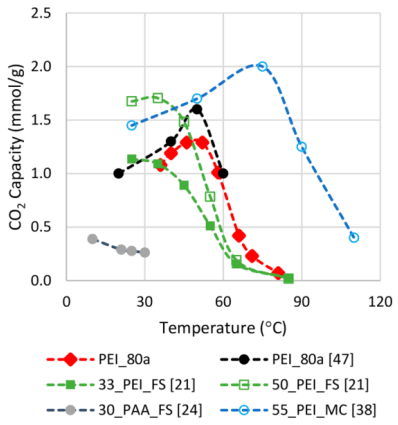

Figure 4. Temperature dependency of the capacity of PEI_80a in comparison to amine impregnated solid sorbents reported in literature.

silica[24] and the 33 wt % PEI loaded silica,[21] no clear peak in the capacity vs temperature curve was identified. For these cases, it is possible that, due to the relatively low amine loadings in these sorbents, the temperature at which capacity is maximized occurred below the range of temperatures studied.

The temperature capacity profiles identified for these sorbents may play a crucial role in choosing sorbents for use in practical air capture applications at different locations. For example, judging from Figure 4, the PEI_80a evaluated in this study would be more appropriate for use in regions of the world with warmer ambient temperatures. In contrast, the 50 wt % PEI loaded fumed silica[21] would be more suitable for regions with lower ambient temperatures.

An interesting observation from the temperature capacity profile of PEI_80a is the steep decrease in capacity (1.29 to 0.07 mmol/g) as the temperature is increased from 46 to 81 °C. The negligible capacity at 81 °C suggests that if adsorption were to be carried out at 46 °C, the sorbent may be effectively regenerated with only a 35 °C increase in temperature. Similarly, for the 50 wt % PEI loaded fumed silica[21] increasing the temperature from 35 to 85 °C reduces the capacity from 1.7 to 0.02 mmol/g. In contrast, although the 55 wt % PEI loaded mesoporous carbon[38] outperformed both of the above-mentioned sorbents in terms of uptake capacity at low temperatures, it retained most of its capacity at temperatures above 80 °C. This suggests that higher temperatures may be necessary for the regeneration which might make the process more energy intensive and thus less economical. However, these are only preliminary inferences from the data made available on the capacity of the sorbents, and practical desorption processes may give different results depending on the specific equipment and the process conditions employed.

The breakthrough curves prepared from the adsorption of CO_2 from 420 ppm of CO_2 in N_2 by PEI_80b at 33, 46, and 58 °C under dry conditions and at various moisture levels are presented in Figure 5. The corresponding capacity curves are also presented in Figure 5. The results depict that the overall effect of temperature on the capture performance remains similar to that of PEI_80a, with a maxima in CO_2 uptake at 46 °C. However, it was noted that the CO_2 uptake was enhanced in comparison to PEI_80a at each of the temperatures studied. While saturation of the sorbent was still not achieved in the 40 h period, both the breakthrough of CO_2 and the appearance of long drawn-out tails were seen to occur later than in the case of PEI_80a (see Figure 2a). The enhancement in performance is also reflected in the capacity curve where the uptake at 40 h increased by 55% at 33 °C, 50% at 46 °C, and 39% at 58 °C, when compared to the performance of PEI_80a under similar adsorption conditions. These results confirm the positive effect of the sonication step on the performance of the sorbent and may be explained by the increased accessibility of the PEI layers due to improved dispersion within the pores of the silica support. The 25% higher specific surface area of PEI_80b in comparison to PEI_80a is also likely a result of the improved dispersion of the amine polymers within the pores.

3.3. Effect of Moisture. To quantify the effect of moisture on the CO_2 capture performance of PEI_80b, the uptake capacities at three different temperatures (33, 46, and 58 °C) for four different moisture levels (0, 0.5, 2, and 3% mol-H_2O) were compared. The breakthrough curves and the corresponding capacity curves plotted for these conditions are depicted in Figure 5. The % RH values corresponding to these conditions are listed in Figure 6. As described in the previous section, saturation of the sorbent was not achieved in the time scale studied due to the slow kinetics of the adsorption. For the purpose of this study, the capacities calculated at the time at which $C_t/C_0 = 0.7$ were used for the comparison (see Figure 6).

At 33 °C, the introduction of moisture level of 0.5% mol-H_2O yielded a 40% increase in capacity from that under dry conditions. Increasing the moisture level further to 2% mol-H_2O resulted in a further 13% increase in capacity. However, at 3% mol-H_2O, the uptake of CO_2 was 22% lower than that under dry conditions. At 33 °C, the highest capacity of 2.36 mmol/g was achieved at a relative humidity of 41%. In the case of the 46 °C experiments, the enhancing effect was lower than at 33 °C and only an 18% enhancement was observed at 0.5% mol-H_2O. Similar to 33 °C, the highest capacity (2.52 mmol/g) at 46 °C was observed at a moisture level of 2% mol-H_2O. These conditions corresponded to an RH of 20%. A moisture level of 3% mol-H_2O appeared to hinder the uptake of CO_2, and the capacity decreased from that at 2% mol-H_2O. At 58 °C, 0.5% mol-H_2O yielded 19% improvement in capacity from dry conditions. Like at the other temperatures, the highest capacity (1.58 mmol/g) at 58 °C was observed at 2% mol-H_2O (corresponding to an RH of 11%). Further increasing the moisture level to 3% mol-H_2O resulted in the reduction of the capacity, consistent with the other two temperatures.

For PEI_80b, the improvements in capacity (at moisture contents below 3% mol-H_2O) were seen to be more significant at lower temperatures. As the evaluation of the effect of temperature on the CO_2 uptake by PEI_80b suggested that temperatures below 46 °C were primarily limited by diffusional resistances, it is likely that the water played a part in improving the accessibility of the amine sites to the CO_2. However, the results do not rule out the possibility of enhancements to capacity being due to the formation of bicarbonates. According to the stoichiometry of the bicarbonate formation reaction, presence of water can theoretically yield up to a twofold enhancement in capacity. In contrast to the study by Sehaqui et al.,[29] where the introduction of moisture yielded up to a 4.9-fold increase in capacity, the enhancements observed in this

DOI: 10.1021/acs.iecr.8b04973
Ind. Eng. Chem. Res. 2019, 58, 3293−3303

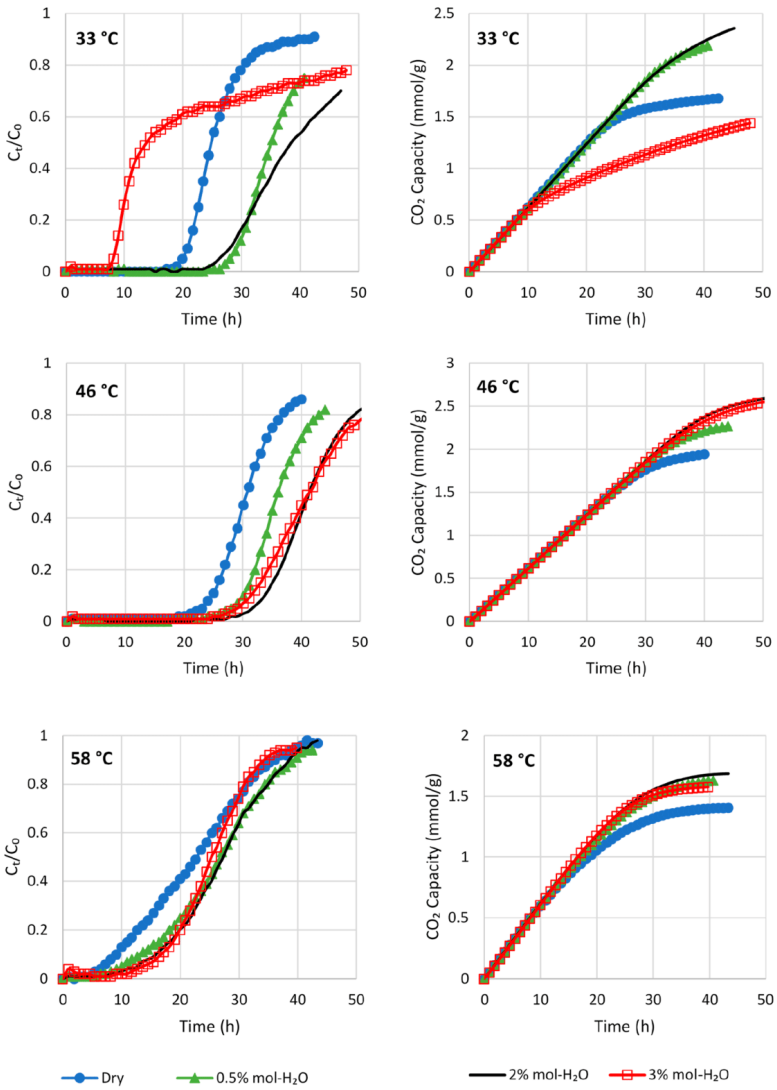

Figure 5. Breakthrough curves (on the left-hand side) and capacity curves (on the right-hand side) for the adsorption of CO_2 by PEI_80b, under dry conditions and different moisture levels, at 33, 46, and 58 °C.

study for PEI_80b were within the theoretical limit. The determination of the exact nature of the enhancing effect of water on the CO_2 uptake by PEI_80b is worthy of further investigation. While the highest enhancements in capacity from the conditions studied were achieved at 2% mol-H_2O at all temperatures, the data suggest that the actual maxima in capacity could occur at a different moisture level between 0.5 and 3% mol-H_2O, where even higher enhancements in capacity than those reported in this paper might be observed.

The results also show that higher moisture content (~3% mol-H_2O) is detrimental to the uptake of CO_2 at all temperatures studied. It is possible that, in the presence of high moisture levels, the sorbent adsorbs large amounts of water, which in turn presents an additional barrier to the diffusion of CO_2 to the amine sites. Liu et al.[44] suggested that

DOI: 10.1021/acs.iecr.8b04973
Ind. Eng. Chem. Res. 2019, 58, 3293−3303

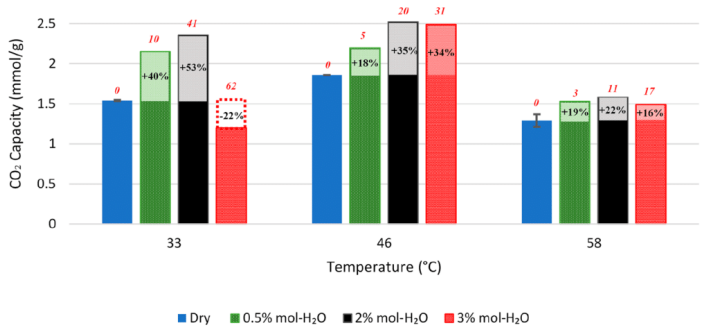

Figure 6. CO_2 capacity of PEI_80b under dry conditions and different moisture levels for CO_2 adsorption from 420 ppm of CO_2 in N_2. The corresponding % RH values at these conditions are listed above the bars, in red colored text. The % change in capacity from dry condition is annotated inside the bars, in black colored text.

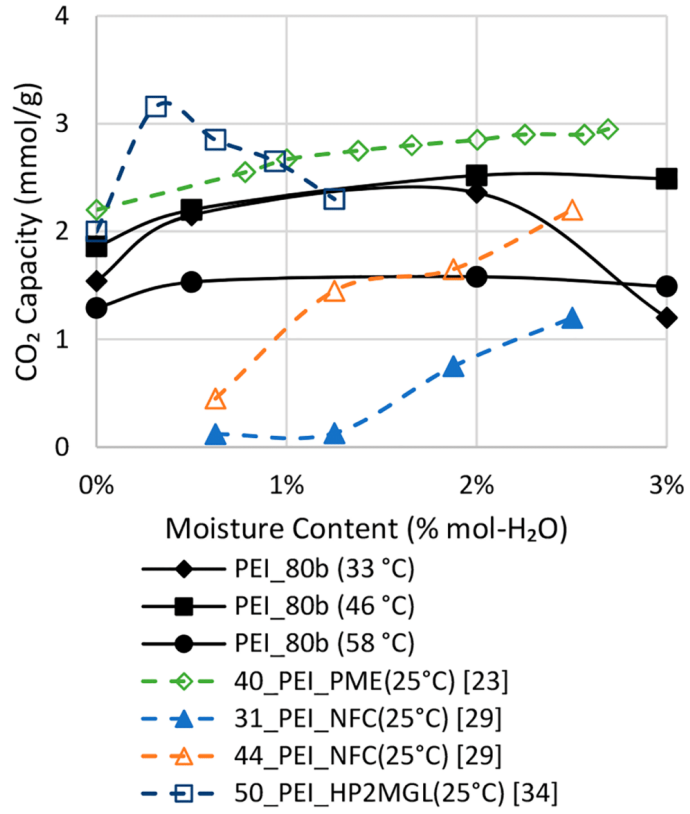

Figure 7. Dependency of the capacity of PEI_80b on the moisture content in comparison to literature data. The % RH values given in the literature were converted to % mol-H_2O basis for comparison, assuming that the experiments were carried out at atmospheric pressure.

DOI: 10.1021/acs.iecr.8b04973
Ind. Eng. Chem. Res. 2019, 58, 3293−3303

this may be due to the adsorbed water forming a film on the surface of the sorbent or due to capillary condensation which led to blockage of the pores in the sorbent.

A similar trend to PEI_80b was observed by Wang et al.[34] for a 50 wt % PEI loaded HP2MGL resin sorbent (see Figure 7), where a moisture level 0.31% mol-H_2O (at 25 °C) was seen to deliver a 58% improvement in capacity in comparison to dry conditions, but further increases in moisture level were seen to be detrimental to the uptake of CO_2. In comparison, PEI_80b appeared to be able to tolerate higher moisture levels without losing capacity. In other studies,[23,29] continuous improvements to capacity were made as the moisture level was increased. However, the capacity profile of the 40 wt % PEI loaded pore expanded MCM-41 sorbent[23] appeared to follow a similar trend to PEI_80b in the range of moisture contents under which it was tested. In the case of these sorbents, it may be that they would have experienced similar inhibitions to the CO_2 uptake if they had been exposed to higher moisture levels.

The amine efficiency can be calculated as the molar ratio between the adsorbed CO_2 and the N atoms in the sorbent. The highest amine efficiency achieved by PEI_80b, under dry conditions, was 0.12 mol-CO_2/mol-N at 46 °C. For PEI_80a, an efficiency of only 0.08 mol-CO_2/mol-N was achieved at the same temperature. The improved efficiency of PEI_80b is likely a product of the improved dispersion of PEI within the silica pores, facilitated by the sonication during the desorption. This would have in turn improved the accessibility of the amine sites to the CO_2. For CO_2 uptake under dry conditions, an amine efficiency of 0.5 mol-CO_2/mol-N can be expected for perfect utilization according to Reaction 1. However, even for adsorption from pure CO_2, PEI_80a only achieved an amine efficiency of 0.25 mol-CO_2/mol-N_2.[46] The low efficiencies can be explained by the fact that a substantial amount of the N atoms in branched PEI exist as tertiary amines,[58] which do not take up CO_2 according to Reaction 1. Typical efficiencies reported for PEI impregnated sorbents for DAC under dry conditions are in the range of 0.11−0.26 mol-CO_2/mol-N.[19,20,22,23,27,34,39] While an amine efficiency of 1 mol-CO_2/mol-N is theoretically possible in the presence of water, according to Reaction 2, only efficiencies up to 0.26 mol-CO_2/mol-N[23,34] have been reported. In comparison, the highest amine efficiency of PEI_80b was 0.17 mol-CO_2/mol-N, at 46 °C and a moisture level of 2% mol-H_2O.

A surface plot of the uptake capacity of PEI_80b plotted from the acquired data is depicted in Figure 8. The plot suggests that the CO_2 uptake is most favored at ∼46 °C under moderate moisture levels (1−3% mol-H_2O). The plot also suggests that the sorbent exhibits a high capacity (>1.2 mmol/g) through a broad range of moisture levels at moderately high temperatures. These results may be taken as a preliminary indication of the suitability of the sorbent for use in a wide range of climates. Warm and moderately humid climates are particularly of interest due to the high capacities (>2.15 mmol/g) exhibited at 33 °C (10 and 40% RH) and 46 °C (20 and 31% RH). However, the enhanced CO_2 capacities at high moisture levels may be accompanied by a significantly higher uptake of H_2O. This additional water uptake would in turn result in a higher energy requirement during the regeneration of the sorbent.[59] Thus, further investigations are required to determine at what humidity level the process can best be operated, such that the benefit of an enhanced CO_2 uptake is reaped without compromising the overall energy requirement of the process.

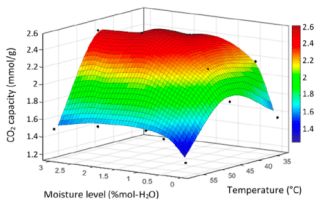

Figure 8. Surface plot of CO_2 capacity of PEI_80b as a function of temperature and moisture level for adsorption from 420 ppm of CO_2 in N_2.

4. CONCLUSION

The two PEI loaded MCF silica sorbents showed a similar trend in capacity when tested under different adsorption temperatures. PEI_80b yielded up to 55% higher uptake capacities relative to PEI_80a when compared at similar adsorption temperatures. This was attributed to the better infiltration and dispersion of the PEI polymers in the MCF pores, facilitated by the sonication of the bulk solution during the synthesis process. At temperatures above 52 °C, the uptake of CO_2 was observed to decrease as higher adsorption temperatures were used, consistent with the thermodynamics of the exothermic reaction. However, at temperatures between 33 and 46 °C, higher adsorption temperatures yielded improved uptake capacities. This was attributed to the reduction in the diffusional resistances in the sorbent, allowing better accessibility of amine sites to the CO_2. PEI_80a was observed to show negligible CO_2 uptake at 81 °C suggesting that, if adsorption were to be carried out at 46 °C, the sorbent may be effectively regenerated with only a 35 °C increase in temperature. For PEI_80b, the highest capacities were observed at a moisture level of 2% mol-H_2O at all temperatures studied. At a moisture content of 3% mol-H_2O, the CO_2 uptake appeared to be negatively affected, suggesting that the adsorbed water may be interfering with the uptake of CO_2. PEI_80b displayed a high CO_2 capacity (>1.2 mmol/g) over a broad range of temperatures and moisture levels and yielded its highest capacity of 2.52 mmol/g at 46 °C and 2% mol-H_2O. The current study did not quantify the water adsorption by the sorbent, but this will be important to determine in future work. Furthermore, given the promising adsorption performance observed for PEI_80b, future research will need to include the evaluation of suitable desorption methods and the optimization of the cycle times of the process.

■ AUTHOR INFORMATION

Corresponding Authors

*Tel.: +61 3 9905 3421; E-mail: Andrew.Hoadley@monash.edu.

*Tel.: +61 3 9905 4626; E-mail: Alan.Chaffee@monash.edu.

ORCID

Andrew F. A. Hoadley: 0000-0001-9605-6858

Alan L. Chaffee: 0000-0001-5100-6910

Notes

The authors declare no competing financial interest.

DOI: 10.1021/acs.iecr.8b04973
Ind. Eng. Chem. Res. 2019, 58, 3293−3303

■ ACKNOWLEDGMENTS

The authors acknowledge Antonio Benci and David Zuidemma, Monash Instrumentation Facility for assistance in designing and programming some of the components in the experimental setup. The authors also acknowledge Zhijian Liang for the production of the MCF and MCF-PEI powder precursors.

■ REFERENCES

(1) IPCC. *IPCC Special Report on Carbon Dioxide Capture and Storage*; Prepared by Working Group III of the Intergovernmental Panel on Climate Change; Metz, B., Davidson, O., de Coninck, H. C., Loos, M., Meyer, L. A., Eds.; Cambridge University Press: Cambridge, U.K. and New York, 2007.

(2) Keith, D. W.; Ha-Duong, M.; Stolaroff, J. K. Climate Strategy with CO_2 Capture from the Air. *Clim. Change* **2006**, *74* (1−3), 17−45.

(3) Kothandaraman, J.; Goeppert, A.; Czaun, M.; Olah, G. A.; Prakash, G. K. S. Conversion of CO_2 from Air into Methanol Using a Polyamine and a Homogeneous Ruthenium Catalyst. *J. Am. Chem. Soc.* **2016**, *138* (3), 778−781.

(4) Graves, C.; Ebbesen, S. D.; Mogensen, M.; Lackner, K. S. Sustainable hydrocarbon fuels by recycling CO_2 and H_2O with renewable or nuclear energy. *Renewable Sustainable Energy Rev.* **2011**, *15* (1), 1−23.

(5) Takeda, Y.; Okumura, S.; Tone, S.; Sasaki, I.; Minakata, S. Cyclizative Atmospheric CO_2 Fixation by Unsaturated Amines with t-BuOI Leading to Cyclic Carbamates. *Org. Lett.* **2012**, *14* (18), 4874−4877.

(6) Hou, C.-L.; Wu, Y.-S.; Jiao, Y.-Z.; Huang, J.; Wang, T.; Fang, M.-X.; Zhou, H. Integrated direct air capture and CO_2 utilization of gas fertilizer based on moisture swing adsorption. *J. Zhejiang Univ., Sci., A* **2017**, *18* (10), 819−830.

(7) Stolaroff, J. K.; Keith, D. W.; Lowry, G. V. Carbon Dioxide Capture from Atmospheric Air Using Sodium Hydroxide Spray. *Environ. Sci. Technol.* **2008**, *42* (8), 2728−2735.

(8) Zeman, F. Experimental results for capturing CO_2 from the atmosphere. *AIChE J.* **2008**, *54* (5), 1396−1399.

(9) Dubey, M. K.; Ziock, H.; Rueff, G.; Elliott, S.; Smith, W. S. Extraction of carbon dioxide from the atmosphere through engineered chemical sinkage. *Prepr. Pap. - Am. Chem. Soc., Div. Fuel Chem.* **2002**, *47* (1), 81−84.

(10) Bandi, A.; Specht, M.; Weimer, T.; Schaber, K. CO_2 recycling for hydrogen storage and transportation —Electrochemical CO_2 removal and fixation. *Energy Convers. Manage.* **1995**, *36* (6), 899−902.

(11) Baciocchi, R.; Storti, G.; Mazzotti, M. Process design and energy requirements for the capture of carbon dioxide from air. *Chem. Eng. Process.* **2006**, *45* (12), 1047−1058.

(12) Zeman, F. Energy and Material Balance of CO_2 Capture from Ambient Air. *Environ. Sci. Technol.* **2007**, *41* (21), 7558−7563.

(13) Petukhov, S. S.; Tumanov, A. I.; Trokhina, G. A. The use of synthetic zeolites in the complete removal of impurities from air. *Chem. Pet. Eng.* **1970**, *6* (1), 23−26.

(14) Kumar, A.; Madden, D. G.; Lusi, M.; Chen, K.-J.; Daniels, E. A.; Curtin, T.; Perry, J. J.; Zaworotko, M. J. Direct Air Capture of CO_2 by Physisorbent Materials. *Angew. Chem.* **2015**, *127* (48), 14580−14585.

(15) Stuckert, N. R.; Yang, R. T. CO_2 Capture from the Atmosphere and Simultaneous Concentration Using Zeolites and Amine-Grafted SBA-15. *Environ. Sci. Technol.* **2011**, *45* (23), 10257−10264.

(16) Lackner, K. S. Capture of carbon dioxide from ambient air. *Eur. Phys. J.: Spec. Top.* **2009**, *176*, 93−106.

(17) Wang, T.; Lackner, K. S.; Wright, A. Moisture Swing Sorbent for Carbon Dioxide Capture from Ambient Air. *Environ. Sci. Technol.* **2011**, *45* (15), 6670−6675.

(18) Song, J.; Liu, J.; Zhao, W.; Chen, Y.; Xiao, H.; Shi, X.; Liu, Y.; Chen, X. Quaternized Chitosan/PVA Aerogels for Reversible CO_2 Capture from Ambient Air. *Ind. Eng. Chem. Res.* **2018**, *57* (14), 4941−4948.

(19) Chaikittisilp, W.; Khunsupat, R.; Chen, T. T.; Jones, C. W. Poly(allylamine)−Mesoporous Silica Composite Materials for CO_2 Capture from Simulated Flue Gas or Ambient Air. *Ind. Eng. Chem. Res.* **2011**, *50* (24), 14203−14210.

(20) Sakwa-Novak, M. A.; Tan, S.; Jones, C. W. Role of Additives in Composite PEI/Oxide CO_2 Adsorbents: Enhancement in the Amine Efficiency of Supported PEI by PEG in CO_2 Capture from Simulated Ambient Air. *ACS Appl. Mater. Interfaces* **2015**, *7* (44), 24748−24759.

(21) Goeppert, A.; Zhang, H.; Czaun, M.; May, R. B.; Prakash, G. K. S.; Olah, G. A.; Narayanan, S. R. Easily Regenerable Solid Adsorbents Based on Polyamines for Carbon Dioxide Capture from the Air. *ChemSusChem* **2014**, *7* (5), 1386−1397.

(22) Pang, S. H.; Lee, L.-C.; Sakwa-Novak, M. A.; Lively, R. P.; Jones, C. W. Design of Aminopolymer Structure to Enhance Performance and Stability of CO_2 Sorbents: Poly(propylenimine) vs Poly(ethylenimine). *J. Am. Chem. Soc.* **2017**, *139* (10), 3627−3630.

(23) Sayari, A.; Liu, Q.; Mishra, P. Enhanced Adsorption Efficiency through Materials Design for Direct Air Capture over Supported Polyethylenimine. *ChemSusChem* **2016**, *9* (19), 2796−2803.

(24) Zerze, H.; Tipirneni, A.; McHugh, A. J. Reusable poly-(allylamine)-based solid materials for carbon dioxide capture under continuous flow of ambient air. *Sep. Sci. Technol.* **2017**, *52* (16), 2513−2522.

(25) Sakwa-Novak, M. A.; Yoo, C.-J.; Tan, S.; Rashidi, F.; Jones, C. W. Poly(ethylenimine)-Functionalized Monolithic Alumina Honeycomb Adsorbents for CO_2 Capture from Air. *ChemSusChem* **2016**, *9* (14), 1859−1868.

(26) Chaikittisilp, W.; Kim, H.-J.; Jones, C. W. Mesoporous Alumina-Supported Amines as Potential Steam-Stable Adsorbents for Capturing CO_2 from Simulated Flue Gas and Ambient Air. *Energy Fuels* **2011**, *25* (11), 5528−5537.

(27) Darunte, L. A.; Oetomo, A. D.; Walton, K. S.; Sholl, D. S.; Jones, C. W. Direct Air Capture of CO_2 Using Amine Functionalized MIL-101(Cr). *ACS Sustainable Chem. Eng.* **2016**, *4* (10), 5761−5768.

(28) McDonald, T. M.; Lee, W. R.; Mason, J. A.; Wiers, B. M.; Hong, C. S.; Long, J. R. Capture of Carbon Dioxide from Air and Flue Gas in the Alkylamine-Appended Metal−Organic Framework mmen-Mg2(dobpdc). *J. Am. Chem. Soc.* **2012**, *134* (16), 7056−7065.

(29) Sehaqui, H.; Gálvez, M. E.; Becatinni, V.; Cheng Ng, Y.; Steinfeld, A.; Zimmermann, T.; Tingaut, P. Fast and Reversible Direct CO_2 Capture from Air onto All-Polymer Nanofibrillated Cellulose—Polyethylenimine Foams. *Environ. Sci. Technol.* **2015**, *49* (5), 3167−3174.

(30) Gebald, C.; Wurzbacher, J. A.; Tingaut, P.; Zimmermann, T.; Steinfeld, A. Amine-Based Nanofibrillated Cellulose As Adsorbent for CO_2 Capture from Air. *Environ. Sci. Technol.* **2011**, *45* (20), 9101−9108.

(31) Birbara, P. J.; Nalette, T. A. A Regenerable Supported Amine-Polyol Sorbent for Carbon Dioxide Removal from Gases. Patent No. WO9413386 A1, 1994.

(32) Choi, S.; Gray, M. L.; Jones, C. W. Amine-Tethered Solid Adsorbents Coupling High Adsorption Capacity and Regenerability for CO_2 Capture From Ambient Air. *ChemSusChem* **2011**, *4* (5), 628−635.

(33) Chen, Z.; Deng, S.; Wei, H.; Wang, B.; Huang, J.; Yu, G. Polyethylenimine-Impregnated Resin for High CO_2 Adsorption: An Efficient Adsorbent for CO_2 Capture from Simulated Flue Gas and Ambient Air. *ACS Appl. Mater. Interfaces* **2013**, *5* (15), 6937−6945.

(34) Wang, J.; Wang, M.; Li, W.; Qiao, W.; Long, D.; Ling, L. Application of polyethylenimine-impregnated solid adsorbents for direct capture of low-concentration CO_2. *AIChE J.* **2015**, *61* (3), 972−980.

(35) Goeppert, A.; Meth, S.; Prakash, G. K. S.; Olah, G. A. Nanostructured silica as a support for regenerable high-capacity organoamine-based CO_2 sorbents. *Energy Environ. Sci.* **2010**, *3* (12), 1949−1960.

(36) Choi, S.; Watanabe, T.; Bae, T.-H.; Sholl, D. S.; Jones, C. W. Modification of the Mg/DOBDC MOF with Amines to Enhance CO_2

DOI: 10.1021/acs.iecr.8b04973
Ind. Eng. Chem. Res. 2019, 58, 3293−3303

Adsorption from Ultradilute Gases. *J. Phys. Chem. Lett.* **2012**, *3* (9), 1136−1141.
(37) Sanz-Pérez, E. S.; Murdock, C. R.; Didas, S. A.; Jones, C. W. Direct Capture of CO_2 from Ambient Air. *Chem. Rev.* **2016**, *116* (19), 11840−11876.
(38) Wang, J.; Huang, H.; Wang, M.; Yao, L.; Qiao, W.; Long, D.; Ling, L. Direct Capture of Low-Concentration CO_2 on Mesoporous Carbon-Supported Solid Amine Adsorbents at Ambient Temperature. *Ind. Eng. Chem. Res.* **2015**, *54* (19), 5319−5327.
(39) Goeppert, A.; Czaun, M.; May, R. B.; Prakash, G. K. S.; Olah, G. A.; Narayanan, S. R. Carbon Dioxide Capture from the Air Using a Polyamine Based Regenerable Solid Adsorbent. *J. Am. Chem. Soc.* **2011**, *133* (50), 20164−20167.
(40) Chang, A. C. C.; Chuang, S. S. C.; Gray, M.; Soong, Y. In-Situ Infrared Study of CO_2 Adsorption on SBA-15 Grafted with γ-(Aminopropyl)triethoxysilane. *Energy Fuels* **2003**, *17* (2), 468−473.
(41) Knöfel, C.; Martin, C.; Hornebecq, V.; Llewellyn, P. L. Study of Carbon Dioxide Adsorption on Mesoporous Aminopropylsilane-Functionalized Silica and Titania Combining Microcalorimetry and in Situ Infrared Spectroscopy. *J. Phys. Chem. C* **2009**, *113* (52), 21726−21734.
(42) Mebane, D. S.; Kress, J. D.; Storlie, C. B.; Fauth, D. J.; Gray, M. L.; Li, K. Transport, Zwitterions, and the Role of Water for CO_2 Adsorption in Mesoporous Silica-Supported Amine Sorbents. *J. Phys. Chem. C* **2013**, *117* (50), 26617−26627.
(43) Su, F.; Lu, C.; Chen, H.-S. Adsorption, Desorption, and Thermodynamic Studies of CO_2 with High-Amine-Loaded Multi-walled Carbon Nanotubes. *Langmuir* **2011**, *27* (13), 8090−8098.
(44) Liu, Q.; Xiong, B.; Shi, J.; Tao, M.; He, Y.; Shi, Y. Enhanced Tolerance to Flue Gas Contaminants on Carbon Dioxide Capture Using Amine-Functionalized Multiwalled Carbon Nanotubes. *Energy Fuels* **2014**, *28* (10), 6494−6501.
(45) Wurzbacher, J. A.; Gebald, C.; Steinfeld, A. Separation of CO_2 from air by temperature-vacuum swing adsorption using diamine-functionalized silica gel. *Energy Environ. Sci.* **2011**, *4* (9), 3584−3592.
(46) Knowles, G. P.; Liang, Z.; Chaffee, A. L. Shaped polyethyleneimine sorbents for CO_2 capture. *Microporous Mesoporous Mater.* **2017**, *238*, 14−18.
(47) Knowles, G. P.; Rahman, R.; Veldman, Z.; Wijesiri, R.; Yeasmin, H.; Hoadley, A.; Chaffee, A. L. *Polyethyleneimine−mesoporous silica composites for CO_2 capture from air*; Presented at The 8th International Symposium on Nanoporous Materials, Ottawa, Canada, July 9−12, 2017.
(48) Knowles, G. P.; Rahman, R.; Veldman, Z.; Negi, A.; Chaffee, A. L. Supported polyethyleneimine sorbents for CO_2 capture from air. Presented at *The 2nd Australia-Japan Symposium on Carbon Resource Utilisation, Brisbane, Australia*, Apr 15−18, 2018.
(49) Subagyono, D. J. N.; Marshall, M.; Knowles, G. P.; Chaffee, A. L. CO_2 adsorption by amine modified siliceous mesostructured cellular foam (MCF) in humidified gas. *Microporous Mesoporous Mater.* **2014**, *186*, 84−93.
(50) Schmidt-Winkel, P.; Lukens, W. W.; Yang, P.; Margolese, D. I.; Lettow, J. S.; Ying, J. Y.; Stucky, G. D. Microemulsion Templating of Siliceous Mesostructured Cellular Foams with Well-Defined Ultra-large Mesopores. *Chem. Mater.* **2000**, *12* (3), 686−696.
(51) Knowles, G. P.; Chaffee, A. L. Pelletized form of a composite material and method of producing same. Patent No. WO/2015/077835, 2015.
(52) Brunauer, S.; Emmett, P. H.; Teller, E. Adsorption of Gases in Multimolecular Layers. *J. Am. Chem. Soc.* **1938**, *60* (2), 309−319.
(53) Barrett, E. P.; Joyner, L. G.; Halenda, P. P. The Determination of Pore Volume and Area Distributions in Porous Substances. I. Computations from Nitrogen Isotherms. *J. Am. Chem. Soc.* **1951**, *73* (1), 373−380.
(54) Holewinski, A.; Sakwa-Novak, M. A.; Jones, C. W. Linking CO_2 Sorption Performance to Polymer Morphology in Aminopolymer/Silica Composites through Neutron Scattering. *J. Am. Chem. Soc.* **2015**, *137* (36), 11749−11759.
(55) Wang, X.; Song, C. Temperature-programmed desorption of CO_2 from polyethylenimine-loaded SBA-15 as molecular basket sorbents. *Catal. Today* **2012**, *194* (1), 44−52.
(56) Wang, X.; Schwartz, V.; Clark, J. C.; Ma, X.; Overbury, S. H.; Xu, X.; Song, C. Infrared Study of CO_2 Sorption over "Molecular Basket" Sorbent Consisting of Polyethylenimine-Modified Mesoporous Molecular Sieve. *J. Phys. Chem. C* **2009**, *113* (17), 7260−7268.
(57) Ma, X.; Wang, X.; Song, C. Molecular Basket" Sorbents for Separation of CO_2 and H_2S from Various Gas Streams. *J. Am. Chem. Soc.* **2009**, *131* (16), 5777−5783.
(58) Knowles, G. P. Amine functionalized ordered mesoporous silicas for the capture of post combustion flue gas CO_2 via adsorption technologies. Ph.D. Thesis, Monash University, Melbourne, Australia, 2013.
(59) Wurzbacher, J. A.; Gebald, C.; Piatkowski, N.; Steinfeld, A. Concurrent Separation of CO_2 and H_2O from Air by a Temperature-Vacuum Swing Adsorption/Desorption Cycle. *Environ. Sci. Technol.* **2012**, *46* (16), 9191−9198.

DOI: 10.1021/acs.iecr.8b04973
Ind. Eng. Chem. Res. 2019, 58, 3293−3303

3. Desorption Process for Capturing CO_2 from Air with Supported Amine Sorbent

This chapter focusses on the second research objective of the thesis: identification of a suitable method of desorbing CO_2 from solid supported amine sorbents. From the two sorbents evaluated in Chapter 2, the one which displayed a larger uptake of CO_2 (PEI_80b) was evaluated under steam assisted temperature vacuum swing desorption (S-TVSD). The chapter describes the desorption performance of the sorbent under a wide range of process conditions.

It was demonstrated that substantial CO_2 desorption could be achieved with S-TVSD under moderate vacuum levels (12 to 56 kPa abs), and relatively low temperatures (70 to 100 °C). It was observed that the lower pressures and higher temperatures made significant enhancements to the CO_2 desorption kinetics. The superiority of the steam assisted process was confirmed by the fact that S-TVSD yielded desorption kinetics which were around 16-fold faster than TVSD at the same desorption temperature and pressure. It was further identified that higher steam flow rates yielded faster desorption at the compromise of a disproportionately higher increase in the thermal energy requirement. An interesting discovery of this study was that while moisture improved the CO_2 uptake as reported in **Chapter 2**, it was observed to negatively affect the desorption performance. This was an effect of the thermal energy consumed for the desorption of the water that gets co-adsorbed on the sorbent. Finally, the desorption conditions studied were observed to cause minimal degradation to the sorbent. It was reported that after 50 cycles of adsorption/desorption which corresponded to over 1500 h of processing time, the sorbent retained 92% of its initial capacity.

In summary, the results indicated the potential of S-TVSD for use in direct air capture processes and highlighted the need to carry out a technoeconomic evaluation to better identify the preferred process conditions.

The content of this chapter has been published in *Ind. Eng. Chem. Res.*

The supporting information for this publication is included in **Appendix A(I)**. The calibration plots for the instruments used for the experimental work in **Chapter 3** are presented in **Appendix E**. The LabVIEW program used for data acquisition is presented in **Appendix F.**

I&EC research
Industrial & Engineering Chemistry Research

Article

Cite This: *Ind. Eng. Chem. Res.* XXXX, XXX, XXX−XXX

pubs.acs.org/IECR

Desorption Process for Capturing CO_2 from Air with Supported Amine Sorbent

Romesh P. Wijesiri,[†,‡] Gregory P. Knowles,[‡] Hasina Yeasmin,[†] Andrew F. A. Hoadley,*[,†] and Alan L. Chaffee*[,‡]

[†]Department of Chemical Engineering, Monash University, Wellington Road, Clayton, Victoria 3800, Australia
[‡]School of Chemistry, Monash University, Wellington Road, Clayton, Victoria 3800, Australia

Supporting Information

ABSTRACT: A polyethylenimine impregnated silica sorbent was evaluated for steam-assisted temperature vacuum swing desorption (TVSD) of CO_2, adsorbed from 420 ppm of CO_2 in N_2. Results indicate that essentially all the CO_2 could be desorbed under mild vacuum levels (12−56 kPa abs) and temperatures (70−100 °C). The fastest average desorption rate (3.75 mmol/g/h) was observed at 12 kPa abs/100 °C at a steam flow rate of 6.2 g/h. In comparison, conventional TVSD under the same conditions only produced an average desorption rate of 0.23 mmol/g/h, confirming the superior kinetics of the steam-assisted process. When adsorption was carried out under humid conditions (1 and 2% mol-H_2O), the co-adsorbed water on the sorbent was observed to slow down the desorption of CO_2, due to the additional energy consumed for the desorption of water. The sorbent displayed excellent stability under the conditions studied, losing only 8% of its capacity after 50 cycles (>1500 h).

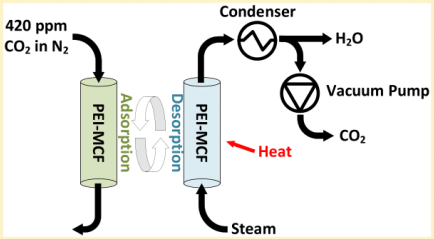

1. INTRODUCTION

Capturing CO_2 directly from air, also known as direct air capture (DAC), is a potential method of compensating for diffuse emissions, which account for close to 50%[1] of the anthropogenic CO_2 released. The captured CO_2 can either be sequestered or utilized as a feed gas to greenhouses[2] or for production of synthetic fuels[3,4] and chemical intermediates.[5] Technologies assessed for DAC include absorption with aqueous hydroxide solutions[6−9] and adsorption with zeolites,[10−12] ion-exchange resin,[13] and solid supported amines (SSA).[14−28] There has been a growing interest in SSAs due to their high uptake capacity and the possibility of regeneration under relatively mild conditions. Additionally, these sorbents have been reported to display enhanced CO_2 uptake capacities when adsorbing in the presence of moisture, which is typically present in air.[16,22,26−28] SSAs are a group of sorbents made of various amines, physically or chemically supported on solid materials. Amines such as polyethylenimine,[14−17,26−30] polypropylenimine,[15] and polyallylamine[18,19] have been loaded onto porous materials such as silica,[14−16,18,19,25,26,28] carbon,[27,31] alumina,[17,24] metal organic frameworks,[20,21] and cellulose.[22,23] The studies on SSA for DAC have largely focused on the development of high-capacity adsorbents, but there has been limited attention given to the development of effective desorption technologies, which are also critical for successful DAC applications. Various desorption technologies have been evaluated for CO_2 capture applications with SSAs. These studies have been undertaken with a variety of sorbents and different desorption conditions, making it difficult to make direct comparisons. To facilitate this, the process conditions of several studies have been summarized in Table 1, where the CO_2 purity and the average desorption rate achieved are noted.

Temperature concentration swing desorption (TCSD)[14,21,27,29,32−37] has been the most widely studied desorption technology. For TCSD, the sorbent is heated and purged with an inert gas to desorb the CO_2. While fast desorption can be achieved, the desorbed CO_2 is produced in a dilute form due to the purge gas. It has been reported that higher desorption temperatures increased both the rate of desorption[14,29,32,35,37] and the concentration of CO_2 in the desorbed product.[14,32] Increasing the flow rate of the purge gas was also reported to increase the rate of desorption, although no effect on the CO_2 concentration was observed.[14] Alternatively, TCSD with a CO_2 purge has been evaluated to desorb CO_2 as a high-purity product, at the expense of a slower desorption rate.[21,34] This poor desorption rate exhibited with the CO_2 purge has been attributed to the significantly higher partial pressure of CO_2 around the sorbent and hence the smaller driving force for desorption.[34] In addition to the slower kinetics of this approach, SSAs reportedly undergo degradation when exposed to high CO_2 concentration atmospheres at elevated temperatures. This has been attributed to the formation of urea linkages.[38−43] However, this type of

Received: June 10, 2019
Revised: July 23, 2019
Accepted: August 5, 2019
Published: August 5, 2019

Table 1. Summary of the Desorption Technologies Evaluated for CO_2 Capture with SSA[a]

				desorption conditions				
ref	type	sorbent[b]	adsorption from	T (°C)	P (kPa abs)[c]	purge gas[d]	average desorption rate[e] (mmol/g/h)	purity (% mol)
14	TCSD	amine/silica (3 g)	air (400−420 ppm of CO_2)	100		335 (N_2)	5.01	10
21	TCSD	amine/MOF (0.09 g)	15% CO_2 in N_2	120		25 (N_2)	10.08	unspecified
	TCSD−CO_2 purge	amine/MOF (0.09 g)	15% CO_2 in N_2	150		25 (CO_2)	4.32	unspecified
27	TCSD	amine/carbon (0.5 g)	5000 ppm of CO_2 in N_2	110		50 (N_2)	5.89	22
32	TCSD	amine/HP2MGL resin (1 g)	5000 ppm of CO_2 in N_2	100		50 (N_2)	3.99	19
33	TCSD	amine/silica (1000 g)	air (394 ppm of CO_2)	130		8000 (9% H_2O/N_2)	0.83	6
35	TCSD	amine/polystyrene (19 g)	45% CO_2 in N_2	100		226 (N_2)	5.00	unspecified
	TVSD	amine/polystyrene (19 g)	45% CO_2 in N_2	100	10		4.20	unspecified
36	TCSD	amine/silica (23 g)	air (400−440 ppm of CO_2)	90		800 (Ar)	0.20	unspecified
	TVSD	amine/silica (23 g)	air (400−440 ppm of CO_2)	90	1		0.15	96
37	TCSD	amine/silica (1 g)	5% CO_2 in N_2	150		50 (N_2)	0.97	unspecified
	TVSD	amine/silica (1 g)	5% CO_2 in N_2	150	10		0.96	unspecified
	TVSD−inert gas purge	amine/silica (1 g)	5% CO_2 in N_2	150	10	50 (N_2)	0.98	unspecified
46	TVSD	amine/cellulose (10 g)	air (400−510 ppm of CO_2 at 80% RH)	95	5		0.65	94−97
47	S-TVSD	unspecified SSA (40 g)	air (40% RH)	100	20	2.5 (steam)	1.35	unspecified
	TVSD	unspecified SSA (40 g)	air (40% RH)	100	20		0.41	unspecified
48	TVSD	amine/cellulose-silica (unspecified)	380 ppm of CO_2/397 ppm of He in N_2	90	0.06−0.7		1.86	98
49	steam stripping	amine/silica (1 g)	10% CO_2 in N_2	110		unspecified (90% H_2O/N_2)	13.86	75
50	steam stripping	amine/silica (2 g)	CO_2 in N_2 (unspecified concentration)	103		72 (steam)	12.47	unspecified
51	steam stripping	amine/silica (1 g)	10% CO_2 in He	105		unspecified (90% H_2O/He)	17.45	75

[a]The data presented here are the desorption conditions with highest average desorption rates reported in the respective studies. [b]Sample mass studied is indicated within parentheses. [c]Desorption pressure for cases where a vacuum was used. [d]Purge gas flow rate in g/h for steam and in mL/min for the rest. The gas used is indicated within parentheses. [e]Average desorption rate calculated as the total desorbed amount divided by the total desorption time.

degradation can be inhibited[41,43−45] or even reversed[39] in the presence of moisture.

Another technology that can be used to desorb CO_2 is vacuum swing desorption (VSD). In this process, the desorption is achieved by applying a vacuum on the sorbent, after the adsorption stage and at the same temperature. This would likely be unsuitable for DAC, as the CO_2 is adsorbed from air, at a partial pressure of ∼0.04 kPa abs. To achieve desorption, the sorbent would need to be evacuated to below this pressure, requiring very large vacuum pumps and, hence, relatively large capital costs for equipment and high-energy requirements.

Alternatively, temperature vacuum swing desorption (TVSD) can be used to avoid the need for high vacuum levels (<0.04 kPa abs) for DAC application. In this type of process, desorption is achieved by applying milder vacuum levels and simultaneously heating the sorbent.[30,35−37,46−48] As no inert gas purge is used, the product gas mainly consists of the adsorbed species (typically CO_2 and H_2O), and the desorbed CO_2 could be obtained at higher concentration. However, while desorption of high-purity CO_2 is made possible with TVSD, it has been reported to produce slower desorption than TCSD with an inert purge gas.[35−37] It has further been identified that for these processes, higher temperatures[30,35−37] and lower pressures[36] led to improved desorption kinetics. Wurzbacher et al.[36,46] evaluated the desorption performance under TVSD when the CO_2 was adsorbed from humid air (20−80% RH). It was observed that while the presence of moisture enhanced the uptake of CO_2, it also resulted in a disproportionately higher uptake of H_2O. This additional uptake of water would in turn result in a higher thermal energy requirement during the regeneration of the sorbent. It was reported that the thermal energy requirement was 30% higher, when CO_2 was adsorbed from air at 80% RH, in comparison to that at 20% RH.[36]

As an alternative approach for desorbing high-purity CO_2, TCSD with steam as a purge gas, also known as steam stripping, has been evaluated.[49−51] As the water in the desorbed product can easily be condensed, CO_2 could be obtained at high purity. In comparison to TCSD with an inert gas, steam stripping showed faster desorption kinetics.[49,51] The authors suggested that this accelerated desorption was a result of the water molecules interacting with the amine sites and displacing the CO_2 adsorbed on these sites. Sandhu et al.[49] reported that the adsorption of water by the sorbent, during steam stripping, released a significant amount of heat, which increased the sorbent temperature by as much as 12 °C.[49] It is possible that this heat generation helped to accelerate the process by increasing the amount of energy available to be utilized for CO_2 desorption, which is endothermic in nature.

DOI: 10.1021/acs.iecr.9b03140
Ind. Eng. Chem. Res. XXXX, XXX, XXX−XXX

As an added advantage of steam stripping, the presence of moisture could be expected to stabilize the sorbent from CO_2 induced degradation. Indeed, Sandhu et al.[49] reported that steam stripping resulted in a 2% loss in the cyclic capacity for a PEI impregnated silica, in comparison to the 6% loss observed with a N_2 purge. Hammache et al.[51] reported no degradation of the amines, negligible leaching, and minimal changes to the structure of the silica sorbent, for desorption with steam stripping at 105 °C, for a PEI functionalized silica sorbent. In contrast, Chaikittisilp et al.[24] reported an 81% reduction in capacity for a PEI loaded SBA-15 sorbent, after steam exposure at 105 °C. It was suggested that this was likely caused by the collapse of the mesostructure. An alumina support, evaluated in the same study showed better stability, losing only 25% of its capacity.

Steam-assisted temperature vacuum swing desorption (S-TVSD) is a hybrid approach.[47] In addition to applying a vacuum and heating the sorbent, a steam purge is used to sweep the desorbed CO_2 from the atmosphere surrounding the sorbent. The sweeping effect lowers the partial pressure of CO_2 below that which could be achieved with pure TVSD, providing a larger driving force for desorption. Additionally, as the process operates under a vacuum, the steam could be produced at lower temperatures (<100 °C). We note that since the steam can be produced at low temperatures, solar thermal energy or waste heat might be used to supply this. The benefit of having a purge gas during TVSD has been demonstrated by Serna-Guerrero et al.,[37] where using a N_2 purge improved the average desorption rate at 70 °C by a factor of ∼3.1. Similarly, Fujiki et al.[52] demonstrated that the use of a steam purge resulted in ∼2-fold faster desorption rates for a VSD process.

In their patent, Gebald et al.[47] described the use of S-TVSD with an amine functionalized sorbent for DAC. They observed that lower pressures combined with higher temperatures yielded higher desorption rates. Gebald et al.[47] also pointed out that while higher steam flow rates led to faster desorption, it would also negatively affect the economics of the process. The preferred steam rate was suggested to be less than 0.1−0.2 kg/h per kg of sorbent. The patent described a two-stage desorption process, which uses TVSD to desorb about half of the CO_2, followed by S-TVSD to desorb the remaining CO_2. At 20 kPa abs/100 °C, the S-TVSD stage (2.5 g/h of steam) was observed to be ∼2.7 times faster, in comparison to the pure TSVD stage. The patent[47] also presented the results of cyclic testing which showed a 13% loss in capacity after 200 cycles of adsorption/desorption.

Our group had previously demonstrated[41,42,53] that branched PEI loaded mesocellular foam (MCF) silica is highly prospective for postcombustion capture applications. Subsequently, two MCF-PEI sorbents, PEI_80a and PEI_80b, were evaluated for adsorption behavior under DAC conditions.[26] The evaluation of the capture performance of the sorbents concluded that both sorbents achieved the highest CO_2 uptake (1.29 mmol/g for PEI_80a and 1.94 mmol/g for PEI_80b) at moderate temperatures (46−52 °C). PEI_80a showed negligible CO_2 uptake at 81 °C suggesting that the sorbent may be effectively regenerated at relatively low temperatures. The presence of low moisture levels (0.5 and 2% mol-H_2O) was seen to enhance the uptake of CO_2 by PEI_80b, when compared to dry conditions. The highest CO_2 capacity of 2.53 mmol/g, was observed at 46 °C with 2% mol-H_2O in the feed gas stream. However, a higher moisture level (3% mol-H_2O) was seen to be detrimental to the uptake of CO_2, by PEI_80b.

Considering the promising adsorption performance by PEI_80b, the current study endeavors to evaluate the sorbent under suitable desorption conditions. S-TVSD was chosen as the technology of interest due to the faster kinetics offered under mild vacuum levels, the possibility of desorbing the CO_2 at high purity, and the improved stability of the sorbent in wet atmospheres. As discussed above, process conditions such as desorption temperature, desorption pressure, and the flow rate of the purge gas (steam for S-TVSD) have been reported to have a significant effect on the desorption performance of CO_2 by SSAs. Furthermore, while moisture was reported to be beneficial for the uptake of CO_2 by PEI_80b during the adsorption stage,[26] studies[36,46] have indicated that the co-adsorbed water may be detrimental to the desorption stage of the process. This study aimed to delineate the relative importance of these various factors in influencing the CO_2 desorption behavior from the MCF-PEI sorbent when used for DAC. Furthermore, it compares the desorption performance for S-TVSD to that of TVSD and TVSD with a N_2 purge.

2. EXPERIMENTAL SECTION

2.1. Material Synthesis and Characterization. Pellets of mesocellular foam (MCF), silica impregnated with an 80% pore volume equivalent of branched PEI (average molecular weight 1200 MW), were produced according to the synthesis method detailed in Wijesiri et al.[26] The results of the material characterization experiments (true density, BET surface area, mesopore volume, and elemental analysis) are also presented in the same publication.

2.2. Experimental Procedure. The experimental setup used to study the adsorption/desorption of CO_2 by the sorbent is depicted in Figure 1. PEI_80b pellets (3.45 g), of an approximate Sauter mean diameter of 1.8 mm, were packed in a glass column (120 mm length × 10 mm i.d.). The bed was contained by 1 cm thick glass wool plugs at each end and terminated with Swagelok fittings. The void fraction of the bed was previously calculated to be 0.54.[26] The experiments were carried out in three stages: adsorption, desorption, and regeneration as depicted in Figure 2.

2.2.1. Adsorption. The oven was set to the desired adsorption temperature. A set of Bronkhorst mass flow controllers was used to blend together N_2 and a custom gas mix of 1000 ppm of CO_2 in N_2 (from Air Liquide) to produce a gas mixture of 420 ppm of CO_2 in N_2 at a flow rate of 200 mL/min. The gas mixture was humidified, when necessary, by passing a portion of it through a gas bubbler filled with deionized water and placed in a temperature-controlled water bath (at 25 °C). The wet gas lines were heated to 30 °C to prevent condensation using HTS/Amptek heat tape. The feed gas prepared was directed through the adsorbent bed. The exhaust gas from the bed was passed through a condenser to knock out any residual water and finally through a 0−1000 ppm Edinburgh Sensors Gascard NG nondispersive infrared CO_2 sensor (±20 ppm accuracy) to measure the CO_2 concentration. Two Vaisala HMP110 RH probes (±1.5% RH accuracy) were used to measure the temperature and relative humidity of the feed gas and the exhaust gas. Type T thermocouples (±1 °C accuracy) placed at the midpoint of the bed and immediately outside the bed were used to measure the bed and oven temperature, respectively.

DOI: 10.1021/acs.iecr.9b03140
Ind. Eng. Chem. Res. XXXX, XXX, XXX−XXX

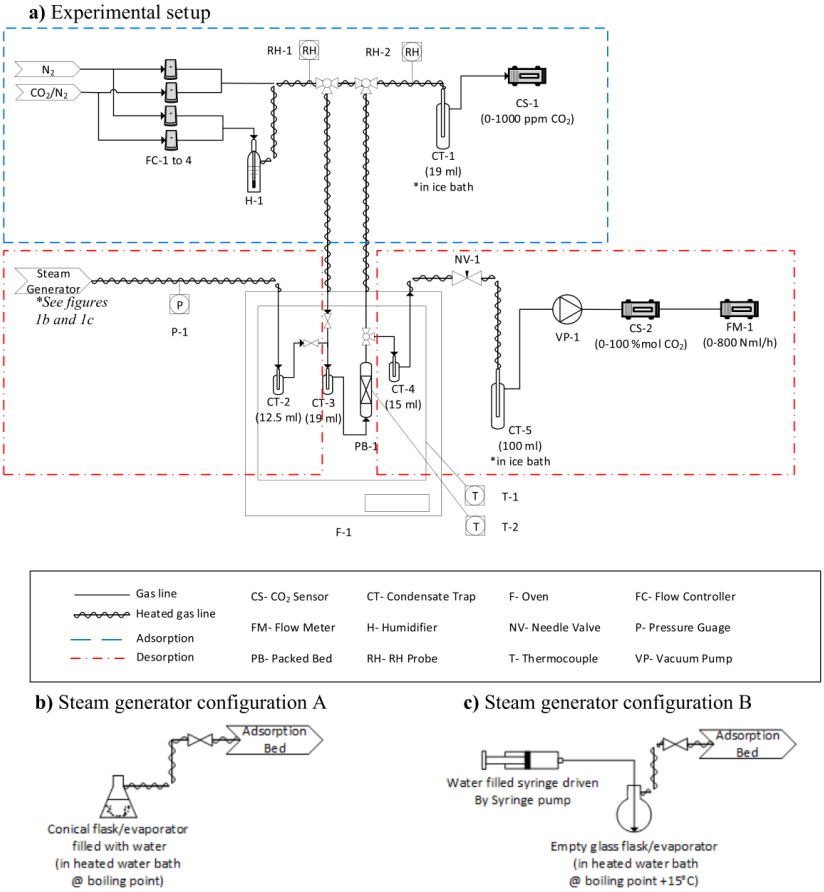

Figure 1. (a) Experimental setup used for studying the adsorption/desorption of CO_2 by PEI_80b, (b) steam generator configuration A, and (c) steam generator configuration B. For TVSD, this step was ignored.

The adsorption of CO_2 and water at a particular time were calculated according to eqs 1 and 2, respectively, where q_{ads} is the amount of CO_2 or H_2O adsorbed (mmol/g), m is the mass of sorbent (g) in the bed, and t_a is the adsorption time (h). C_f and C_e are the concentrations (mmol/mmol) in the feed gas to and the exhaust gas from the bed, respectively. $\dot{n}_f$ is the flow rate of the feed gas (mmol/h), which was assumed to be the same as that of the exhaust gas, as the adsorbates, CO_2 and H_2O, were present in low concentrations (0.042% and 1−2%, respectively). Moreover, the adsorption of H_2O was very fast, and the H_2O content in the exhaust gas increased back to its feed concentration within ∼10% of the total adsorption time. Thus, while there was a slight difference in the molar flow rate for the initial period of the adsorption, this results in a negligible difference to the calculated integral and has been ignored.

$$q_{\mathrm{ads,CO_2}} = \int_0^{t_a} \frac{\dot{n}_f (C_{f,CO_2} - C_{e,CO_2})}{m} \, dt_a \quad (1)$$

$$q_{\mathrm{ads,H_2O}} = \int_0^{t_a} \frac{\dot{n}_f (C_{f,H_2O} - C_{e,H_2O})}{m} \, dt_a \quad (2)$$

The feed and exhaust concentrations of H_2O (C_{f,H_2O} and C_{e,H_2O}) were calculated according to eq 3, where RH is the relative humidity (%) as measured by the RH probes, p_{sat,H_2O} is the saturation vapor pressure of water (kPa abs) at the respective temperature, and P is the total pressure of the gas (kPa abs).

$$C_{H_2O} = \mathrm{RH} \times \frac{p_{sat,H_2O}}{P} \quad (3)$$

The saturation vapor pressure (p_{sat,H_2O}) was calculated according to the Antoine correlation (eq 4) for water, where

DOI: 10.1021/acs.iecr.9b03140
Ind. Eng. Chem. Res. XXXX, XXX, XXX−XXX

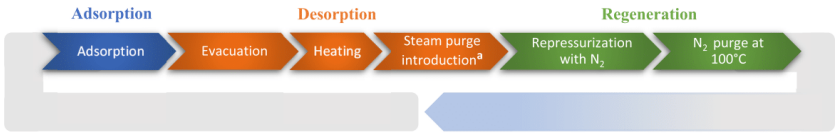

[a]*For TVSD, this step was ignored. For N_2 assisted TVSD, a N_2 purge was used*

Figure 2. Flow diagram of the experimental procedure used.

T_g is the temperature of the gas (°C) as measured by the RH probes.

$$p_{sat,H_2O} = 10^{8.07131-\frac{1730.63}{233.426+T_g}} \quad \text{for } 1\ °C \le T \le 100\ °C \tag{4}$$

For each experiment, adsorption was carried out at 46 °C until 1.66 ± 0.05 mmol/g of CO_2 was adsorbed by the PEI_80b pellets.

2.2.2. Desorption. Upon completion of the adsorption stage, the bed was switched from the adsorption system to the desorption system (refer to Figure 1a), using an arrangement of valves in the gas lines inside the oven. The system was evacuated with the vacuum pump, and the pressure was monitored using the vacuum pressure gauge. Depending on the desorption pressure chosen, one of the following three vacuum pumps were selected: KNF N86 (12 kPa abs), KNF NMP830 (26 kPa abs), or KNF NMP05 (56 kPa abs). The CO_2 concentration in the exhaust gas from the vacuum pump was measured using a Gas Sensing Solutions Sprint IR6S 0−100% CO_2 sensor (accuracy, ±5% reading). The gas flow rate of the exhaust gas was measured using a Bioprocess Control μFlow 0−800 N mL/h flow meter (accuracy, ±5% reading). The oven was set to the desorption temperature, and the gas lines during desorption runs were heated to above the dew point temperature of steam to prevent the condensation of steam. The temperatures of the adsorbent bed and the oven were monitored using type T thermocouples. Once the bed reached the dew point temperature of water (at the respective desorption pressure), steam was introduced through the bed by opening the valve in the steam generator system. The corresponding dew (or boiling) point temperatures were calculated as 50 °C (12 kPa abs), 66 °C (26 kPa abs), and 85 °C (56 kPa abs). The exhaust gas from the bed was passed through a condenser, to condense and collect the water, after which the exhaust gas was recompressed via the vacuum pump. Condensate traps were connected upstream and downstream of the adsorbent bed, as a precaution, to prevent the sorbent from coming into contact with liquid water.

Two configurations of steam generators were used depending on the desired rate of steam generation. Configuration A (Figure 1b) was used for a steam generation rate of 6.4 ± 1.2 g/h, where a conical flask filled with deionized water was placed in a temperature-controlled water bath heated to the boiling point temperature of water. The steam boiling off the liquid was sucked into the desorption system through the vacuum lines. The steam flow rate was calculated by measuring the difference in the weight of the conical flask, before and after the experiment. It was assumed that the evaporation rate was constant throughout the experiment.

Configuration B (Figure 1c) was used for steam generation rates of ≤1.5 g/h. In this case, water was delivered using a 5 mL glass syringe, driven by a New Era NE-300 syringe pump, to a small glass vessel. The glass vessel was heated to 15 °C higher than the boiling point temperature, using the heated water bath, to ensure rapid evaporation of water. Similar to configuration A, the steam generated was sucked into the desorption system using the vacuum lines. The flow rate of steam was controlled by adjusting the rate of delivery of water by the syringe pump.

For the pure TVSD experiment, the same procedure was used, with the exception that the steam generator was turned off. For the N_2 assisted TVSD experiment, instead of the steam generator, the desorption system was connected to a N_2 gas supply, via a Bronkhorst mass flow controller.

The CO_2 desorption capacity of PEI_80b was calculated according to eq 5, where q_{des} is the amount of CO_2 desorbed(mmol/g), $\dot{n}_e$ is the flow rate of the exhaust gas (mmol/h), m is the mass of sorbent (g) in the bed, and t_d is desorption time (h). C_{e,CO_2} is the concentration of CO_2 (mmol/mmol) in the exhaust gas from the bed.

$$q_{des,CO_2} = \int_0^{t_d} \frac{\dot{n}_e C_{e,CO_2}}{m}\, dt_d \tag{5}$$

The average desorption rate was calculated according to eq 6.

$$\text{average desorption rate (mmol/g/h)} = \frac{\text{total amount of desorbed } CO_2 \left(\frac{\text{mmol}}{\text{g}}\right)}{\text{total time for desorption (h)}} \tag{6}$$

2.2.3. Regeneration. After the end of the desorption experiment, the vacuum pump was turned off and the system was repressurized with N_2. The bed was switched back to the adsorption system (see Figure 1a). The sorbent bed was regenerated by heating to 100 °C and purging with 190 mL/min of N_2 to remove any residual H_2O and CO_2. The amount of CO_2 and H_2O left on the sorbent, after the desorption stage was quantified by measuring the CO_2 concentration and the relative humidity of the exhaust gas, during the regeneration step, using the 0−1000 ppm of CO_2 sensor and the exhaust RH probe, respectively. Thereafter, the residual amounts of CO_2 and H_2O were calculated according to eqs 1−4. The residual amount of CO_2 was indicative of the extent of desorption, while the residual amount of H_2O was taken as the equilibrium amount of water adsorbed by the sorbent under the desorption conditions employed.

2.3. Measurement of the Leak Rate in the Experimental Setup under Vacuum. The experimental setup, with a clean bed (no adsorbed CO_2/H_2O) and with the steam inlet closed off, was evacuated to 12 kPa abs using the KNF N86 vacuum pump. The setup was left under vacuum for 90 min, and the gas flow rate out of the vacuum pump was measured using the flow meter (FM-1). A gas leak of 35 ± 4 N mL/h was recorded, indicating that there were one or more

DOI: 10.1021/acs.iecr.9b03140
Ind. Eng. Chem. Res. XXXX, XXX, XXX−XXX

small leaks in the system. However, the readings from the vacuum pressure gauge (P-1) confirmed that the final pressure of 12 kPa abs was achieved and that the leaks were not significant enough to prevent the evacuation of the system to the desired pressure.

2.4. Effect of the Void Volume in the Desorption System. This void volume in the desorption system was calculated to be 146.5 mL for the four condensate traps and 29 mL for the connecting tubing (see Figure 1). It was suspected that this may cause a lag in the CO_2 desorption profiles. To validate this, the experiment at 26 kPa abs/100 °C with 0.5 g/h steam flow rate was repeated after removing the condensate traps inside the oven (CT-2,3,4) and replacing CT-4 with a 12.5 mL condensate trap filled with 2 mm glass beads.

2.5. Calculation of the Thermal Energy Requirement for Steam Production. The amount of thermal energy required to produce steam for the desorption of CO_2 was calculated according to eq 7, where E_{steam} is the thermal energy requirement (J/g), $\dot{m}_{steam}$ is the steam flow rate (g/h), t_d is the desorption time (h), C_p is the specific heat capacity (J/g °C), H_{lat} is the latent heat of vaporization (J/g), and m_{CO_2} is the mass of CO_2 desorbed (g). T_{boil}, T_{in} and T_d are the boiling point temperature (°C), initial temperature of water (°C), and the desorption temperature (°C). The initial temperature of water was assumed to be 25 °C. The C_p of water and steam were assumed to be constant at 4.2 J/g °C and 2.0 J/g °C, respectively. H_{lat} was 2384 J/g at 12 kPa abs and 2188 J/g at 26 kPa abs. E_{steam} was converted to a GJ/t basis for presentation in this paper.

$$E_{steam} = \frac{\dot{m}_{steam} t_d (C_{p,water}(T_{boil} - T_{in}) + H_{lat} + C_{p,steam}(T_d - T_{boil}))}{m_{CO_2}} \quad (7)$$

3. RESULTS

The amounts of CO_2 adsorbed and desorbed and the residual amount in the sorbent after the experiment for different desorption pressures and temperatures at a steam flow rate of 6.4 ± 1.2 g/h are depicted in Figure 3. In the figure, the total height of the bar represents the adsorbed amount. The "residual amount" refers to the CO_2 left over on the sorbent after the S-TVSD step, as quantified during the regeneration step (see section 2.2.3). For most cases, negligible amounts of residual CO_2 (≤0.01 mmol/g) were measured, indicating that essentially all the adsorbed CO_2 was released during the desorption at the conditions studied here. The only exception to this were the runs at 56 kPa abs/100 °C and at 26 kPa abs/80 °C, where 0.04 mmol/g (~2% of adsorbed amount) of CO_2 was left over after the desorption, in each case. "Discrepancy" refers to the difference between the adsorbed amount and the sum of the desorbed and residual amounts of CO_2.

The CO_2 desorption profiles and bed temperature profiles at different desorption pressures and temperatures are depicted in Figure 4. The steam was introduced after the bed temperature reached the dew point temperature at the respective desorption pressure (50 °C for 12 kPa abs, 66 °C for 26 kPa abs, and 85 °C for 56 kPa abs). Under all conditions, rapid desorption was observed initially. At lower desorption temperatures and higher pressures, the desorption rate was seen to decay much faster, leading to longer desorption times.

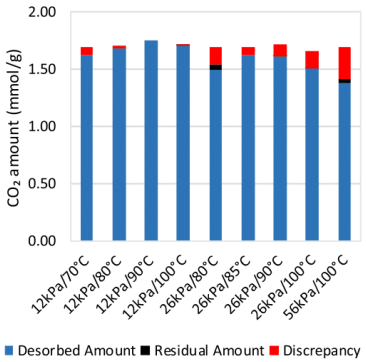

Figure 3. Amounts of CO_2 adsorbed and desorbed and the residual CO_2 in the sorbent after the experiment for different desorption pressures and temperatures at a steam flow rate of 6.4 ± 1.2 g/h. The adsorbed amount is represented by the total height of the bar.

During each desorption experiment, a sharp increase in the bed temperature was observed immediately after the introduction of steam. Except for the 90 and 100 °C runs at 12 kPa abs, the bed temperature was momentarily seen to overshoot the temperature of the oven containing the bed. Following the initial increase in temperature, the bed temperature was then observed to fall back toward the oven temperature.

The CO_2 desorption profiles and bed temperature profiles for different steam flow rates at 12 kPa abs/100 °C and 26 kPa abs/100 °C are depicted in Figure 5. It was observed that lower steam flow rates resulted in longer desorption times. Moreover, when using lower steam flow rates, there appeared to be a lag between ~~the~~ when steam is introduced and when desorption starts. When comparing the temperature profiles, the dips in the bed temperatures were seen to be shallower and longer lasting for the experiments with lower steam flow rates.

This lag in CO_2 desorption observed for lower flow rates was suspected to be due to the residence time for the desorbed gas to reach the CO_2 sensor, due to the void volume present in the desorption system. To validate this, the experiment at 26 kPa abs/100 °C with 0.5 g/h steam flow rate was repeated ~~with~~ after reducing the void volume, as described in section 2.4. As shown in Figure S1 in the Supporting Information, this significantly reduced the lag before desorption started.

The equilibrium amount of water adsorbed on the sorbent under different temperatures and pressures were calculated as outlined in section 2.2.3 and are plotted in Figure 6. Higher pressures and lower temperatures were observed to result in larger amounts of water adsorption.

It is critical that DAC systems are resilient to the moisture that is to some extent always present in air. We previously demonstrated that during the adsorption stage, moisture contents of 0.5 to 2% mol-H_2O in the feed gas yielded up to 53% enhancements to the CO_2 uptake by PEI_80b.[26] To evaluate the effect of adsorption under wet conditions on the desorption performance, the adsorption experiment (at 46 °C) was also carried out from 420 ppm of CO_2 in N_2 at moisture contents of 1 and 2% mol-H_2O. The corresponding amounts of H_2O adsorbed on the sorbent before desorption (referred to from here onward as preadsorbed water) were calculated as 2.1

DOI: 10.1021/acs.iecr.9b03140
Ind. Eng. Chem. Res. XXXX, XXX, XXX−XXX

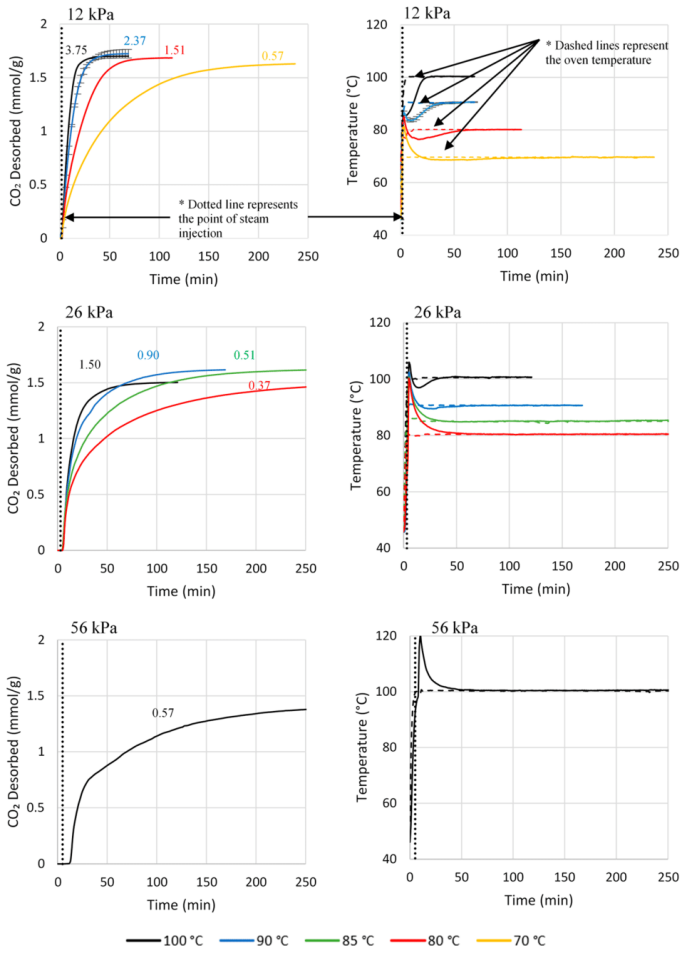

Figure 4. CO_2 desorption (left-hand side) and bed temperature (right-hand side) for S-TVSD at pressures of 12 kPa abs, 26 kPa abs, and 56 kPa abs at a steam flow rate of 6.4 ± 1.2 g/h. The average desorption rate (mmol/g/h) for each run is denoted in text next to the data sets. Error bars included for the 12 kPa abs/90 °C data are based on duplicate runs. The error is assumed to be similar for the other data sets.

mmol/g and 5.4 mmol/g, respectively. The desorption was carried out at 26 kPa abs/100 °C and a steam flow rate of 1.5 g/h.

The bed temperature profiles (see Figure 7) for the experiments with preadsorbed water on the sorbent were seen to lag behind that of the experiment with the dry sorbent. This deviation in temperature was more prominent as the amount of preadsorbed water was increased from 2.1 mmol/g to 5.4 mmol/g. It was also observed that the CO_2 desorption rate was initially slower when there was preadsorbed water.

The CO_2 adsorption capacity of the sorbent over 50 cycles is plotted in Figure 8. The data presented represents the adsorption at 46 °C from dry 420 ppm of CO_2 in N_2. The desorption for these cycles was carried out at varying pressures (12−56 kPa abs), temperatures (70−100 °C), and steam flow rates (0.3−9 g/h). The capacities after 29.5 h of adsorption at the same condition was used for this comparison. The missing bars in the plot are experiments where adsorption was carried out under different adsorption conditions or where the data acquisition system failed. In comparison to the 1.69 mmol/g of CO_2 that was adsorbed in the first experiment, the 50th experiment only yielded a capacity of 1.56 mmol/g. This translates to an 8% loss in capacity over the 50 cycles (>1500 h). It can be noted that the capacity appeared to be relatively stable up until about 30 cycles. Following this, the loss of capacity appeared to accelerate.

Desorption of CO_2 under two other desorption technologies was also carried out to make comparisons with S-TVSD. First, a pure TVSD experiment at 12 kPa abs/100 °C was done to evaluate the effect of using a steam-aided process. Next, TVSD

DOI: 10.1021/acs.iecr.9b03140
Ind. Eng. Chem. Res. XXXX, XXX, XXX−XXX

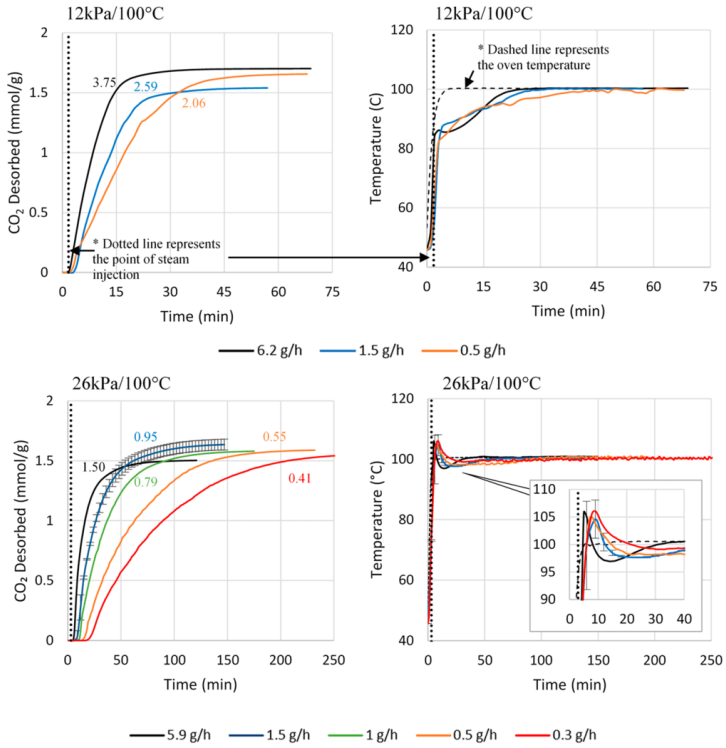

Figure 5. CO_2 desorption (left-hand side) and bed temperature (right-hand side) for S-TVSD at 12 kPa abs/100 °C and 26 kPa abs/100 °C under different steam flow rates. The average desorption rate (mmol/g/h) for each run is denoted in text next to the data sets. Error bars included for the 1.5 g/h data at 26 kPa abs/100 °C are based on duplicate runs. The error is assumed to be similar for the other data sets.

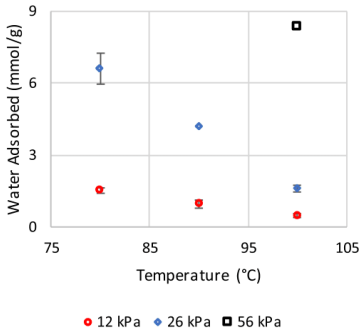

Figure 6. Equilibrium amounts of water adsorbed on the sorbent under the various desorption pressures and temperatures. Error bars presented are based on replicated experiments.

with a 162 mL/min N_2 purge at 26 kPa abs/90 °C was done to determine if the promoting effect on the desorption was due to the interaction of water with the amine sites, as suggested by other studies,[49,51] or simply due to the sweeping effect of the purge gas.

When compared to pure TVSD at 12 kPa abs/100 °C, S-TVSD with a steam flow rate of 6.4 g/h showed significantly faster desorption of CO_2 (see Figure 9). Furthermore, it can be noted that even the S-TVSD case with the weakest vacuum (56 kPa abs) outperformed TVSD (12 kPa abs) at 100 °C. This confirms the superiority of the desorption kinetics offered by the S-TVSD, in comparison to conventional TVSD. In comparison to TVSD assisted by a N_2 purge, it was observed that while the initial desorption rate of CO_2 was similar in S-TVSD, the rate decayed much faster leading to a longer desorption time.

4. DISCUSSION

4.1. Effect of Desorption Pressure, Temperature, and Steam Flow Rate. As depicted in Figure 3, negligible amounts of residual CO_2 (≤0.01 mmol/g) were measured for most desorption pressures and temperatures, indicating that essentially complete desorption of CO_2 had taken place. It is likely that the residual 0.04 mmol/g of CO_2 measured for 56 kPa abs/100 °C and 26 kPa abs/80 °C would also have been removed if the desorption had been continued for longer. The discrepancy between the adsorbed amount of CO_2 and the desorbed amount of CO_2 was attributed to two factors. First, there was a brief period (1−4 min) at the start of the

DOI: 10.1021/acs.iecr.9b03140
Ind. Eng. Chem. Res. XXXX, XXX, XXX−XXX

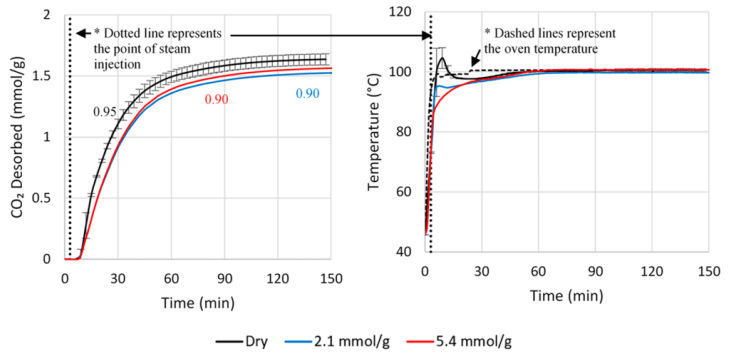

Figure 7. CO_2 desorption (left-hand side) and bed temperature (right-hand side) for S-TVSD at 26 kPa abs/100 °C with different amounts of preadsorbed water. The average desorption rate (mmol/g/h) for each run is denoted in text next to the data sets. Error bars included for the dry data are based on duplicate runs. The error is assumed to be similar for the other data sets.

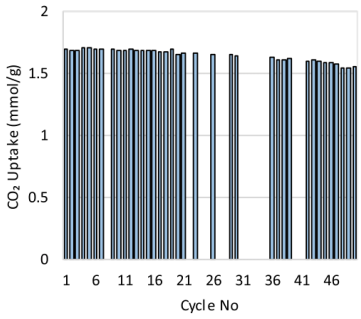

Figure 8. Adsorption capacity of PEI_80b from dry 420 ppm of CO_2 at 46 °C over 50 cycles of S-TVSD. Desorption carried out at varying pressures (12−56 kPa abs), temperatures (70−100 °C), and steam flow rates (0.3−9 g/h).

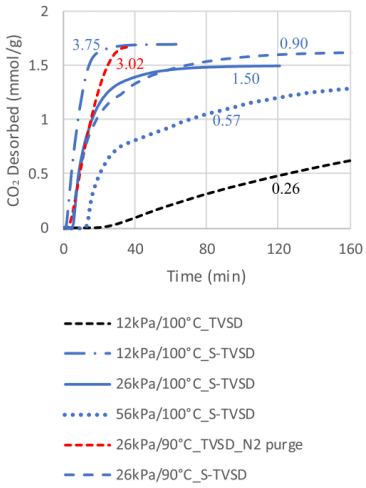

Figure 9. Comparison of CO_2 desorption under S-TVSD with TVSD and with TVSD with N_2 purge. The S-TVSD runs were at a steam flow rate of 6.4 ± 1.2 g/h. The average desorption rate (mmol/g/h) for each run is denoted in text next to the data sets.

desorption experiment where the flow rate exceeded the upper limit of range of the flow meter. As a result, the amount of CO_2 desorbed would have been underestimated. It was observed that at the higher pressures, the flow rate exceeded the range of the flow meter for a longer period than at the lower pressures. The larger discrepancies at higher pressures are consistent with this. This is perhaps attributed to the fact that the vacuum pumps used for achieving higher pressures were not as powerful and could only displace gases at a lower flow rate. As such, they would have taken longer to fully displace the noncondensable gases in the desorption lines, upon the introduction of steam at the start of the desorption. The slow evacuation of these noncondensable gases is likely the cause of the extended period of high flow rate. Second, the discrepancy may have also been due to the measurement errors in the CO_2 sensor and flow meter (±5% of reading for both) used for the desorption stage.

When comparing the effect of temperature and pressure on the CO_2 desorption kinetics (refer to Figure 4), rapid desorption was observed initially under all conditions. However, at lower desorption temperatures and higher pressures, the desorption rate was seen to decrease much faster, leading to longer desorption times and lower average desorption rates. The fastest average desorption rate of 3.75 mmol/g/h was observed at 12 kPa abs/100 °C. When compared with the data reported in the literature (see Table 1), this is the fastest desorption rate reported for TVSD type processes for DAC. While a desorption rate of 4.2 mmol/g/h was reported by Bos et al.,[35] it was for a process capturing CO_2 from a much higher concentration gas (45% mol).

For 56 kPa abs, desorption was only carried out at 100 °C, as higher temperatures were expected to potentially lead to degradation of the sorbent and lower temperatures posed the risk of water condensation in the sorbent bed, which might cause the leaching of PEI. In any case, 56 kPa abs yielded significantly slower desorption than at the lower pressures at 100 °C, as expected for TVSD type processes. As such, lower desorption temperatures at 56 kPa abs would likely result in

DOI: 10.1021/acs.iecr.9b03140
Ind. Eng. Chem. Res. XXXX, XXX, XXX−XXX

even longer desorption times, which would likely be undesirable for practical applications.

The shorter desorption times achieved at lower pressures would mean lower thermal energy requirements owing to the reduced steam requirement. However, lower pressures would increase the electrical energy requirement for the vacuum generation, which may offset the savings in thermal energy. The larger vacuum pumps needed to reach lower pressures may also represent significantly higher capital costs.

The sharp increases and decreases in the bed temperature observed (refer to Figure 4) were presumed to be an effect of the energy released by adsorption of water and the energy consumed by the desorption of CO_2. The initial increase in temperature observed at the introduction of steam could be attributed to the fast water adsorption at the beginning of desorption stage. Similar observations were reported by Sandhu et al.[49] for steam stripping. The increase was more prominent in the experiments with lower temperatures and higher desorption pressures, where the desorption of CO_2 was slower and the sorption of water was more preferred (as depicted in Figure 6). Conversely, the most significant dips in temperature were observed for the experiments with higher temperatures and lower pressures, where desorption of CO_2 was faster and the sorption of water was less preferred. Similar results have been reported for desorption under TVSD,[36] where lower pressures led to more prominent dips in the bed temperature.

From Figure 5, it was evident that lower steam flow rates resulted in longer desorption times. As the steam flow rate is lowered, the rate at which the desorbed CO_2 is swept away by the steam is also reduced, resulting in a higher partial pressure of CO_2 in the atmosphere around the sorbent. The higher partial pressure would produce a lower driving force for desorption, resulting in slower overall mass transfer. When comparing the temperature profiles, shallower and longer dips can be observed for lower steam flow rates, consistent with the slower desorption rate of CO_2. The lag in CO_2 desorption seen for lower steam flow rates was attributed to the residence time for the desorbed gas to reach the CO_2 sensor due to the void volume present in the desorption system. Minimizing the void volume in the system was seen to significantly reduce the lag (see Figure S1). It is likely that minimizing the volume in the connecting tubes by using shorter, smaller i.d. tubing would further reduce this apparent lag.

4.2. Effect of Preadsorbed Water. The differences in the temperature profiles when there was preadsorbed water on the sorbent (see Figure 7) was attributed to the energy consumed for the desorption of water. As the preadsorbed amounts of water (2.1 and 5.4 mmol/g) were more than the equilibrium adsorbed amount of water (1.61 mmol/g) at the desorption conditions, some of this water would be expected to desorb consuming thermal energy. This is reaffirmed by the observation that the deviation in the temperature profiles increased as the amount of preadsorbed water was increased. Similar observations have been made for TVSD[36] where the presence of preadsorbed water resulted in a dip in the temperature profile. Both cases with preadsorbed water displayed a similar average desorption rate of 0.90 mmol/g/h, while this was slightly higher for the dry case (0.95 mmol/g/h). This slower average desorption rate was likely a result of the lower temperature of the bed during the start of the desorption, which would have resulted in slower kinetics.

This indicates that carrying out the adsorption step under humid conditions may not be preferred due to the additional energy requirement for desorption. However, CO_2 adsorption would be faster under wet conditions,[26] allowing for shorter adsorption times. For example, under dry adsorption 29.7 h were needed to capture 1.66 mmol/g of CO_2, while both wet adsorption conditions studied here captured the same amount in 27.9 h. This means that less air needs to be pushed through the sorbent, resulting in a reduced electrical energy requirement. These inferences place emphasis on the need to carry out a techno-economic analysis on the process, to determine the preferred operating conditions.

4.3. Concentration of the Desorbed CO_2. The concentration measurements (see Figures S2−S4) during the experiments depicted that at the start of the desorption, the CO_2 concentration of the exhaust gas rapidly rises, reaching >99% mol in some cases. Following this, the concentration was seen to undergo a gradual decrease until finally approaching 0% mol. This reduction in concentration was likely caused by the diluting effect of the small vacuum leaks identified in the section 2.3. Therefore, the current paper makes no further discussion on the concentration of the CO_2 desorbed. However, it should be noted that with a well-sealed system, the initial concentration can be expected to be retained throughout the duration of the desorption.

4.4. Stability of the Sorbent. The small loss in capacity of the sorbent, as seen in Figure 8, after exposure to multiple cycles indicates that the sorbent displays good stability under the process conditions that have been studied here. This may be attributed to the stabilizing effect of moisture against CO_2 induced degradation as observed in other studies.[39,41,43−45] In comparison, a prior study[42] by our group, evaluating an MCF-PEI sorbent for postcombustion capture with VSD under dry conditions, reported an 8% loss in capacity over 60 cycles. In other studies,[41,43] we presented that the presence of moisture better preserved the CO_2 capacity of similar sorbents.

It was also noted that the gas lines, downstream of the adsorbent bed in the desorption system, were coated with a film of a yellow substance. This was likely PEI which had leached off from the sorbent during the desorption experiments. Our group had previously reported that PEI impregnated MCF sorbents incurred small losses in mass when exposed to a vacuum (0.02 kPa abs) at 110 °C[41,54] and under a wet Ar purge at 105 °C,[55] which were attributed to the loss of low-molecular weight (volatile) PEI in the sorbent. In the current study, this apparent leaching effect was noticed even after the first few cycles, despite seeing no significant loss in capacity. This may be explained by the fact that typically not all amine sites are accessible to the CO_2 due to the diffusional limitation.[26] The initial losses may have been comprised of these unutilized amine sites. Alternatively, it is possible that as the outer layers of PEI were leached off, the inner layers which were previously inaccessible would have become exposed and thus compensated for the losses. The accelerated reduction in capacity which was observed after ∼30 cycles may indicate that the leaching of PEI had finally become significant enough to cause a loss in capacity, which could not be compensated for by the previously inaccessible PEI. While no detailed investigations have been done in the current study to confirm this postulation, it would be of interest to quantify the loss of sorbent in this manner. This is important for practical DAC systems as in addition to the loss of the productivity of the

DOI: 10.1021/acs.iecr.9b03140
Ind. Eng. Chem. Res. XXXX, XXX, XXX−XXX

system, leaching of PEI, which is basic in nature, could lead to the degradation of downstream equipment.

4.5. Comparison to Other Desorption Technologies. When compared to pure TVSD at 12 kPa abs/100 °C, S-TVSD with a steam flow rate of 6.2 g/h showed significantly faster desorption of CO_2 (see Figure 9), confirming the superior desorption kinetics offered by the steam-aided process. Furthermore, it can be noted that even the S-TVSD case with the weakest vacuum (56 kPa abs) outperformed TVSD at 12 kPa abs, indicating that the use of a steam purge allows the process to use lower vacuums to achieve similar if not better results. In the TVSD experiment, the initial lag before the desorption of CO_2 starts is likely an effect of the large volume in the condensers and connecting tubes, as described earlier.

In comparison to TVSD assisted by a N_2 purge, it was observed that while the initial desorption rate of CO_2 was similar in S-TVSD, the rate decayed much faster. This slowing down of the kinetics is likely attributed to the increased diffusional limitations imposed by the water adsorbed on the sorbent. A similar phenomena of water hindering the transportation of CO_2 inside the sorbent was previously discussed by our group[26] for the adsorption stage of the process, where adsorption under high moisture levels led to reduced CO_2 uptake. It was suggested that this was likely due to the water presenting an additional barrier for the diffusion of CO_2 to/from the sorbent. This is in contradiction to the reports of Sandhu et al.[49] and Hammache et al.,[51] where TCSD with a steam purge yielded superior kinetics to purging with N_2. In both studies, it was suggested that the steam had a displacing effect on the CO_2, thus enhancing the desorption. Despite the faster kinetics offered by the N_2 assisted case, the product CO_2 was largely diluted with N_2 (4% mol CO_2 concentration at its highest). Depending on the preferred method of utilization/storage of the desorbed CO_2, the product gas may need to be purified further. However, CO_2 at this concentration may be sufficient for use as a feed for greenhouses or algae cultivations.

4.6. Thermal Energy Requirement. The thermal energy requirement for steam generation for desorption at 100 °C at 12 and 26 kPa abs at various steam flow rates is depicted in Figure 10. The calculations were only done for this temperature, as it produced the fastest desorption of CO_2. It can be seen that significant reductions to the energy requirement can be made by reducing the steam flow rate as suggested by Gebald et al.[47] For desorption of 99% of the adsorbed CO_2, the lowest energy requirement was 12.1 GJ/t at 26 kPa abs/100 °C at a steam rate of 0.3 g/h and 4.0 GJ/t at 12 kPa abs/100 °C at a steam rate of 0.5 g/h.

As evident from the CO_2 desorption profiles (Figures 4 and 5), the desorption rate toward the end of the desorption is significantly slower than at the beginning. This suggests that for DAC systems, it may be preferable to carry out partial desorption of the CO_2 reaping the benefits of faster desorption rates. The faster rates would in turn lead to energy savings due to lower steam consumption. To validate this, the energy calculations were repeated for desorption of 75% of the adsorbed CO_2. As seen in Figure 10, significantly lower energy requirements were calculated for these cases. At 12 kPa abs/100 °C, the lowest energy requirement reduced to 2.3 GJ/t, and at 26 kPa abs/100 °C, it reduced to 7.6 GJ/t.

In comparison, the thermal energy requirements for TVSD processes for DAC reported in the literature are in the range of

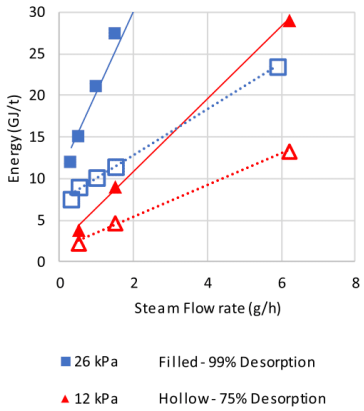

Figure 10. Thermal energy requirement for steam production for desorption at 100 °C at 12 and 26 kPa abs at various steam flow rates.

1.3[56] to 14.5[46] GJ/t. However, it should be noted that the calculations in the current study only consider the energy for steam production and do not include the thermal energy provided to the sorbent from the oven. Furthermore, the electrical energy requirement for the operation of the vacuum pump was also not included. A more detailed techno-economic evaluation is recommended to calculate the total energy requirement and to identify the preferred operating conditions.

5. CONCLUSIONS

It was demonstrated that CO_2 could be desorbed from PEI_80b with steam-assisted temperature vacuum swing under moderate vacuum levels (12−56 kPa abs), and relatively low temperatures (70−100 °C). The fastest desorption was achieved at 12 kPa abs/100 °C, with an average desorption rate of 3.75 mmol/g/h. In comparison, TVSD under the same temperature and pressure only had an average desorption rate of 0.23 mmol/g/h, confirming the superior kinetics offered by S-TVSD. When adsorption was carried under humid conditions (1 and 2% mol-H_2O), the co-adsorbed water on the sorbent was observed to slow down the desorption of CO_2, due to the additional energy required for the desorption of water. Evaluation of the adsorption capacity of CO_2 over 50 cycles (>1500 h) revealed an 8% loss in capacity, indicating the stability of the sorbent under the conditions studied. Of the desorption conditions studied, the lowest thermal energy requirement for steam production was calculated to be 2 GJ/t for desorption at 12 kPa abs/100 °C at a steam flow rate of 0.5 g/h. To better evaluate the energy consumption of the process and determine the preferred conditions for practical DAC systems, a techno-economic evaluation is recommended to be carried out. It should also be noted that while these investigations were in the context of DAC, the observations here could be extended to other CO_2 capture applications with solid supported amines.

■ ASSOCIATED CONTENT

Supporting Information

The Supporting Information is available free of charge on the ACS Publications website at DOI: 10.1021/acs.iecr.9b03140.

DOI: 10.1021/acs.iecr.9b03140
Ind. Eng. Chem. Res. XXXX, XXX, XXX−XXX

CO_2 desorption profiles before and after minimization of the dead volume in the system and CO_2 concentration profiles for desorption under various conditions (PDF)

AUTHOR INFORMATION

Corresponding Authors

*Phone: +61 3 9905 3421. E-mail: Andrew.Hoadley@monash.edu.

*Phone: +61 3 9905 4626. E-mail: Alan.Chaffee@monash.edu.

ORCID

Andrew F. A. Hoadley: 0000-0001-9605-6858

Alan L. Chaffee: 0000-0001-5100-6910

Notes

The authors declare no competing financial interest.

ACKNOWLEDGMENTS

The authors acknowledge Antonio Benci and David Zuidema, Monash Instrumentation Facility, for assistance in designing and programming some of the components in the experimental setup.

NOMENCLATURE

DAC = direct air capture
MCF = mesocellular foam silica
PEI = polyethylenimine
SSA = solid supported amine
TCSD = temperature concentration swing desorption
TVSD = temperature vacuum swing desorption
S-TVSD = steam-assisted temperature vacuum swing desorption
VSD = vacuum swing desorption

REFERENCES

(1) IPCC. *IPCC Special Report on Carbon Dioxide Capture and Storage*, Prepared by Working Group III of the Intergovernmental Panel on Climate Change. Metz, B., Davidson, O., de Coninck, H. C., Loos, M., Meyer, L. A., Eds.; Cambridge University Press: Cambridge, U.K., 2007.

(2) Hou, C.-L.; Wu, Y.-S.; Jiao, Y.-Z.; Huang, J.; Wang, T.; Fang, M.-X.; Zhou, H. Integrated direct air capture and CO_2 utilization of gas fertilizer based on moisture swing adsorption. *J. Zhejiang Univ., Sci., A* **2017**, *18* (10), 819−830.

(3) Kothandaraman, J.; Goeppert, A.; Czaun, M.; Olah, G. A.; Prakash, G. K. S. Conversion of CO_2 from Air into Methanol Using a Polyamine and a Homogeneous Ruthenium Catalyst. *J. Am. Chem. Soc.* **2016**, *138* (3), 778−781.

(4) Graves, C.; Ebbesen, S. D.; Mogensen, M.; Lackner, K. S. Sustainable hydrocarbon fuels by recycling CO_2 and H_2O with renewable or nuclear energy. *Renewable Sustainable Energy Rev.* **2011**, *15* (1), 1−23.

(5) Takeda, Y.; Okumura, S.; Tone, S.; Sasaki, I.; Minakata, S. Cyclizative Atmospheric CO_2 Fixation by Unsaturated Amines with t-BuOI Leading to Cyclic Carbamates. *Org. Lett.* **2012**, *14* (18), 4874−4877.

(6) Stolaroff, J. K.; Keith, D. W.; Lowry, G. V. Carbon Dioxide Capture from Atmospheric Air Using Sodium Hydroxide Spray. *Environ. Sci. Technol.* **2008**, *42* (8), 2728−2735.

(7) Zeman, F. Experimental results for capturing CO_2 from the atmosphere. *AIChE J.* **2008**, *54* (5), 1396−1399.

(8) Bandi, A.; Specht, M.; Weimer, T.; Schaber, K. CO_2 recycling for hydrogen storage and transportation —Electrochemical CO_2 removal and fixation. *Energy Convers. Manage.* **1995**, *36* (6−9), 899−902.

(9) Dubey, M. K.; Ziock, H.; Rueff, G.; Elliott, S.; Smith, W. S. Extraction of carbon dioxide from the atmosphere through engineered chemical sinkage. In *ACS Division of Fuel Chemistry, Preprints*, 1st ed.; American Chemical Society, 2002; Vol. *47*, pp 81−84.

(10) Petukhov, S. S.; Tumanov, A. I.; Trokhina, G. A. The use of synthetic zeolites in the complete removal of impurities from air. *Chem. Pet. Eng.* **1970**, *6* (1), 23−26.

(11) Kumar, A.; Madden, D. G.; Lusi, M.; Chen, K.-J.; Daniels, E. A.; Curtin, T.; Perry, J. J.; Zaworotko, M. J. Direct Air Capture of CO_2 by Physisorbent Materials. *Angew. Chem.* **2015**, *127* (48), 14580−14585.

(12) Stuckert, N. R.; Yang, R. T. CO_2 Capture from the Atmosphere and Simultaneous Concentration Using Zeolites and Amine-Grafted SBA-15. *Environ. Sci. Technol.* **2011**, *45* (23), 10257−10264.

(13) Lackner, K. S. Capture of carbon dioxide from ambient air. *Eur. Phys. J.: Spec. Top.* **2009**, *176*, 93−106.

(14) Goeppert, A.; Zhang, H.; Czaun, M.; May, R. B.; Prakash, G. K. S.; Olah, G. A.; Narayanan, S. R. Easily Regenerable Solid Adsorbents Based on Polyamines for Carbon Dioxide Capture from the Air. *ChemSusChem* **2014**, *7* (5), 1386−1397.

(15) Pang, S. H.; Lee, L.-C.; Sakwa-Novak, M. A.; Lively, R. P.; Jones, C. W. Design of Aminopolymer Structure to Enhance Performance and Stability of CO2 Sorbents: Poly(propylenimine) vs Poly(ethylenimine). *J. Am. Chem. Soc.* **2017**, *139* (10), 3627−3630.

(16) Sayari, A.; Liu, Q.; Mishra, P. Enhanced Adsorption Efficiency through Materials Design for Direct Air Capture over Supported Polyethylenimine. *ChemSusChem* **2016**, *9* (19), 2796−2803.

(17) Sakwa-Novak, M. A.; Yoo, C.-J.; Tan, S.; Rashidi, F.; Jones, C. W. Poly(ethylenimine)-Functionalized Monolithic Alumina Honeycomb Adsorbents for CO_2 Capture from Air. *ChemSusChem* **2016**, *9* (14), 1859−1868.

(18) Chaikittisilp, W.; Khunsupat, R.; Chen, T. T.; Jones, C. W. Poly(allylamine)−Mesoporous Silica Composite Materials for CO_2 Capture from Simulated Flue Gas or Ambient Air. *Ind. Eng. Chem. Res.* **2011**, *50* (24), 14203−14210.

(19) Zerze, H.; Tipirneni, A.; McHugh, A. J. Reusable poly-(allylamine)-based solid materials for carbon dioxide capture under continuous flow of ambient air. *Sep. Sci. Technol.* **2017**, *52* (16), 2513−2522.

(20) Darunte, L. A.; Oetomo, A. D.; Walton, K. S.; Sholl, D. S.; Jones, C. W. Direct Air Capture of CO_2 Using Amine Functionalized MIL-101(Cr). *ACS Sustainable Chem. Eng.* **2016**, *4* (10), 5761−5768.

(21) McDonald, T. M.; Lee, W. R.; Mason, J. A.; Wiers, B. M.; Hong, C. S.; Long, J. R. Capture of Carbon Dioxide from Air and Flue Gas in the Alkylamine-Appended Metal−Organic Framework mmen-Mg2(dobpdc). *J. Am. Chem. Soc.* **2012**, *134* (16), 7056−7065.

(22) Sehaqui, H.; Gálvez, M. E.; Becatinni, V.; cheng Ng, Y.; Steinfeld, A.; Zimmermann, T.; Tingaut, P. Fast and Reversible Direct CO_2 Capture from Air onto All-Polymer Nanofibrillated Cellulose—Polyethylenimine Foams. *Environ. Sci. Technol.* **2015**, *49* (5), 3167−3174.

(23) Gebald, C.; Wurzbacher, J. A.; Tingaut, P.; Zimmermann, T.; Steinfeld, A. Amine-Based Nanofibrillated Cellulose As Adsorbent for CO_2 Capture from Air. *Environ. Sci. Technol.* **2011**, *45* (20), 9101−9108.

(24) Chaikittisilp, W.; Kim, H.-J.; Jones, C. W. Mesoporous Alumina-Supported Amines as Potential Steam-Stable Adsorbents for Capturing CO_2 from Simulated Flue Gas and Ambient Air. *Energy Fuels* **2011**, *25* (11), 5528−5537.

(25) Sakwa-Novak, M. A.; Tan, S.; Jones, C. W. Role of Additives in Composite PEI/Oxide CO_2 Adsorbents: Enhancement in the Amine Efficiency of Supported PEI by PEG in CO_2 Capture from Simulated Ambient Air. *ACS Appl. Mater. Interfaces* **2015**, *7* (44), 24748−24759.

(26) Wijesiri, R. P.; Knowles, G. P.; Yeasmin, H.; Hoadley, A. F. A.; Chaffee, A. L. CO_2 Capture from Air Using Pelletised Polyethyleneimine Impregnated MCF Silica. *Ind. Eng. Chem. Res.* **2019**, *58* (8), 3293−3303.

(27) Wang, J.; Huang, H.; Wang, M.; Yao, L.; Qiao, W.; Long, D.; Ling, L. Direct Capture of Low-Concentration CO_2 on Mesoporous Carbon-Supported Solid Amine Adsorbents at Ambient Temperature. *Ind. Eng. Chem. Res.* **2015**, *54* (19), 5319−5327.

DOI: 10.1021/acs.iecr.9b03140
Ind. Eng. Chem. Res. XXXX, XXX, XXX−XXX

(28) Goeppert, A.; Czaun, M.; May, R. B.; Prakash, G. K. S.; Olah, G. A.; Narayanan, S. R. Carbon Dioxide Capture from the Air Using a Polyamine Based Regenerable Solid Adsorbent. *J. Am. Chem. Soc.* **2011**, *133* (50), 20164−20167.
(29) Monazam, E. R.; Spenik, J.; Shadle, L. J. CO_2 Desorption Kinetics for Immobilized Polyethylenimine (PEI). *Energy Fuels* **2014**, *28* (1), 650−656.
(30) Liu, Y.; Yu, X. Carbon dioxide adsorption properties and adsorption/desorption kinetics of amine-functionalized KIT-6. *Appl. Energy* **2018**, *211*, 1080−1088.
(31) Gargiulo, V.; Alfè, M.; Ammendola, P.; Raganati, F.; Chirone, R. CO_2 sorption on surface-modified carbonaceous support: Probing the influence of the carbon black microporosity and surface polarity. *Appl. Surf. Sci.* **2016**, *360* (A), 329−337.
(32) Wang, J.; Wang, M.; Li, W.; Qiao, W.; Long, D.; Ling, L. Application of polyethylenimine-impregnated solid adsorbents for direct capture of low-concentration CO_2. *AIChE J.* **2015**, *61* (3), 972−980.
(33) Zhang, W.; Liu, H.; Sun, C.; Drage, T. C.; Snape, C. E. Capturing CO_2 from ambient air using a polyethyleneimine−silica adsorbent in fluidized beds. *Chem. Eng. Sci.* **2014**, *116*, 306−316.
(34) Hoffman, J. S.; Hammache, S.; Gray, M. L.; Fauth, D. J.; Pennline, H. W. Parametric study for an immobilized amine sorbent in a regenerative carbon dioxide capture process. *Fuel Process. Technol.* **2014**, *126*, 173−187.
(35) Bos, M. J.; Kroeze, V.; Sutanto, S.; Brilman, D. W. F. Evaluating Regeneration Options of Solid Amine Sorbent for CO_2 Removal. *Ind. Eng. Chem. Res.* **2018**, *57* (32), 11141−11153.
(36) Wurzbacher, J. A.; Gebald, C.; Steinfeld, A. Separation of CO_2 from air by temperature-vacuum swing adsorption using diamine-functionalized silica gel. *Energy Environ. Sci.* **2011**, *4* (9), 3584−3592.
(37) Serna-Guerrero, R.; Belmabkhout, Y.; Sayari, A. Influence of regeneration conditions on the cyclic performance of amine-grafted mesoporous silica for CO_2 capture: An experimental and statistical study. *Chem. Eng. Sci.* **2010**, *65* (14), 4166−4172.
(38) Drage, T. C.; Arenillas, A.; Smith, K. M.; Snape, C. E. Thermal stability of polyethylenimine based carbon dioxide adsorbents and its influence on selection of regeneration strategies. *Microporous Mesoporous Mater.* **2008**, *116* (1−3), 504−512.
(39) Sayari, A.; Belmabkhout, Y. Stabilization of Amine-Containing CO_2 Adsorbents: Dramatic Effect of Water Vapor. *J. Am. Chem. Soc.* **2010**, *132* (18), 6312−6314.
(40) Yu, Q.; Delgado, J.; Veneman, R.; Brilman, D. W. F. Stability of a Benzyl Amine Based CO_2 Capture Adsorbent in View of Regeneration Strategies. *Ind. Eng. Chem. Res.* **2017**, *56* (12), 3259−3269.
(41) Knowles, G. P.; Liang, Z.; Chaffee, A. L. Shaped polyethyleneimine sorbents for CO_2 capture. *Microporous Mesoporous Mater.* **2017**, *238*, 14−18.
(42) Knowles, G. P.; Sher, J. L.; Xiao, P.; Webley, P. A.; Chaffee, A. L. Novel adsorption process technologies for CO_2 post combustion capture via amine type adsorbents. Presented at the *14th International Conference on Greenhouse Gas Control Technologies*, Melbourne, Australia, October 21−26, 2018.
(43) Subagyono, D. J. N.; Marshall, M.; Knowles, G. P.; Chaffee, A. L. CO_2 adsorption by amine modified siliceous mesostructured cellular foam (MCF) in humidified gas. *Microporous Mesoporous Mater.* **2014**, *186*, 84−93.
(44) Gebald, C.; Wurzbacher, J. A.; Tingaut, P.; Steinfeld, A. Stability of Amine-Functionalized Cellulose during Temperature-Vacuum-Swing Cycling for CO_2 Capture from Air. *Environ. Sci. Technol.* **2013**, *47* (17), 10063−10070.
(45) Heydari-Gorji, A.; Sayari, A. Thermal, Oxidative, and CO_2-Induced Degradation of Supported Polyethylenimine Adsorbents. *Ind. Eng. Chem. Res.* **2012**, *51* (19), 6887−6894.
(46) Wurzbacher, J. A.; Gebald, C.; Piatkowski, N.; Steinfeld, A. Concurrent Separation of CO_2 and H_2O from Air by a Temperature-Vacuum Swing Adsorption/Desorption Cycle. *Environ. Sci. Technol.* **2012**, *46* (16), 9191−9198.
(47) Gebald, C.; Repond, N.; Wurzbacher, J. A. *Steam assisted vacuum desorption process for carbon dioxide capture*. U.S. Patent Application 20170203249 A1, 2017.
(48) Sujan, A. R.; Pang, S. H.; Zhu, G.; Jones, C. W.; Lively, R. P. Direct CO_2 Capture from Air using Poly(ethylenimine)-Loaded Polymer/Silica Fiber Sorbents. *ACS Sustainable Chem. Eng.* **2019**, *7* (5), 5264−5273.
(49) Sandhu, N. K.; Pudasainee, D.; Sarkar, P.; Gupta, R. Steam Regeneration of Polyethylenimine-Impregnated Silica Sorbent for Postcombustion CO_2 Capture: A Multicyclic Study. *Ind. Eng. Chem. Res.* **2016**, *55* (7), 2210−2220.
(50) Li, W.; Choi, S.; Drese, J. H.; Hornbostel, M.; Krishnan, G.; Eisenberger, P. M.; Jones, C. W. Steam-Stripping for Regeneration of Supported Amine-Based CO_2 Adsorbents. *ChemSusChem* **2010**, *3* (8), 899−903.
(51) Hammache, S.; Hoffman, J. S.; Gray, M. L.; Fauth, D. J.; Howard, B. H.; Pennline, H. W. Comprehensive Study of the Impact of Steam on Polyethyleneimine on Silica for CO_2 Capture. *Energy Fuels* **2013**, *27* (11), 6899−6905.
(52) Fujiki, J.; Chowdhury, F. A.; Yamada, H.; Yogo, K. Highly efficient post-combustion CO_2 capture by low-temperature steam-aided vacuum swing adsorption using a novel polyamine-based solid sorbent. *Chem. Eng. J.* **2017**, *307*, 273−282.
(53) Knowles, G. P.; Chaffee, A. L. Shaped Silica-polyethyleneimine Composite Sorbents for CO_2 Capture via Adsorption. *Energy Procedia* **2017**, *114*, 2219−2227.
(54) Knowles, G. P.; Chaffee, A. L. *Pelletized form of MCF-PEI composite and method of producing same*. World Patent No. 2015/077835, 2015.
(55) Knowles, G. P.; Webley, P. A.; Liang, Z.; Chaffee, A. L., Silica/Polyethyleneimine Composite Adsorbent S-PEI for CO_2 Capture by Vacuum Swing Adsorption (VSA). In *Recent Advances in Post-Combustion CO_2 Capture Chemistry*; Attalla, M. I., Ed.; ACS Symposium Series, Vol. *1097*; American Chemical Society: Washington, DC, 2012; pp 177−205.
(56) Sinha, A.; Darunte, L. A.; Jones, C. W.; Realff, M. J.; Kawajiri, Y. Systems Design and Economic Analysis of Direct Air Capture of CO_2 through Temperature Vacuum Swing Adsorption Using MIL-101(Cr)-PEI-800 and mmen-Mg2(dobpdc) MOF Adsorbents. *Ind. Eng. Chem. Res.* **2017**, *56* (3), 750−764.

DOI: 10.1021/acs.iecr.9b03140
Ind. Eng. Chem. Res. XXXX, XXX, XXX−XXX

4. Technoeconomic Evaluation of a Process Capturing CO_2 Directly from Air

This chapter focusses on the third research objective of the thesis: evaluating the technoeconomic feasibility of a DAC process. A process model which could accurately predict the adsorption/desorption of CO_2 was developed and validated using the experimental data obtained in Chapters 2 and 3. In addition to the data presented in Chapters 2 and 3, adsorption experiments were carried out at 27 °C, to get the required data for developing the process model. The process model was then subjected to a multi-objective optimisation to determine the preferred process conditions.

The optimisation identified the minimum cost of capture to be 612 USD/tonne for a process with air entering at 25°C under dry conditions, and 657 USD/tonne for air entering at 22 °C and 39% RH. In both of the cases, the incoming air to the process was heated to 27 °C, before passing through the air-sorbent contactors, to benefit from the reduced mass transfer limitations achieved at higher temperatures, as identified in **Chapter 2**. An adsorption temperature of 27 °C was considered for this study, although 46 °C was previously reported to produce a larger uptake of CO_2. This was done as an average ambient temperature of 46 °C corresponds to unrealistically warm climates, and heating the air to this temperature would require a significant amount of energy. The largest contributors to the cost of capture were identified to be the cost of the air-sorbent contactors, and the cost of providing the thermal energy required for the desorption. The higher cost for adsorption under humid conditions was attributed to the additional energy requirement for desorbing the co-adsorbed water. Despite the higher cost of capture, it was noted that the humid conditions represent more practical values, as it would be unrealistic to expect completely dry climates in any region of the world.

Finally, the study also evaluated different scenarios under which the cost of capture could be reduced. It was determined that the utilisation of waste heat from other processes would have the largest effect on the economics of the process, with a 42% reduction in the cost of capture. In terms of how the sorbent development could improve the economics, it was determined that a sorbent with two-fold faster kinetics would reduce the cost of capture by 27%. A combination of these two scenarios could cut the cost by 54%.

The content of this chapter has been published in *Processes.*

The supporting information for this publication is included in **Appendix A(II)**.

processes

MDPI

Article

Technoeconomic Evaluation of a Process Capturing CO_2 Directly from Air

Romesh Pramodya Wijesiri [1,2], Gregory Paul Knowles [2], Hasina Yeasmin [1], Andrew Forbes Alexander Hoadley [1,*] and Alan Loyd Chaffee [2,*]

[1] Department of Chemical Engineering, 16 Alliance Lane, Clayton Campus, Monash University, Clayton, VIC 3800, Australia
[2] School of Chemistry, 17 Rainforest Walk, Clayton Campus, Monash University, Clayton, VIC 3800, Australia
* Correspondence: Andrew.Hoadley@monash.edu (A.F.A.H.); Alan.Chaffee@monash.edu (A.L.C.); Tel.: +61-3-9905-3421 (A.F.A.H.); Tel.: +61-3-9905-4626 (A.L.C.)

Received: 30 June 2019; Accepted: 28 July 2019; Published: 2 August 2019

Abstract: Capturing CO_2 directly from air is one of the options for mitigating the effects global climate change, and therefore determining its cost is of great interest. A process model was proposed and validated using laboratory results for adsorption/desorption of CO_2, with a branched polyethyleneimine (PEI) loaded mesocellular foam (MCF) silica sorbent. The model was subjected to a Multi-Objective Optimization (MOO) to evaluate the technoeconomic feasibility of the process and to identify the operating conditions which yielded the lowest cost. The objectives of the MOO were to minimize the cost of CO_2 capture based on a discounted cash flow analysis, while simultaneously maximizing the quantity of CO_2 captured. This optimization identified the minimum cost of capture as 612 USD tonne^{-1} for dry air entering the process at 25 °C, and 657 USD tonne^{-1} for air at 22 °C and 39% relative humidity. The latter represents more realistic conditions which can be expected for subtropical climates. The cost of direct air capture could be reduced by ~42% if waste heat was utilized for the process, and by ~27% if the kinetics of the sorbent could be improved by a factor of two. A combination of both would allow cost reductions of ~54%.

Keywords: direct air capture; economic; cost; model; steam; temperature vacuum swing; adsorption; polyethyleneimine; carbon capture

1. Introduction

The increase in anthropogenic CO_2 emissions has been identified as a main cause of global climate change. Close to half [1] of these emissions are accounted for by diffuse sources such as motor vehicles, homes and offices. Capturing these emissions at the source would require the fitting of capture systems to each of these, which would neither be economical, nor practical. Alternatively, the effect of these emissions could be compensated for with "Direct Air Capture" (DAC) systems, i.e., processes which capture CO_2 directly from the atmosphere. The captured CO_2 could either be sequestered or utilized for application in various industries [2]. The technologies evaluated for DAC include absorption with aqueous hydroxide solutions, adsorption with solid inorganic bases, and adsorption with solid-supported amines (SSA). A review of the studies done on DAC has been detailed in Sanz-Pérez et al. [3]. Of these technologies, adsorption with SSA has presented itself to be promising for DAC.

SSAs are a group of sorbents made of various amines, physically or chemically supported on porous solid materials [3]. They are well suited for DAC applications, due to their high uptake capacity and selectivity, resilience to moisture which is present in air, and the possibility of regeneration under relatively mild conditions. While significant research has been done on SSA for DAC, its focus

has mainly been on sorbent development. There have only been a few reports [4–9] on the energy requirements and the cost of capture of such systems, and there is significant discrepancy between their results. These reports [4–9] evaluated DAC systems which used temperature concentration swing adsorption (TCSA) [5,6], temperature vacuum swing adsorption (TVSA) [9] and steam-assisted temperature vacuum swing adsorption (S-TVSA) [4,7,8] type processes. For TCSA, after the CO_2 is adsorbed on to the sorbent, the sorbent is heated and purged with a gas (steam in Krekel et al. [5] and Zhang et al. [6]) to effect desorption. In TVSA, desorption is achieved by heating the sorbent and applying a vacuum. S-TVSA is a hybrid of the two approaches, where in addition to applying heat and a vacuum, a steam purge is also used.

In two of the early studies, Kulkarni and Sholl [7] and Zhang et al. [6] carried out an economic analysis based only on the operating cost of the processes. They reported costs of CO_2 capture of 43–494 [7] and 91–227 [6] USD tonne^{-1}. Krekel et al. [5] expanded on the work carried out by Zhang et al. [6], and reported that once the capital expenses are included, the cost of capture would be increased significantly to 792–1200 USD tonne^{-1}. Sinha et al. [4] estimated a cost of capture of 60–190 USD tonne^{-1}.

Several companies are active in the field of DAC with SSA. The most well-known of these are Climeworks [10] and Global Thermostat [11]. The cost of capture reported for the operations of first-generation DAC system by Climeworks was estimated to be 600 USD tonne^{-1} [12]. This is an important benchmark, as it is based on a commercially operating system, as opposed to results of studies which are sensitive to the scope and assumptions used. Climeworks has further expressed their confidence in reducing this cost down to 200 USD tonne^{-1} by 2021, and down to 100 USD tonne^{-1} by 2030 [12]. Similarly, Global Thermostat expects a cost of capture of 100 USD tonne^{-1} for their first commercial DAC process [12]. Carbon Engineering [13] is another company which is developing a DAC process, although they focus on an aqueous hydroxide-based process. The projected cost of capture with this process has been reported to be 94–232 USD tonne^{-1} [14], but this process requires very high temperatures for regeneration of the sorbent.

In comparison, removing CO_2 from air via afforestation and forest management has a cost of capture of 15–50 USD tonne^{-1} [15]. However, this approach carries a large land requirement, which would compete with the land available for food production. Moreover, the land available also enforces an upper limit on the scale at which CO_2 can be removed. In comparison, CO_2 removal by DAC faces less stringent limitations on the degree of possible scaling. However, it is important to stress that DAC is not envisioned to be an alternative for good forest management practices, but rather as a technology to supplement the rate of CO_2 removal by the natural carbon cycle.

The energy requirements of the DAC processes in prior works, is largely accounted for by the thermal energy required for the desorption process. This mainly consists of the sensible heat required to heat up the sorbent to the desorption temperature, and the large heat of desorption for CO_2. [5-7] When adsorption is considered under humid conditions, the heat of desorption of water, which gets co-adsorbed on SSA, adds to the thermal energy demand [9]. Another big contributor to the energy consumption is that needed for pushing air through the air-sorbent contactors. [4-6] Due to the low concentration of CO_2 in air, large amounts of air need to be processed to capture the CO_2. This results in large energy requirements, even for low pressure drop contactor configurations as are described in some studies [4,7].

It was previously reported [16] that branched polyethyleneimine (PEI) loaded mesocellular foam (MCF) silica sorbent in pelletized form is promising for CO_2 adsorption under DAC conditions. The study identified that while low temperatures were better for the thermodynamics of the reaction between the CO_2 and amine sites, the uptake of CO_2 was limited by diffusional resistances in the sorbent. In contrast, higher temperatures allowed for better diffusion of CO_2, but the thermodynamics were less favored. The amount of CO_2 adsorbed by the sorbent was determined by the combined effect of these two factors. Due to the large diffusional resistances of the sorbent studied, the highest uptake

was achieved under relatively warm conditions (46 °C). The study further identified that low levels of moisture in the gas (0.5 to 2% mol-H_2O), enhanced the CO_2 uptake by up to 53%.

The same sorbent was evaluated using a S-TVSA adsorption/desorption cycle [17]. It was identified that substantial CO_2 desorption could be achieved with mild vacuum levels (12 to 56 kPa abs), and temperatures (70 to 100 °C). This indicated that the process could benefit from a reduced electrical energy demand for vacuum generation and a lower capital cost owing to the use of smaller vacuum pumps. It was further noted that as desorption is possible at relatively low temperatures, the thermal energy requirement could be supplied with low grade heat. The desorption conditions (pressure, temperature, steam flow rate) were seen to have a significant effect on the desorption performance. Moreover, it was identified that while the presence of moisture enhanced CO_2 adsorption, it also resulted in a significant uptake of H_2O, which increased the thermal energy demand for the desorption stage.

Building on this prior work, the present study aimed to (1) identify operating conditions which yield the lowest cost of DAC, (2) determine the relative effects of varying operating conditions on its technoeconomic performance and (3) identify promising directions for research on sorbent development that could foster further cost reduction for DAC.

To address the first two aims, a DAC technoeconomic model was developed based on the results of laboratory scale experimental data [17]. Next, the process model was subjected to a Multi-Objective Optimization (MOO) to minimize the cost of capture, while simultaneously maximizing the amount of CO_2 captured. In contrast to prior studies [4–7] which fixed on particular process conditions, the present study considers a range of conditions, seeking to minimize the cost. Moreover, adsorption from dry versus and humid air was compared, to evaluate the effect of the water, which co-adsorbs, on the process. Previous technoeconomic studies do not appear to have addressed this aspect [4–7]. The final aim was addressed through the use of case studies exploring the relative effect that sorbent modifications could have on the cost of capture.

2. Methods

2.1. Adsorption/Desorption Model

To develop a process model and evaluate the economics, the laboratory scale data was fitted to a simplified heat and mass transfer model, which accurately predicts the performance of the sorbent. In this simplified model, it is assumed that the adsorption bed has no concentration or temperature gradients in either the radial or the axial direction. With this assumption, it is possible to develop a sorbent column transport model, without using isotherm data. This simple empirical model is used to simulate the adsorption/desorption behavior of the sorbent for a specific sorbent bed configuration. The model is limited to predicting the performance with a single bed thickness and is not able to account for different bed thicknesses, as these would require isotherm and bed dispersion experimental data. The following assumptions were made to develop the model:

- Ideal gas law is assumed for all gases;
- "Air" in this study comprises of 420 ppm CO_2 in N_2;
- Only CO_2 and H_2O interact with the sorbent;
- Adsorption and desorption occur under isobaric conditions;
- There are no heat losses to the surroundings.

2.1.1. CO_2/H_2O Mass Transfer Kinetics

The mass transfer rate of CO_2 and H_2O from/to the sorbent was approximated by the linear driving force (LDF) model [18,19] (Equation (1)) where $\frac{dq}{dt}$ is the mass transfer rate (mol kg-sorbent^{-1} s^{-1}), q_{eq} is the equilibrium adsorbed amount of CO_2 or H_2O (mol kg^{-1}) under the specified process condition, and q_t is the amount adsorbed on the sorbent (mol kg^{-1}) at time t. k is the LDF mass transfer

coefficient (s^{-1}) which is a lumped parameter accounting for all the resistances to mass transfer. i refers to the components H_2O or CO_2 and j refers to ads (adsorption) or des (desorption).

$$\frac{dq_{i,j}}{dt} = k_{i,j}\left(q_{eq,i,j} - q_{t,i,j}\right) \tag{1}$$

As the desorption kinetics are affected by the temperature and the partial pressure of CO_2, the LDF mass transfer coefficient, $k_{CO_2,des}$, was expanded to account for temperature in Equation (2) and partial pressure in Equation (3). Due to the lack of isotherm data, an empirical relationship (Equation (3)) with the steam flow rate and the desorption pressure was used to predict the effect of the partial pressure of CO_2 on the desorption kinetics. In Equation (2), E_a is the activation energy (J mol^{-1}), R is the gas constant (J mol^{-1} K^{-1}) and T is temperature (°C). k_{0,CO_2} is a constant (s^{-1}) which follows an empirical relationship with the pressure (kPa abs), P, and steam flow rate (kg-steam h^{-1} kg-sorbent^{-1}), $\dot{m}_{steam}$, according to Equation (3). k_{1-5} are empirical constants.

$$k_{CO_2,des} = k_{0,CO_2} e^{-\frac{E_{a,CO_2}}{R(T+273)}} \tag{2}$$

$$k_{0,CO_2} = k_1\left(k_2 - e^{-\frac{\dot{m}_{steam}}{k_3}}\right)(k_4 P + k_5) \tag{3}$$

For H_2O mass transfer in the desorption stage, the LDF mass transfer coefficient, $k_{H_2O,des}$, was expanded according to Equation (4), to account for the effect of temperature on the kinetics.

$$k_{H_2O,des} = k_{0,H_2O} e^{-\frac{E_{a,H_2O}}{R(T+273)}} \tag{4}$$

For the adsorption stage, this study only considered a single adsorption temperature (27 °C). Therefore, the LDF constants, $k_{H_2O,ads}$ and $k_{CO_2,ads}$, were estimated as fixed values and not as relationships to the process conditions.

2.1.2. Equilibrium Model for H_2O Uptake During the Desorption Stage

The equilibrium uptake of water by the sorbent under the desorption conditions were fitted to a Freundlich isobar equation [20] (Equations (5) and (6)), where q_{eq} is the equilibrium adsorbed amount of water (mol kg^{-1}), R is the gas constant (J mol^{-1} K^{-1}), T is the temperature (°C) and P is the pressure (kPa abs). K_0 (mol kg^{-1} $kPa^{-1/n0}$), α and A_0 (J mol^{-1}) are constants.

$$q_{eq,H_2O,des} = K_0 e^{-\frac{\alpha R(T+273)}{A_0}} P^{\frac{1}{n_0}} \tag{5}$$

$$n_0 = \frac{A_o}{R(T+273)} \tag{6}$$

2.1.3. Heat Transfer Model

The heat transfer to/from the sorbent was modelled according to the energy balance given by Equation (7), where $m_{sorbent}$ is the mass of sorbent (kg), $C_{p,sorbent}$ is the specific heat capacity of the sorbent (J kg^{-1} °C^{-1}), T_{bed} is the bed temperature (°C), t is time (s), $T_{heat/cool}$ is the temperature (°C) of the medium used to heat up or cool down the sorbent bed, U is the overall heat transfer coefficient (W m^{-2} °C^{-1}) between the heating/cooling medium and the sorbent bed, A is the heat transfer area of the bed (m^2), $\dot{m}$ is mass flow rate (kg s^{-1}) and h is the specific enthalpy (J kg^{-1}).

$$\begin{aligned} m_{sorbent} C_{p,sorbent} \frac{dT_{bed}}{dt} &= UA(T_{heat/cool} - T_{bed}) + \dot{m}_{in,H_2O} h_{in,H_2O} - \dot{m}_{out,H_2O} h_{out,H_2O} \\ &+ \dot{m}_{in,CO_2} h_{in,CO_2} - \dot{m}_{out,CO_2} h_{out,CO_2} \end{aligned} \tag{7}$$

The specific enthalpies of the components were calculated according to Equation (8) where H_{ads} is the heat of adsorption (J kg^{-1}), C_p is the specific heat capacity (J kg^{-1} °C^{-1}), T is the temperature (°C) and T_{ref} is a reference temperature (°C), taken to be 50 °C for this study. H_{ads,CO_2} for this type of sorbent was previously reported to be 2270 kJ kg^{-1} [21] and $C_{p,sorbent}$ was measured to be 2 kJ kg^{-1} °C^{-1} using a SETARAM micro DSC III. H_{ads,H_2O} of 2611 kJ kg^{-1} was adopted from Wurzbacher et al. [9].

$$h_i = H_{ads,i} + C_{p,i}\left(T - T_{ref}\right) \tag{8}$$

i refers to the component CO_2 or H_2O.

2.1.4. Experimental Validation of Adsorption/Desorption Model and Parameter Estimation

The experimental data for the validation of the adsorption/desorption model was acquired using the procedure described in Wijesiri et al. [17].

The parameters for Equation (1) for the mass transfer kinetics in the adsorption stage ($k_{i,ads}$ and $q_{eq,i,ads}$) were determined by doing a least squares regression fit of the LDF model on the experimental data for CO_2/H_2O uptake ($q_{t,ads}$) from 420 ppm CO_2 at 27 °C, under dry conditions and with 1% mol-H_2O. The experimental data showed minimal changes in temperature (≤ 1 °C) for both cases, so the adsorption stage was assumed to be isothermal.

For the desorption stage, the CO_2 mass transfer kinetics were experimentally determined for the range of desorption conditions discussed in this study. Essentially all the CO_2 was desorbed [17] and therefore the equilibrium adsorbed amount ($q_{eq,CO_2,des}$ term in Equation (1)) was assumed to be 0.00 mol kg^{-1} for all the desorption conditions. The constants E_{a,CO_2} and k_1 to k_5, were estimated by least squares regression of the experimental CO_2 desorption data ($q_{t,des}$).

Similarly, the parameters for the Freundlich isobar (Equations (5) and (6)) were estimated by least squares regression of the experimental equilibrium H_2O uptake data.

As it was not possible to obtain data on the H_2O mass transfer kinetics during the desorption stage with the experimental set up used, it had to be approximated by using the bed temperature data and the heat transfer model (Equation (7)). To do this, the heat transfer coefficient from the oven to the sorbent bed, U was obtained by fitting the heat transfer model of the clean sorbent bed, Equation (7), (with no CO_2 or H_2O adsorbed) against the experimental bed temperature data (T_{bed}).

The mass transfer kinetics of H_2O during the desorption stage were determined by coupling the mass transfer model (Equations (1)–(4)) with the heat transfer model (Equation (7)). The $\dot{m}_{out,H_2O}$ term in Equation (7) was defined according Equation (9), where MW_{H_2O} is the molar mass of H_2O (kg mol^{-1})

$$\dot{m}_{out,H_2O} = \dot{m}_{in,H_2O} - \frac{dq_{H_2O}}{dt} \times m_{sorbent} \times MW_{H_2O} \tag{9}$$

k_{0,H_2O} and E_{a,H_2O} in Equation (4) were determined by least squares regression fitting Equation (7) to the experimental bed and oven temperature data with the $\dot{m}_{in,CO_2}$, $\dot{m}_{out,CO_2}$ and $\dot{m}_{in,H_2O}$ data from the experiments.

2.2. Process Model and Economic Model

2.2.1. Air-Sorbent Contactor Configuration

For the scaled-up process, an air-sorbent contact similar to that described in Patent WO2014170184A1 [22] was considered. This consists of a series of stacked thin cylindrical adsorption beds contained in a larger contactor (see Figure 1a). In such a contactor, air flows in through the inlet on one side, flows up across the thickness of the sorbent bed, and exits through another side of the contactor. The heating and cooling of the bed is envisioned to be done by heat transfer coils directly under the sorbent beds. When scaling up, it was assumed that the ratio of heat transfer to mass of sorbent would be kept the same as the lab scale experimental set up used. The beds were

2.26 m in diameter $\left(d_{bed,contactor}\right)$ which is close to the maximum recommended for adsorption beds [23]. The height ($H_{bed,contactor}$) was 0.10 m; this being the same height as the laboratory scale experiments. The void factor (ϵ) of the beds was assumed to be 0.5. It was also assumed that the diameter of the sorbent pellets, d_{pellet}, used in the contactor would be the same as the lab scale set up (1.8 mm). These dimensions correspond to 250 kg of sorbent per bed. For the current study, a contactor with 16 beds, with a total of 4000 kg of sorbent per contactor, was considered.

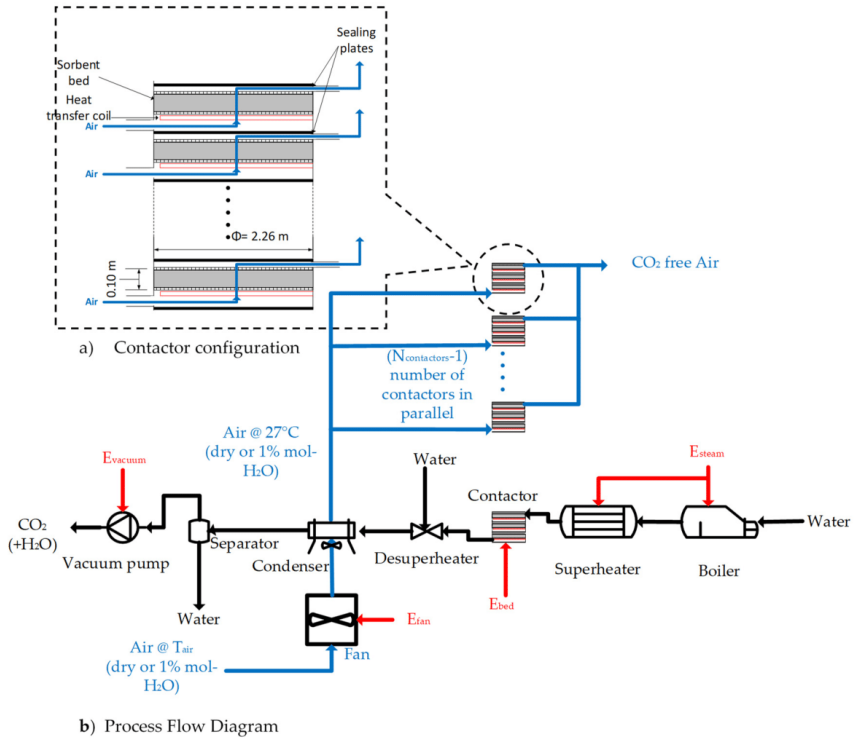

Figure 1. (**a**) A schematic of the proposed air-sorbent contactor configuration and (**b**) the process flow diagram of the proposed Direct Air Contact (DAC) system.

2.2.2. Process Description

The process model considers two scenarios in order to determine the effect of moisture inherent in air collected from the surroundings: adsorption from dry air and adsorption from air with a moisture content of 1% mol-H_2O. In both scenarios, the adsorption is carried out at 27 °C. These two scenarios are referred to as the "dry case" and "humid case".

A schematic of the process considered for the current study is depicted in Figure 1b. The process consists of multiple contactors adsorbing CO_2 from air in parallel, and a single contactor desorbing CO_2. In the adsorption stage, the incoming air is heated up to the adsorption temperature (27 °C) and pushed through the contactors using a fan. The air is heated, as it was previously discovered [16] that higher temperatures led to higher CO_2 uptake, due to improved diffusion kinetics. Heating the air also provides the cooling necessary for the condensation of steam in the desorption stage. A previous study [16] reported that this sorbent had the highest CO_2 uptake at 46 °C. However, as this temperature

corresponds to unrealistically warm climates, and heating the air to 46 °C would require a significant amount of energy, a milder adsorption temperature of 27 °C is considered for the current study.

The temperature at which the air could enter the process, T_{air} (°C), was calculated according to Equation (10), where $Q_{condenser}$, is the cooling duty of the condenser (W) (refer Section S1 of the Supplementary Information), $\dot{m}_{air}$ is the mass flow rate of air per contactor (kg s^{-1}), C_p is the specific heat capacity of air (J kg^{-1} $°C^{-1}$) and $N_{contactors}$ is the number of contactors in the system. The relative humidity (RH) values corresponding to 1% mol-H_2O for the humid case were calculated according to Equation (11), where P_{air} is the pressure of the air which is assumed to be 101 kPa abs, and p_{sat,H_2O} is the saturation vapour pressure of water, calculated according to the Antoine correlation [24].

$$T_{air} = 27 - \frac{Q_{condenser}}{\dot{m}_{air} C_{p.air} \times (N_{contactors} - 1)} \quad (10)$$

$$RH = \frac{P_{air} \times 1\%}{P_{sat,H_2O}} \quad (11)$$

In the desorption stage, water is boiled and superheated to produce steam, which is then passed through the contactor. Downstream of the contactor, the steam is desuperheated via the addition of water, and passed through the condenser, which cools the CO_2/H_2O mixture down to 45 °C. Following this, the condensate is separated from the gas and returned to the boiler. The gas stream from the condenser, consisting of CO_2 saturated with H_2O, is compressed to atmospheric pressure using the vacuum pump. The calculations for the unit operations in the process are described in S1 in the Supplementary Information.

The adsorption/desorption cycle the contactors are subjected to is shown in Figure 2a. The cycle is split into three stages. Firstly, the contactor goes through the adsorption stage, until a predetermined amount of CO_2 (q_{ads}) is adsorbed into the bed. The desorption stage starts by first evacuating the contactor to the desorption pressure and heating up the sorbent to the desorption temperature. The heating is provided by a heat transfer fluid, at 10 °C higher than the desorption temperature, passing through the heating coils shown in Figure 1. After the sorbent is heated to just above the steam dew point temperature, the steam purge is started. Following the introduction of steam, heat is continuously supplied to the bed, to maintain the desorption temperature, for the remainder of the desorption stage. The desorption stage ends after a predetermined amount of CO_2 (q_{des}) is desorbed. Following this, the bed goes into the cooling stage, where the bed is cooled down to the adsorption temperature by passing water, at 25 °C, through the cooling coils. Finally, the contactor is re-pressurized and goes back into the adsorption stage. For this study, it was assumed that the evacuation and re-pressurization steps would take negligible time. The operational sequence of the contactors is shown in Figure 2b, which shows how the contactors are subjected to the cycles, with one bed in desorption at all times.

2.2.3. Energy Consumption

The energy requirements considered for the evaluation are the electrical energy required to operate the fan (E_{fan}) in the adsorption stage and the vacuum pump (E_{vacuum}) in the desorption stage, and the thermal energy required to heat the sorbent beds (E_{bed}) and to produce steam (E_{steam}). The methods for calculating these are presented in Section S2 of the Supplementary Information.

2.2.4. Capital Cost

The purchased equipment costs of the major equipment were estimated using cost correlations [23,25,26]. The cost correlations were adjusted for inflation using the chemical engineering plant cost index (CEPCI). The total plant cost was calculated by accounting for insulation, piping, instrumentation, electrical work, civil and structures, and lagging [27]. The detailed calculations are included in Section S3 of the Supplementary Information.

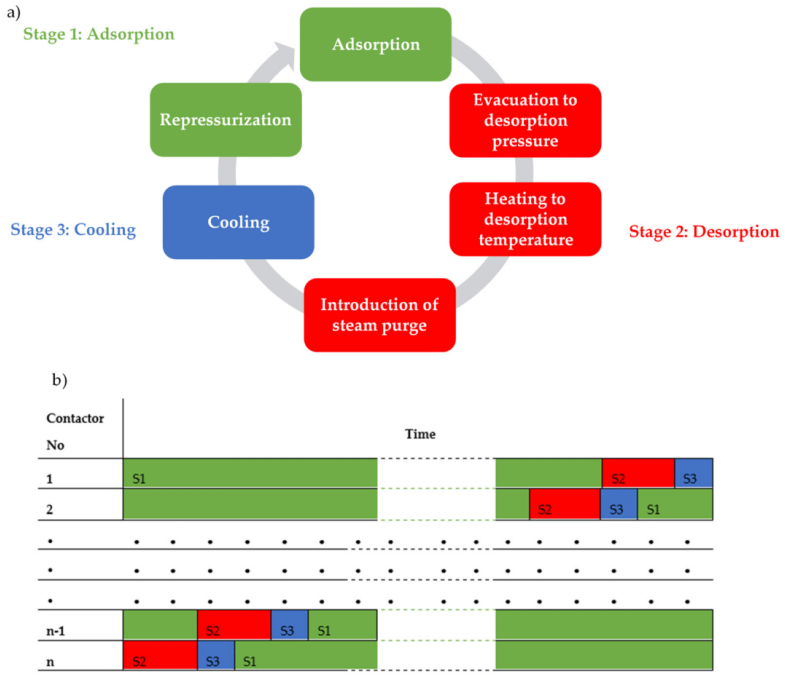

Figure 2. (**a**) The adsorption/desorption cycle the contactors are subjected to. (**b**) The operational sequence of the contactors, with one bed in desorption at all times and the rest in adsorption. S1 to S3 refer to the stages in the adsorption/desorption cycle (adsorption, desorption and cooling).

2.2.5. Operating Cost

The energy requirements of the process were assumed to be met by a solar thermal hot water system and a solar photovoltaic system to minimize the CO_2 emissions from the process. The energy costs were taken to be 50 USD MWh^{-1} for thermal energy [28] and 100 USD MWh^{-1} for electrical energy [29]. The cost of water was taken to be 3 USD m^{-3} [30] and the annual maintenance was assumed to be 2% of the total plant cost [27]. The sorbent was assumed to cost 8.1 USD kg^{-1} and have a lifetime of 4 years. The cost of the sorbent was estimated by calculating the cost of the raw materials required and multiplying it by a factor of 3 to account for the production costs. More details are included in Section S4 of the Supplementary Information.

2.2.6. Cost of Capture

The cost of capture of CO_2 (C_{CO_2}) in USD $tonne^{-1}$ is calculated from a discounted cash flow calculation to obtain a zero Net Present Value (NPV) at the end of the project life using Equation (12), where C_{CO_2} is the cost of capture (USD $tonne^{-1}$), C_{plant}, $C_{annual\ opex}$ and $C_{sorbent}$ are the capital cost of the plant, annual operating cost, and the cost of sorbent, respectively.

CR is the annual capture rate (tonne yr^{-1}) as calculated according to Equation (13), where q_{des} is the amount of CO_2 desorbed (referred to as the extent of desorption from hereon) per cycle (mol kg^{-1}), $m_{sorbent}$ is the mass of sorbent in a single contactor (kg), MW_{CO_2} is the molar mass of CO_2 (kg mol^{-1}), $N_{contactors}$ is the number of contactors in the system, and t_{cycle} is the total cycle time (h). The process was assumed to run 360 days a year for 24 h a day. More details are given in Section S5 of

the Supplementary Information. For the NPV analysis, the plant operating lifetime is 20 years and a discount rate of 10% is used.

$$C_{CO_2} = \frac{(C_{plant} + C_{annual\ opex} \sum_{x=1}^{20} \frac{1}{(1+0.1)^x} + C_{sorbent} \sum_{y=0,4,\ldots,16,20} \frac{1}{(1+0.1)^y})}{CR \times \sum_{x=1}^{20} \frac{1}{(1+0.1)^x}} \quad (12)$$

$$CR = \frac{(q_{des} \times m_{sorbent} \times MW_{CO_2} \times N_{contactors})}{t_{cycle}} \times 8.64\ h\ year^{-1}\ t\ kg^{-1} \quad (13)$$

2.3. Multi-Objective Optimization

To determine the preferred operating conditions which would result in the lowest cost of capture and the highest capture rate, a multi-objective optimization (MOO) was carried out on the process model using the MATLAB *gamultiobj* function. This uses a controlled, elitist genetic algorithm (a variant of NSGA-II [31]). The objectives for the MOO were to minimize (C_{CO_2}) and maximize (CR). The objectives, variables and the constraints of the MOO problem are listed in Table 1.

Table 1. Definition of multi-objective optimization problem.

Objectives		
Min (C_{CO_2}) and Max (CR)		
Variables		
Variable		*Range*
Adsorption air flow rate to a single contactor ($m^3\ h^{-1}$ kg-sorbent^{-1})	$\dot{V}_{air}$	2 to 10
Total number of contactors	$N_{contactors}$	2 to 60
Desorption temperature (°C)	T_d	80 to 100
Desorption pressure (kPa abs)	P_d	12 to 26
Desorption steam flow rate (kg h^{-1} kg-sorbent^{-1})	$\dot{m}_{steam}$	0.09 to 1.86
Extent of adsorption (mol kg^{-1})	q_{ads}	0.25 to 1.50 (dry case) 0.25 to 2.75 (humid case)
Extent of desorption (mol kg^{-1})	q_{des}	0.20 to 1.45 (dry case) 0.20 to 2.70 (humid case)

Additionally, the constraint in Equation (14) was enforced to ensure that all the contactors can be desorbed within a single cycle, where t_{ads} and t_{des} are the durations of the adsorption and desorption stages (h) and $N_{contactors}$ is the number of contactors in the system.

$$t_{ads} \geq t_{des} \times (N_{contactors} - 1) \quad (14)$$

2.4. Sensitivity Analysis

Two sensitivity analyses were carried out. Firstly, the sensitivity of the results of the cost of capture to some of the values in the model which carried uncertainty were tested. This was done by varying these values by ±10% from the original values and observing the change in the cost of capture in the lowest cost scenario. The values of interest chosen were cost of energy, cost of the contactor, discount rate, sorbent cost and lifetime and the plant lifetime.

Next, the sensitivity of the results to the MOO parameters used was tested. This was done by varying the parameters used for the original MOO.

3. Results of Model Validation and Parameter Estimation

The experimental data and the model predictions for CO_2/H_2O mass transfer in the adsorption stage are presented in Figure 3. The CO_2 mass transfer, equilibrium H_2O uptake, H_2O mass transfer kinetics and heat transfer in the desorption stage are presented in Figures 4–6. The figures show that

the experimental data are in close agreement with the model predictions. The results of the parameter estimations are listed in Table 2 along with the constants used.

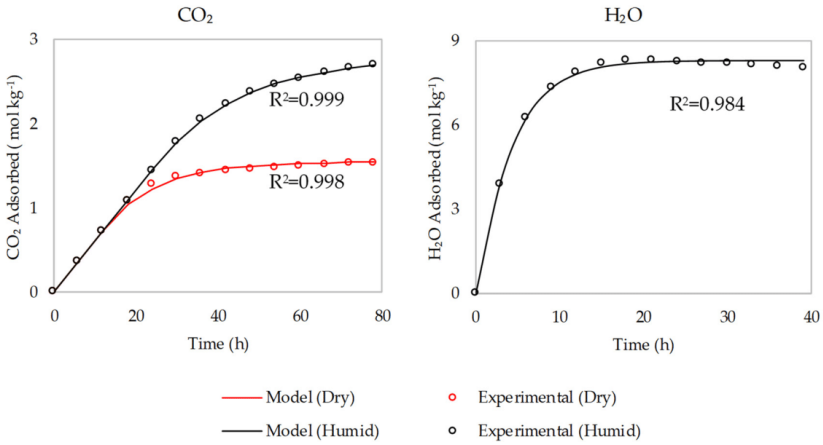

Figure 3. The experimental data and the model predictions for CO_2 and H_2O adsorption from 420 ppm CO_2 in N_2 in the dry and humid cases.

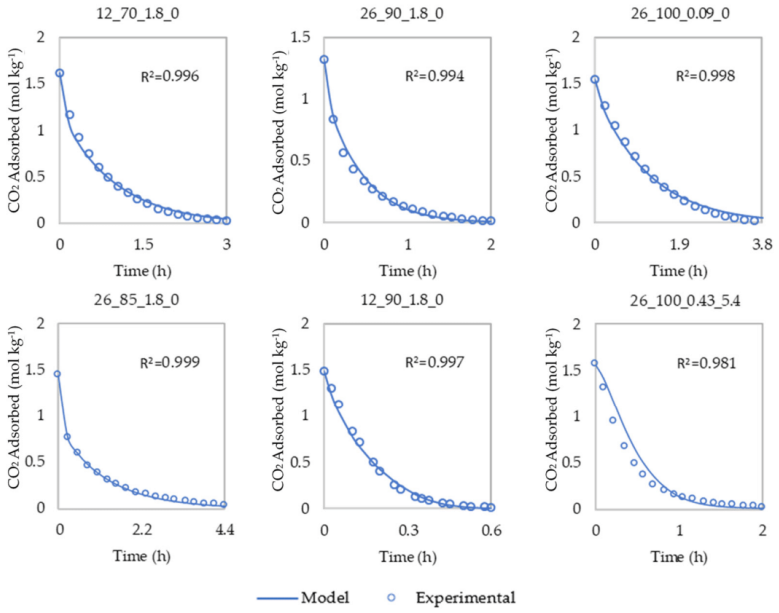

Figure 4. The experimental data and the model predictions for CO_2 mass transfer kinetics in the desorption stage. Legend for titles AA_BBB_CCC_DD (AA- desorption pressure (kPa abs), BBB-desorption temperature (°C), CCC- desorption steam flow rate (kg h^{-1} kg-sorbent^{-1}), DD- amount of water adsorbed during adsorption stage (mol kg^{-1})). More results are depicted in Figure S1 in the Supplementary Information.

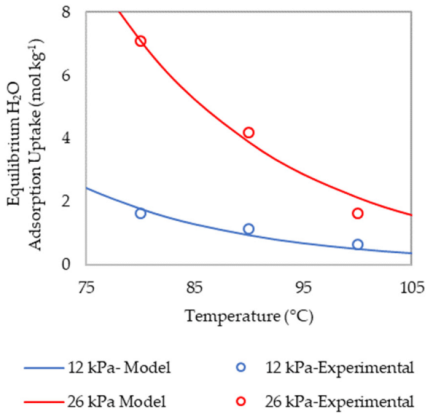

Figure 5. The experimental data and the model predictions for equilibrium H_2O adsorption amount in the desorption stage at desorption pressures of 12 kPa and 26 kPa abs.

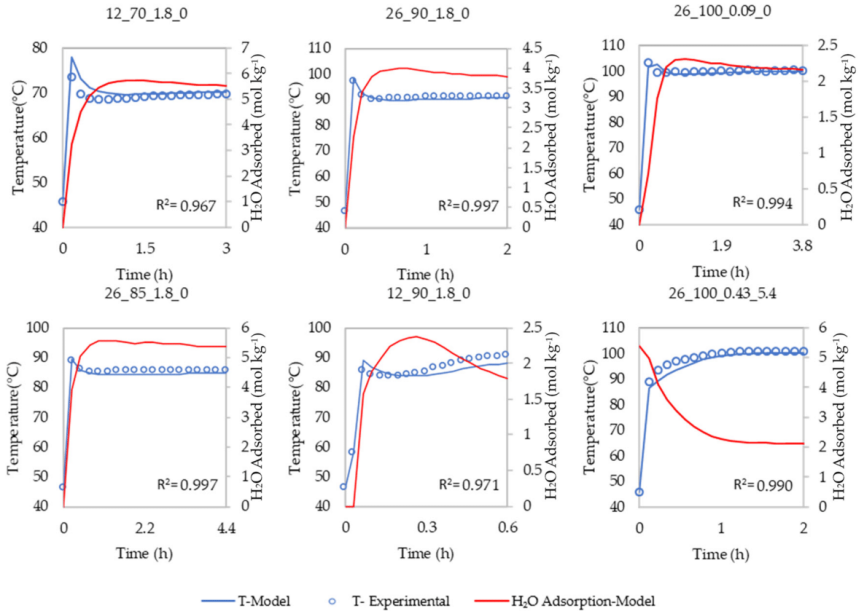

Figure 6. The experimental data and the model predictions for heat transfer and H_2O mass transfer kinetics in the desorption stage. Legend for titles AA_BBB_CCC_DD (AA- desorption pressure (kPa abs), BBB-desorption temperature (°C), CCC- desorption steam flow rate (kg h^{-1} kg-sorbent^{-1}), DD- amount of water adsorbed during adsorption stage (mol kg^{-1})). More results are depicted in Figure S2 in the Supplementary Information.

Table 2. The results of the parameter estimation for the adsorption/desorption model and the constants used.

Parameter	Value
Adsorption stage mass transfer	
Dry case	
$k_{CO_2,ads}$ (s^{-1})	2.21×10^{-5}
$q_{eq,CO_2,ads}$ (mol kg^{-1})	1.55×10^{0}
Humid case	
$k_{CO_2,ads}$ (s^{-1})	1.31×10^{-5}
$q_{eq,CO_2,ads}$ (mol kg^{-1})	2.80×10^{0}
$k_{H_2O,ads}$ (s^{-1})	6.74×10^{-5}
$q_{eq,H_2O,ads}$ (mol kg^{-1})	8.30×10^{0}
Desorption stage mass transfer	
CO_2 mass transfer kinetics	
E_{a,CO_2} (J mol^{-1})	1.44×10^{5}
k_1 (s^{-1})	1.06×10^{0}
k_2	1.03×10^{0}
k_3 (kg-steam h^{-1} kg-sorbent^{-1})	7.56×10^{-1}
k_4 (kPa^{-1})	-2.29×10^{13}
k_5	6.66×10^{14}
Freundlich isobar for H_2O	
K_0 (mol kg^{-1} $kPa^{-1/n0}$)	1.30×10^{7}
α	1.51×10^{1}
A_0 (j mol^{-1})	1.63×10^{3}
H_2O mass transfer kinetics	
E_{a,H_2O} (J mol^{-1})	4.05×10^{3}
k_{0,H_2O} (s^{-1})	1.90×10^{3}
Desorption stage heat transfer	
U_{lab} (W m^{-2} °C^{-1})	1.70×10^{1}
Lab scale sorbent bed dimensions	
A_{lab} (m^2)	3.14×10^{-3}
$m_{sorbent,lab}$ (kg)	3.45×10^{-3}
Thermodynamic properties and constants	
$C_{p,sorbent}$ (J kg^1 °C^{-1})	2.00×10^{3}
C_{p,CO_2} (J kg^1 °C^{-1})	9.00×10^{2}
$C_{p,steam}$ (J kg^1 °C^{-1})	2.00×10^{3}
$C_{p,air}$ (J kg^1 °C^{-1})	1.00×10^{3}
H_{ads,H_2O}(J kg^{-1})	2.61×10^{6}
H_{ads,CO_2}(J kg^{-1})	2.27×10^{6}

4. Results of Multi-Objective Optimization

The plots of the Pareto non-dominated fronts from the results of the MOO are presented in Figures 7 and 8 for the dry and the humid cases. From Figure 7, it is apparent that the dry case allows for a lower cost of capture than the humid case for all capture rates. Moreover, it can be seen that the cost of capture increases as the capture rate is increased for both cases. From Figure 8, it is apparent that as the capture rate is increased, $N_{contactors}$, $\dot{m}_{steam}$ and q_{ads} are also increased. Additionally, P_d is reduced for the humid case. Negligible changes are seen in the other parameters.

The set of variables which yielded the lowest cost scenarios for the humid and the dry cases are listed in Table 3, along with the resulting cycle times and energy requirements of the process.

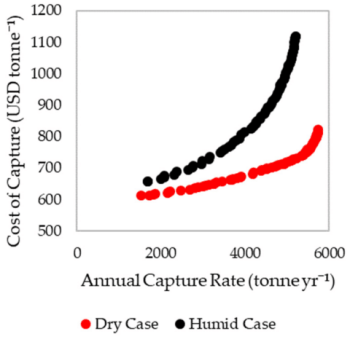

Figure 7. Pareto plots for the objective functions of the Multi-Objective Optimization (MOO) for the dry and the humid cases.

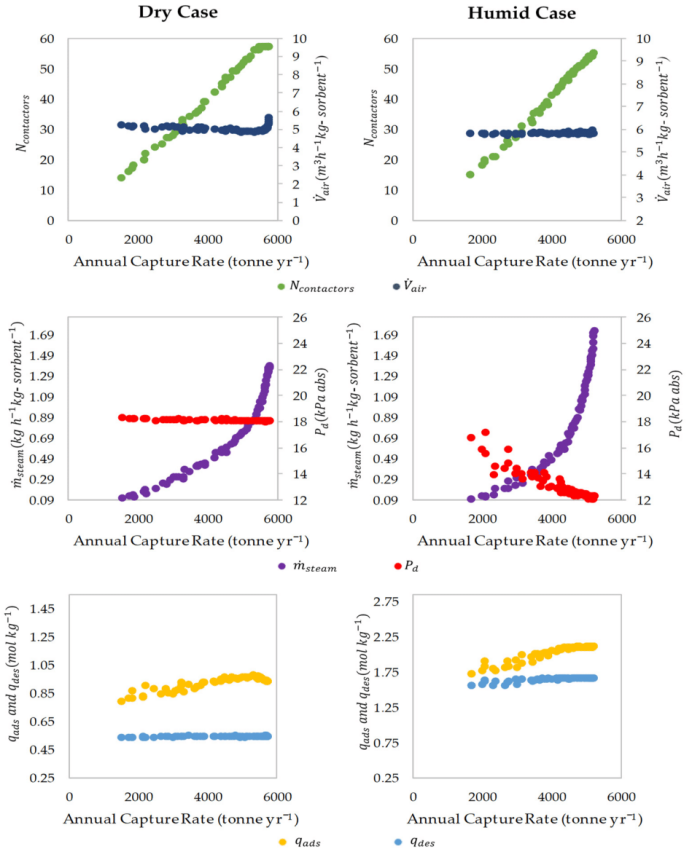

Figure 8. Pareto plots for the variables plotted against the capture rate, for the humid and the dry case. The limits for the y-axes are the bounds for each parameter used in the MOO. T_d was not plotted as it was constant at 100 °C across all the data points.

Table 3. The process conditions which yield the lowest cost scenarios and the resulting cycle times and energy requirements of the process.

Parameter		Dry	Humid
Variables			
Adsorption air flow rate to a single contactor (m^3 h^{-1} kg-sorbent^{-1})	$\dot{V}_{air}$	5.23	5.81
Total no of contactors	$N_{contactors}$	14	15
Desorption temperature (°C)	T_d	100	100
Desorption pressure (kPa abs)	P_d	18.33	16.85
Desorption steam flow rate (kg h^{-1} kg-sorbent^{-1})	$\dot{m}_{steam}$	0.11	0.11
Extent of adsorption (mol kg^{-1})	q_{ads}	0.79	1.72
Extent of desorption (mol kg^{-1})	q_{des}	0.54	1.55
Cycle times			
Adsorption (h)	t_{ads}	6.87	19.53
Desorption (h)	t_{des}	0.52	1.39
Cooling(h)	t_{cool}	0.11	0.11
Full cycle (h)	t_{cycle}	7.51	21.03
Energy requirement			
Electrical energy for fan (GJ $tonne^{-1}$)	E_{fan}	1.35	1.71
Electrical energy for vacuum pump (GJ $tonne^{-1}$)	E_{vacuum}	0.61	0.65
Thermal energy for steam (GJ $tonne^{-1}$)	E_{steam}	7.05	6.26
Thermal energy to heat sorbent (GJ $tonne^{-1}$)	E_{bed}	6.14	9.45
Total electrical (GJ $tonne^{-1}$)	$E_{electrical}$	1.96	2.36
Total thermal (GJ $tonne^{-1}$)	$E_{thermal}$	13.18	15.71
Total (GJ $tonne^{-1}$)	E_{total}	15.14	18.08
Cost and capture rate			
Cost of capture (USD $tonne^{-1}$)	C_{CO2}	612	657
Annual capture rate (tonne yr^{-1})	CR	1521	1682

The temperature and RH at which the air could enter the process for each of the points in the Pareto plots, as calculated with Equations (10) and (11), are depicted in Figure 9.

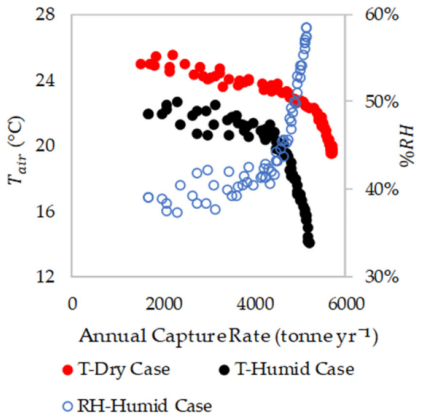

Figure 9. The temperature and RH of the inlet air to the process for each of the points in the Pareto plots.

The breakdown of the cost of capture for the preferred conditions is shown in Figure 10. It was observed that both the dry and humid case showed a similar cost breakdown. The biggest contributors were identified as the cost of thermal energy and the contactors.

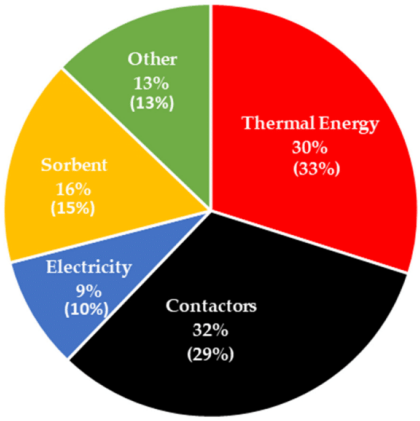

Figure 10. The contributions of various components to the cost of capture for the lowest cost case for the dry and humid case. The value for the humid case is given inside brackets in the data labels.

The results of the sensitivity analysis on the model values is shown in Figure 11. As the two cases had a similar cost breakdown, the sensitivities were almost identical.

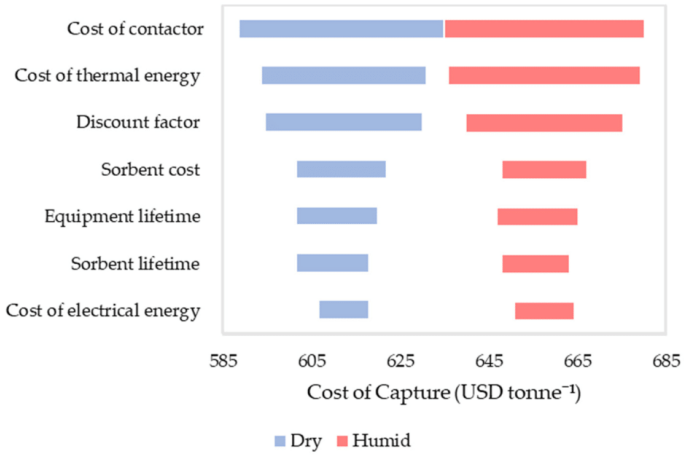

Figure 11. Tornado plot of the sensitivity of the cost of capture of the lowest cost scenarios for ± 10% changes in the model values.

5. Discussion

5.1. Influence of Process Conditions

It can be noted that the cost of capturing under humid conditions is higher than that under dry conditions for all the capture rates in the Pareto fronts (Figure 7). The presence of moisture allows the process to take advantage of the improved CO_2 adsorption capacities of the sorbent [16] as indicated by the higher q_{ads} and q_{des} in the humid case. However, this also leads to a longer t_{ads} and t_{des}, which increases t_{cycle}. This reduces the annual capture rate, and so increases the cost of capture (see Equations (12) and (13)).

In the humid case, the process is restricted from using smaller q_{ads} and q_{des}, due to the large amount of water adsorbed. As the water adsorption/desorption is significantly faster than that of CO_2 (see Figure 3), at lower q_{ads} and q_{des} (shorter t_{ads} and t_{des}) values, there is a much higher proportion of H_2O adsorbed in comparison to CO_2. This in turn translates to a proportionately higher cost of thermal energy consumed for desorbing the H_2O. And as the thermal energy accounts for a large fraction of the cost, this has a significant impact on the economics of the process. These results indicate that using a sorbent with a reduced affinity for water may improve the economics of the process.

When comparing the process conditions which yielded the lowest cost scenario, both the humid and the dry case had a similar adsorption air flow rate ($\dot{V}_{air}$), desorption temperature (T_d) and desorption pressure (P_d). At high $\dot{V}_{air}$, the rate at which CO_2 can be captured is increased, which can reduce the cycle time. However, this is done at the compromise of higher pressure drops across the contactors resulting in an increased electrical energy consumption.

The preferred T_d was identified as 100 °C which is the upper limit used for the optimization. This is due to the faster desorption kinetics presented at higher temperatures [17], which leads to shorter cycle times. The upper limit for this study was set at 100 °C, as solid supported amines have been reported to undergo degradation at high temperatures [32]. However, the sorbent in this study was previously reported [17] to be stable at temperatures up to 100 °C, under the desorption conditions evaluated here. In the case of P_d, the preferred value is a balance between benefitting from the faster desorption rates (shorter cycle times) offered by the lower pressures [17] and the increased expenses for electrical energy.

The identification of the preferred steam flow rate, $\dot{m}_{steam}$, is similar to that of P_d. The preferred value is a balance between benefitting from the faster desorption rates (shorter t_{des}) offered by the faster steam flow rates [17] at the compromise of increased cost of thermal energy. In both cases, the steam flow rate with the lowest cost was the close to its lower bounds, indicating that benefit of shorter t_{des} is not justified by the higher energy cost. This can be attributed to the fact that thermal energy demand has the one of the biggest impacts on the economics of the process (see Figure 10).

When comparing the energy requirements, the electrical energy consumption was similar for both cases. However, the humid case needed more thermal energy to heat up the sorbent during the desorption. This is because the energy consumed by the water being desorbed from the sorbent, cools it down [17]. Therefore, more heat needs to be provided in the humid case, to maintain the desired desorption temperature.

From Figure 11, it can be seen that both cases display similar sensitivities to the values studied. The final result was seen to be relatively insensitive to the values studied, as the cost was seen to vary by <±4% for a variation of ±10% in the parameters. The cost of thermal energy and the contactor were identified to be the variables which most affected the cost of capture. This is consistent with the fact that thermal energy and the cost of the contactor are the two largest contributions to the cost (see Figure 10). The discount factor was also seen to have a large impact on the cost of capture and a value of 10% is conservative for the current economic conditions.

5.2. Pareto Non-Dominated Fronts

In both cases, the cost of capture increases as the capture rate increases. As seen in the Pareto plots of the variables (Figure 8), the increase in the capture rate is achieved mainly by using a higher $N_{contactors}$ which increases the amount of CO_2 captured. However, to increase $N_{contactors}$, either t_{ads} needs to be increased or t_{des} needs to be decreased to satisfy the inequality constraint in Equation (14). This is fulfilled by increasing $\dot{m}_{steam}$, which shortens t_{des} by improving the CO_2 desorption kinetics. P_d is also decreased for the humid case, which can be attributed to the comparatively longer t_{des}, which demands a greater increase in the kinetics to satisfy the inequality constraint in Equation (14). Furthermore, q_{ads} is increased to increase the t_{ads} and q_{des} is kept relatively constant which shortens t_{des} when used in combination with higher $\dot{m}_{steam}$, and lower P_d. These changes to the process conditions (except q_{des}) increase the annual capture rate while incurring additional expenses as explained in Section 5.1.

The increases in the thermal energy demand and the contactors are particularly significant as they are the two biggest contributors to the economics of the process.

$\dot{V}_{air}$, can be seen to be relatively constant for most of the Pareto front. This can be expected since it is selected based on the compromise between the positive effect of a shorter t_{ads} and the negative of a higher energy requirement for high flow rates. It is likely that the balance between the two does not significantly vary for the different points in the Pareto plot. In the dry case, there is a steep increase in $\dot{V}$ at the higher capture rate end which coincides with a steep increase in the cost. This highlights that while slightly higher capture rates can be achieved with higher $\dot{V}_{air}$, it is accompanied by a significant increase in the cost.

The results of the sensitivity analysis carried out on the MOO options is included in Section S6 of the Supplementary Information, and it is evident that the Pareto fronts are insensitive to the MOO options used.

5.3. Temperature and RH of the Incoming Air to the Process

For the lowest cost cases, the incoming air temperature, T_{air}, was calculated to be 25 °C for the dry case and 22 °C for the humid case (see Figure 9). The RH of the humid case was calculated to be 39%. It is noted that, while the dry case yielded a lower cost, it is unrealistic to expect completely dry conditions anywhere in the world. However, the conditions calculated for the humid case are far more realistic and can be expected of regions with sub-tropical climates.

T_{air} can be seen to reduce with increases in the capture rate (see Figure 9). This can be attributed to the higher steam flow rates available at the higher capture rate/higher cost end of the Pareto fronts. It is also apparent that the humid case allows for significantly lower temperatures. This is owing to the water which gets desorbed from the sorbent which condenses, releasing additional thermal energy. These results indicate that the process could operate in colder climates with higher humidity, at the compromise of a higher cost of capture. It is also noteworthy that when operating at a higher moisture level than 1% mol-H_2O, lower T_{air} may be achieved due to the increased adsorption of water, although this would also likely lead to a higher cost of capture.

5.4. Comparison to Results of Other Studies

The cost and energy data for the lowest cost case described in the current study is presented alongside data found for other DAC processes [4–9,12,14,33] in Figure 12. The data are that of the lowest cost case described in the respective studies.

It is evident that the cost of capture presented in the current study is in the upper end of the range of costs reported for similar processes. However, it can be noted that the cost in the current study is similar to that reported by Climeworks based on the actual performance of their first-generation DAC system (DAC-1) [12]. In comparison, the other values depicted in Figure 12 are subjective to the scope of the respective study and the assumptions that were used. For example, Kulkarni and Sholl [7] and Zhang et al. [6] did not include the capital expenses of the equipment in their studies. Krekel et al. [5] expanded on the work carried out by Zhang et al. [6], and reported that once the capital expenses are included, the cost of capture is increased significantly. Moreover, the costs of capture depicted in Figure 12 for Zhang et al. [6] and Krekel et al. [5] are based on scenarios where the energy is supplied with fossil fuels, as opposed to the low carbon solar energy used here. Krekel et al. [5] reported that the cost of capture increases from 792 to 1333 USD tonne^{-1} when the emissions from energy generation are considered. They further reported that if wind energy is used, a capture cost of 824 USD tonne^{-1} can be achieved. Zhang et al. [6] estimated an increase from 91 to 225 USD tonne^{-1} for a system utilizing wind and nuclear energy.

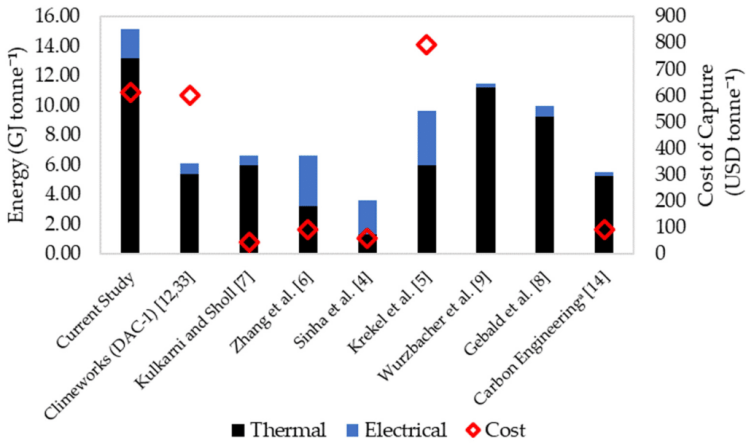

Figure 12. Comparison of the cost and energy data from this study to that of previous studies. The data are that of the lowest cost case described in the respective studies. [a] Carbon Engineering refers to an aqueous hydroxide-based process for DAC.

The large difference between the results of this study and that of the Sinha et al. [4] is in part due to the two main differences. Firstly, the cash flow was not discounted [4]. The second reason is due to the nature of the sorbent used. Sinha et al. [4] evaluated a monolithic sorbent which was assumed to be self-contained. In comparison, the pelletized sorbent in the current study needs to be contained in contactors which contribute to about a third of the total cost. This may indicate the advantage that monolithic sorbents have over pelletized ones. Furthermore, Sinha et al. [4] also did not consider the CO_2 emissions from energy generation in their calculations.

Apart from these, another major reason for the higher cost reported in the current study is the slower kinetics of the sorbent evaluated. It was previously reported [16] that the large loading of PEI in this sorbent resulted in a large CO_2 uptake capacity although at the sacrifice of significant mass transfer limitations, which resulted in a slow uptake rate of CO_2. The effect of this is evident here, where long cycle times are required for the process (7.51 h for the dry case). In comparison, for other studies, the reported cycle times are in the range of 1.27 [4] to 4 h [7]. These long cycle times result in a lower annual capture rate and hence a larger cost. Furthermore, it should be noted that the subject sorbent was shown to provide better adsorption performance at the higher temperature of 46 °C [16]; thus, it may be that further improvements in the process economics could be achieved by tailoring the design of sorbent material so that its optimum sorption performance occurs at the intended adsorption temperature.

The slow kinetics also have a large effect on the energy requirement of the process. As seen in Table 3, the thermal energy requirement is dominated by the energy for steam generation, and for longer desorption times, larger amounts of steam are needed to desorb the CO_2. This would explain the larger thermal energy requirement of the process in comparison to the other studies depicted in Figure 12. However, the electrical energy requirement of the process is in close agreement with most of the values reported in literature. While Wurzbacher et al. [9] and Gebald et al. [8] reported much lower values, they only evaluated the desorption stage and did not include the energy needed to pump the air through contactors during adsorption.

It is difficult to make direct comparisons with the costs reported by Carbon Engineering [14], as this corresponds to a completely different type of process. However, it is noted that the need for very high temperatures (900 °C) for the regeneration of the sorbent, may make the process more reliant

on fossil fuel-based energy. In comparison, the processes using SSA could more easily be powered with relatively inexpensive low carbon energy sources like solar thermal hot water systems.

5.5. Case Studies

In this section, the effect of five different scenarios on the cost of capture is evaluated. The scenarios were selected based on the main cost drivers and the limitations of the process identified in the previous sections. For these evaluations, the MOO was repeated with the respective changes described below for each scenario.

Case study A: Thermal energy from waste heat utilization—This scenario was chosen because the main contributor to the cost of the capture was identified to be the thermal energy requirement. Moreover, the low temperatures (≤100 °C) used for the desorption process makes it possible for integration with waste heat sources. It was assumed that this energy could be achieved free of charge.

Case study B: Hypothetical sorbent with faster kinetics—This scenario addresses the limitation of slow mass transfer kinetics of the sorbent (longer cycle times). Here a hypothetical sorbent, with improved mass transfer kinetics of CO_2 is used. Potential means of achieving this include using additives which improve CO_2 diffusion in the amine phase [34–37] and using support materials with high surface areas [38] and/or large pore sizes [39] to better disperse the amines and thus improve their accessibility to the CO_2. To carry out the evaluation, $k_{CO_2,ads}$ in Equation (1) and k_1 in Equation (3) were multiplied by a factor of 2, to emulate a sorbent with twice as faster CO_2 mass transfer kinetics.

Case study C: Hypothetical sorbent with faster kinetics but lower CO_2 uptake capacity—This scenario considers an iteration of case study B. It is possible that the improvements made to the kinetics would come at the expense of a smaller CO_2 uptake capacity. For example, it has been reported in literature that lower PEI loadings (% wt) on the sorbent results in lower uptake capacities and faster kinetics [40,41]. For this scenario, a hypothetical sorbent where the kinetics are increased by a factor of 2, at the compromise of a halved equilibrium capacity, is evaluated. To carry out the evaluation, $k_{CO_2,ads}$ in Equation (1) and k_1 in Equation (3) were multiplied by a factor of 2, and $q_{eq,CO_2,ads}$ in Equation (1) was multiplied by 0.5.

Case study D: Combination of case studies A and B, where a sorbent with superior kinetics is used with waste heat utilization.

Case study E: Hypothetical sorbent with lower H_2O uptake capacity—As mentioned earlier, while adsorbing from humid air enhances the CO_2 uptake, a proportionately higher amount of water is also adsorbed. This results in a higher energy requirement for desorption of water. It has been reported [42] that the water uptake by PEI-silica sorbents could be reduced by using hydrophobic silica as the support material. The study [42] further demonstrated that the benefit of enhanced CO_2 capacities when adsorbing in the presence of moisture could be retained, in spite of the reduction of the water uptake. Modifications to the amine such as reducing the proportion of primary amines [43] and introduction of methyl groups [44] have also been reported to reduce the water uptake by these sorbents. For this scenario, a hypothetical sorbent, with half the water uptake capacity is evaluated. To carry out the evaluation, $q_{eq,H_2O,ads}$ in Equation (1) and K_0 in Equation (5) were multiplied by a factor of 0.5.

For case studies B–E, the current study does not attempt to identify exactly how the sorbent may be developed to meet the specified criteria but simply aims to estimate the impact each modification would have on the economics of the process. The results of this exercise are meant to be taken as a guide, for identifying the direction future research into sorbent development may head towards.

The results of the case studies are depicted in Figure 13. From the results, it is evident that using waste heat to provide the thermal energy yields the biggest reduction (~ 42%) in the cost of capture. This reduction is an effect of two things. Firstly, the large contribution of the thermal energy to the cost is eliminated. Secondly, the process takes advantage of the free thermal energy and utilizes higher $\dot{m}_{steam}$ to increase the capture rate. This is evident in the thermal energy demands which are more than 3-fold higher than that of the base case. The higher $\dot{m}_{steam}$ facilitates faster desorption

which reduces t_{cycle}, which in turn lowers the cost of capture. While the reductions are attractive, it should also be noted that the utilization of waste heat would restrict the locations where DAC systems could be operated to areas such as industrial parks. DAC systems with waste heat utilization would also likely be more practical for carbon capture and utilization projects rather than carbon capture and sequestration projects. This is because sequestration sites would likely be located far away from industrial sites, which would require the transportation of CO_2, incurring additional costs. In comparison, the utilization could be done at the same site the capture is done.

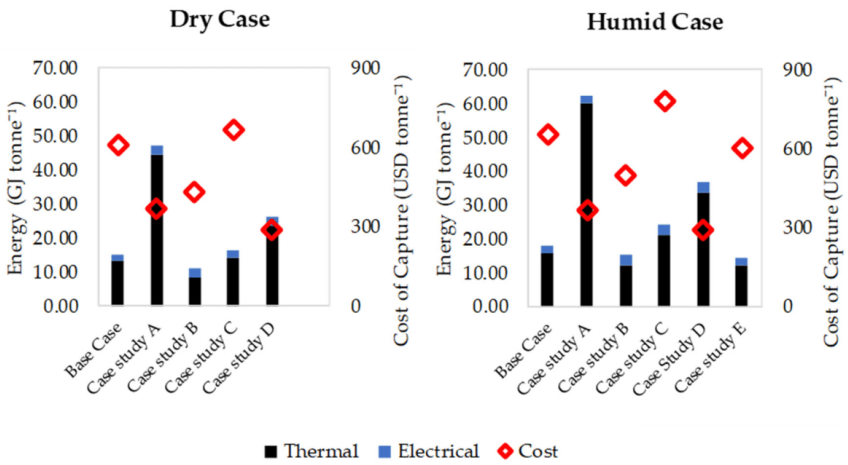

Figure 13. Results of the case studies for the dry and the humid case.

When comparing cases B to E, it can be seen that developing sorbents with improved CO_2 mass transfer kinetics would have the biggest impact on reducing the cost (~27% reduction). With faster kinetics, shorter t_{cycle} could be achieved, which reduces the cost of capture. The thermal energy demand can also be seen to reduce as hypothesized. However, case study C shows that the improvements to the kinetics of the sorbent should not be made at the expense of the CO_2 uptake capacity. Case study D shows that combining faster sorbents with waste heat utilization could lower the cost of capture by ~54%. Finally, case study E shows that an 8% reduction in cost can be achieved by using less hygroscopic sorbents, which can be attributed to the reduced thermal energy requirement. Although the costs for these case studies are still quite high, these give an indication of the relative impact each modification could have on the economics of the process.

6. Conclusions

A process model was proposed, for a DAC process employing a S-TVSA cycle, and validated with laboratory experimental results. To evaluate the technoeconomic performance of the process, the model was subjected to a MOO with the objectives of minimizing the cost of capture and maximizing the amount of CO_2 captured. A minimum cost of capture of 612 USD tonne^{-1} was calculated for a process with air entering at 25 °C under dry conditions, and a cost of 657 USD tonne^{-1} was calculated for air entering at 22 °C and 39% RH. The humid case yielded higher costs than the dry case, as an effect of the additional energy required to desorb the water that gets co-adsorbed on the sorbent. While the dry case yielded the lower cost, it is noted that the humid case is more realistic for practical DAC systems, and that the inlet air conditions correspond to that typical of subtropical climates. It was observed that the capture rate of the process could be increased (at the expense of a higher cost of capture) by increasing the number of contactors, using more aggressive desorption conditions and changing the

cycle times. The process variables which had the most effect on the results were identified as the steam flow rate and the number of contactors. The relatively higher costs calculated here, in comparison to the results of prior studies, were identified to be a result of the differences in the assumptions and scope of the respective studies, and the slower kinetics of the sorbent evaluated in the current study. It was identified that using a sorbent with two-fold faster kinetics could reduce the cost by ~27% and that the utilization of waste heat could produce a ~42% reduction in cost. A combination of both would allow the cost to be reduced by ~54%.

In summary, the process evaluated in this study does not appear to be economically feasible in the current state. However, the study identified several avenues which could lead to improvements. Of these, the improvements in sorbent design suggested here could realistically be achieved even with the current state of the technology. However, further research is needed for areas such as the development of low-cost contactors. If a combination of these improvements is achieved, this DAC process has the potential to be economically feasible and a valuable tool for combatting climate change in the future.

Supplementary Materials: The following are available online at http://www.mdpi.com/2227-9717/7/8/503/s1, Section S1: Calculations for the unit operations, Section S2: Calculation of energy consumption, Section S3: Capital cost estimation, Section S4: Estimation of cost of sorbent, Section S5: NPV analysis, S6: Desorption Stage: Model Validation *contd.*, S7: Sensitivity of the results to the MOO options

Author Contributions: Conceptualization, R.P.W., G.P.K., H.Y., A.F.A.H. and A.L.C.; methodology, R.P.W., G.P.K., H.Y., A.F.A.H. and A.L.C.; software, R.P.W.; validation, R.P.W., G.P.K., H.Y., A.F.A.H. and A.L.C.; investigation, R.P.W.; resources, G.P.K., H.Y., A.F.A.H. and A.L.C.; writing—original draft preparation, R.P.W.; writing—review and editing, R.P.W., G.P.K., H.Y., A.F.A.H. and A.L.C.; visualization, R.P.W.; supervision, G.P.K., H.Y., A.F.A.H. and A.L.C.; project administration, A.F.A.H. and A.L.C.; funding acquisition, A.F.A.H. and A.L.C.

Funding: This research received no external funding.

Acknowledgments: The authors acknowledge Antonio Benci and David Zuidema, Monash Instrumentation Facility, for assistance in designing and programming some of the componentry in the experimental set up.

Conflicts of Interest: The authors declare no conflict of interest.

References

1. IPCC. *IPCC Special Report on Carbon Dioxide Capture and Storage; Prepared by Working Group III of the Intergovernmental Panel on Climate Change*; Cambridge University Press: Cambridge, UK; New York, NY, USA, 2005.
2. Koytsoumpa, E.I.; Bergins, C.; Kakaras, E. The CO_2 economy: Review of CO_2 capture and reuse technologies. *J. Supercrit. Fluids* **2018**, *132*, 3–16. [CrossRef]
3. Sanz-Pérez, E.S.; Murdock, C.R.; Didas, S.A.; Jones, C.W. Direct Capture of CO_2 from Ambient Air. *Chem. Rev.* **2016**, *116*, 11840–11876. [CrossRef] [PubMed]
4. Sinha, A.; Darunte, L.A.; Jones, C.W.; Realff, M.J.; Kawajiri, Y. Systems Design and Economic Analysis of Direct Air Capture of CO_2 through Temperature Vacuum Swing Adsorption Using MIL-101(Cr)-PEI-800 and mmen-Mg_2(dobpdc) MOF Adsorbents. *Ind. Eng. Chem. Res.* **2017**, *56*, 750–764. [CrossRef]
5. Krekel, D.; Samsun, R.C.; Peters, R.; Stolten, D. The separation of CO_2 from ambient air—A techno-economic assessment. *Appl. Energy* **2018**, *218*, 361–381. [CrossRef]
6. Zhang, W.; Liu, H.; Sun, C.; Drage, T.C.; Snape, C.E. Capturing CO_2 from ambient air using a polyethyleneimine–silica adsorbent in fluidized beds. *Chem. Eng. Sci.* **2014**, *116*, 306–316. [CrossRef]
7. Kulkarni, A.R.; Sholl, D.S. Analysis of Equilibrium-Based TSA Processes for Direct Capture of CO_2 from Air. *Ind. Eng. Chem. Res.* **2012**, *51*, 8631–8645. [CrossRef]
8. Gebald, C.; Repond, N.; Wurzbacher, J.A. Steam Assisted Vacuum Desorption Process for Carbon Dioxide Capture. U.S. Patent No. US20170203249A1, 20 July 2017.
9. Wurzbacher, J.A.; Gebald, C.; Piatkowski, N.; Steinfeld, A. Concurrent Separation of CO_2 and H_2O from Air by a Temperature-Vacuum Swing Adsorption/Desorption Cycle. *Environ. Sci. Technol.* **2012**, *46*, 9191–9198. [CrossRef]

10. Climeworks. Our Technology. Available online: https://www.climeworks.com/our-technology/ (accessed on 14 June 2019).
11. Gobal Thermostat. A Unique Capture Process. Available online: https://globalthermostat.com/a-unique-capture-process/ (accessed on 14 June 2019).
12. Kramer, D. Can carbon capture from air shift the climate change equation? *Phys. Today* **2018**, *71*, 26–29. [CrossRef]
13. Carbon Engineering. Carbon Engineering: CO_2 Capture and the Synthesis of Clean Transportation Fuels. Available online: https://carbonengineering.com/ (accessed on 16 July 2019).
14. Keith, D.W.; Holmes, G.; St. Angelo, D.; Heidel, K. A Process for Capturing CO_2 from the Atmosphere. *Joule* **2018**, *2*, 1573–1594. [CrossRef]
15. Jackson, R.B.; Baker, J.S. Opportunities and Constraints for Forest Climate Mitigation. *Bioscience* **2010**, *60*, 698–707. [CrossRef]
16. Wijesiri, R.P.; Knowles, G.P.; Yeasmin, H.; Hoadley, A.F.A.; Chaffee, A.L. CO_2 Capture from Air Using Pelletised Polyethyleneimine Impregnated MCF Silica. *Ind. Eng. Chem. Res.* **2019**, *58*, 3293–3303. [CrossRef]
17. Wijesiri, R.P.; Knowles, G.P.; Yeasmin, H.; Hoadley, A.F.A.; Chaffee, A.L. Desorption Process for Capturing CO_2 from Air with Supported Amine Sorbent. *Ind. Eng. Chem. Res.*. under review.
18. Glueckauf, E.; Coates, J.I. 241. Theory of chromatography. Part IV. The influence of incomplete equilibrium on the front boundary of chromatograms and on the effectiveness of separation. *J. Chem. Soc.* **1947**, 315–1321. [CrossRef]
19. Sircar, S.; Hufton, J.R. Why Does the Linear Driving Force Model for Adsorption Kinetics Work? *Adsorption* **2000**, *6*, 137–147. [CrossRef]
20. Do, D.D. *Adsorption Analysis: Equilibria and Kinetics*; Imperial College Press: London, UK, 1998.
21. Knowles, G.P.; Chaffee, A.L. Shaped Silica-polyethyleneimine Composite Sorbents for CO_2 Capture via Adsorption. *Energy Procedia* **2017**, *114*, 2219–2227. [CrossRef]
22. Gebald, C.; Piatkowski, N.; Rüesch, T.; Wurzbacher, J.A. Low-Pressure Drop Structure of Particle Adsorbent Bed for Adsorption Gas Separation Process. Patent No. WO2014170184A1, 23 October 2014.
23. Couper, J.R. *Chemical Process Equipment: Selection and Design*, 2nd ed.; Elsevier/Butterworth-Heinemann: Amsterdam, The Netherlands, 2010.
24. Antoine, L.C. Tensions des vapeurs; nouvelle relation entre les tensions et les températures Comptes Rendus. *Comptes Rendus des Séances de l'Acad. des Sci.* **1888**, *107*, 681–836.
25. Seider, W.D. *Product and Process Design Principles: Synthesis, Analysis, and Evaluation*, 3rd ed.; John Wiley: Hoboken, NJ, USA, 2009.
26. Sinnott, R.K. Coulson & Richardson's chemical engineering. In *Chemical Engineering Design*, 4th ed.; Elsevier Butterworth-Heinemann: Oxford, UK, 2005; Volume 6.
27. Brennan, D. *Process Industry Economics: An International Perspective*; IChemE: Rugby, UK, 1998.
28. IEA Solar Heating & Cooling Programme. *Solar Heat Worldwide 2018*; International Energy Agency: Paris, France, 2018.
29. IRENA. *Renewable Power Generation Costs in 2017*; International Renewable Energy Agency: Abu-Dhabi, UAE, 2018.
30. South East Water Corporation. *2018-19 Pricing Handbook*; South East Water Corporation: Melbourne, Australia, 2018.
31. Deb, K. *Multi-Objective Optimization Using Evolutionary Algorithms*, 1st ed.; John Wiley & Sons: New York, NY, USA, 2001.
32. Jahandar Lashaki, M.; Khiavi, S.; Sayari, A. Stability of amine-functionalized CO_2 adsorbents: A multifaceted puzzle. *Chem. Soc. Rev.* **2019**, *48*, 3320–3405. [CrossRef]
33. Bajamundi, C.J.E.; Koponen, J.; Ruuskanen, V.; Elfving, J.; Kosonen, A.; Kauppinen, J.; Ahola, J. Capturing CO_2 from air: Technical performance and process control improvement. *J. CO_2 Util.* **2019**, *30*, 232–239. [CrossRef]
34. Wang, J.; Huang, H.; Wang, M.; Yao, L.; Qiao, W.; Long, D.; Ling, L. Direct Capture of Low-Concentration CO_2 on Mesoporous Carbon-Supported Solid Amine Adsorbents at Ambient Temperature. *Ind. Eng. Chem. Res.* **2015**, *54*, 5319–5327. [CrossRef]
35. Goeppert, A.; Meth, S.; Prakash, G.K.S.; Olah, G.A. Nanostructured silica as a support for regenerable high-capacity organoamine-based CO_2 sorbents. *Energy Environ. Sci.* **2010**, *3*, 1949–1960. [CrossRef]

36. Sakwa-Novak, M.A.; Tan, S.; Jones, C.W. Role of Additives in Composite PEI/Oxide CO_2 Adsorbents: Enhancement in the Amine Efficiency of Supported PEI by PEG in CO_2 Capture from Simulated Ambient Air. *ACS Appl. Mater. Interfaces* **2015**, *7*, 24748–24759. [CrossRef]
37. Choi, S.; Gray, M.L.; Jones, C.W. Amine-Tethered Solid Adsorbents Coupling High Adsorption Capacity and Regenerability for CO_2 Capture from Ambient Air. *ChemSusChem* **2011**, *4*, 628–635. [CrossRef]
38. Lu, W.; Sculley, J.P.; Yuan, D.; Krishna, R.; Zhou, H.C. Carbon Dioxide Capture from Air Using Amine-Grafted Porous Polymer Networks. *J. Phys. Chem. C* **2013**, *117*, 4057–4061. [CrossRef]
39. Chen, Z.; Deng, S.; Wei, H.; Wang, B.; Huang, J.; Yu, G. Polyethylenimine-Impregnated Resin for High CO_2 Adsorption: An Efficient Adsorbent for CO2 Capture from Simulated Flue Gas and Ambient Air. *ACS Appl. Mater. Interfaces* **2013**, *5*, 6937–6945. [CrossRef]
40. Darunte, L.A.; Oetomo, A.D.; Walton, K.S.; Sholl, D.S.; Jones, C.W. Direct Air Capture of CO_2 Using Amine Functionalized MIL-101(Cr). *ACS Sustain. Chem. Eng.* **2016**, *4*, 5761–5768. [CrossRef]
41. Goeppert, A.; Zhang, H.; Czaun, M.; May, R.B.; Prakash, G.K.S.; Olah, G.A.; Narayanan, S.R. Easily Regenerable Solid Adsorbents Based on Polyamines for Carbon Dioxide Capture from the Air. *ChemSusChem* **2014**, *7*, 1386–1397. [CrossRef]
42. Zhang, H.; Goeppert, A.; Olah, G.A.; Prakash, G.K.S. Remarkable effect of moisture on the CO_2 adsorption of nano-silica supported linear and branched polyethylenimine. *J. CO_2 Util.* **2017**, *19*, 91–99. [CrossRef]
43. Didas, S.A.; Kulkarni, A.R.; Sholl, D.S.; Jones, C.W. Role of Amine Structure on Carbon Dioxide Adsorption from Ultradilute Gas Streams such as Ambient Air. *ChemSusChem* **2012**, *5*, 2058–2064. [CrossRef]
44. Sehaqui, H.; Gálvez, M.E.; Becatinni, V.; cheng Ng, Y.; Steinfeld, A.; Zimmermann, T.; Tingaut, P. Fast and Reversible Direct CO_2 Capture from Air onto All-Polymer Nanofibrillated Cellulose—Polyethylenimine Foams. *Environ. Sci. Technol.* **2015**, *49*, 3167–3174. [CrossRef]

5. Conclusions and Recommendations

In this thesis, a Direct Air Capture (DAC) process, i.e. a process capturing CO_2 directly from air, was developed and characterised in detail. The sorbent evaluated in the current work was branched polyethyleneimine (PEI) functionalised mesocellular foam (MCF) silica, with a high amine loading, in pelletised form. The amine loading of this sorbent is among the highest for PEI impregnated solid sorbents evaluated for DAC. The sorbent was selected as the large PEI content allowed for substantial uptake of CO_2, as had previously been demonstrated under post combustion capture conditions. The process development was carried out systematically in three stages; first studying the adsorption of CO_2 by the sorbent, second identifying a suitable method of desorption, and finally evaluating the technoeconomic feasibility of a scaled-up DAC process. The results of each stage have been published in peer-reviewed journals.

In the first stage, the PEI-MCF sorbent was evaluated under a series of temperatures and moisture levels. This stage aimed to identify the relative effect of these two process variables on the CO_2 adsorption performance by the sorbent, and the process conditions which would provide a larger uptake of CO_2. This was critical for process development, as the operating conditions of DAC processes would be location specific and may vary from sub-zero temperatures to about 55 °C, under various moisture levels, depending on the local climate. At the time of carrying out this research, there was no information on the effect of moisture and temperature for highly loaded (>55% wt) PEI impregnated sorbents, under DAC conditions. Furthermore, up to date, this is the only study which evaluated the effect of moisture at a series of different temperatures for PEI sorbents under DAC conditions.

The results of this study identified that while the large amine loading produced a large CO_2 uptake, it also resulted in significant mass transfer limitations and hence slower adsorption kinetics. The highest CO_2 uptake was observed at 46°C under both dry and humid conditions. It was observed that at temperatures higher than this, the CO_2 adsorption was reduced, consistent with the thermodynamics of the exothermic reaction between the CO_2 and the amine sites. A reduced uptake was also observed at temperatures below 46 °C. This was attributed to the large mass transfer resistances in the sorbent, which hindered the accessibility of the amine sites to the CO_2, at lower temperatures. The presence of moisture was observed to enhance the CO_2 uptake by up to 53%. Of the moisture levels studied, the highest uptake was observed for adsorption at 2% mol-H_2O for all temperatures evaluated. At 46°C this corresponded to a CO_2 uptake of 2.52 mmol/g. It was also noted that the CO_2 uptake was negatively affected at a higher moisture level of 3% mol-H_2O, which suggested that the large amounts of co-adsorbed water may be interfering with the adsorption of CO_2. The study concluded that while

the sorbent displayed a high CO_2 uptake (>1.2 mmol/g) under a broad range of temperature and moisture levels, it would be better suited for warm climates with a moderate humidity.

The second stage of the research evaluated the performance of the sorbent under steam-assisted temperature vacuum swing desorption (S-TVSD). In this process, the desorption was carried out by applying a vacuum and heating up the sorbent, while simultaneously purging with steam. S-TVSD was chosen as the technology of interest due to the fast kinetics offered under mild vacuum levels, the possibility of desorbing the CO_2 at high purity, and the improved stability of the sorbent in wet atmospheres. At the time of carrying out the research, S-TVSD for DAC applications had been described only in a single patent which disclosed minimal information of the desorption kinetics. In comparison, the research described in this thesis carried out a rigorous investigation on desorption performance of the sorbent under a wide array of process conditions.

The results demonstrated that substantial CO_2 desorption could be achieved with S-TVSD under moderate vacuum levels (12 to 56 kPa abs), and relatively low temperatures (70 to 100 °C). The moderate vacuum levels required suggested that the process could be developed with low capital and operating expenses. The low temperatures needed indicated opportunities for process integration with low temperature solar thermal systems or waste heat from other processes. Higher temperatures and greater vacuum levels produced significantly faster kinetics, and the fastest desorption was achieved at 12 kPa abs/100 °C. Under the same temperature and pressure, the desorption kinetics of a TVSD process was observed to be around 16 times slower, which confirmed the superior kinetics offered by the steam assisted process. It was further identified that higher steam flow rates yielded faster desorption at the compromise of a disproportionately higher increase in the thermal energy requirement. An interesting discovery of this study was that while moisture improved the CO_2 uptake, it also resulted in an additional thermal energy requirement for the desorption of the water that gets co-adsorbed on the sorbent. The desorption was also observed to be slightly slower in comparison to that when adsorption was under dry conditions. Finally, it was observed that the sorbent underwent minimal degradation under the process conditions studied. After 50 cycles of adsorption/desorption which corresponded to over 1500 h of processing time, the sorbent retained 92% of its initial capacity. The study concluded that S-TVSD presented itself to be a promising technology for DAC and highlighted the need to identify the preferred process conditions, after taking into consideration their impact on the economics of the DAC process.

The final stage of the research focussed on evaluation of the technoeconomic feasibility of a scaled-up DAC process. At the time of carrying out this work, only limited studies had evaluated the economics of DAC processes using solid supported amines, and there was considerable discrepancy between

their results. Furthermore, it was noted that these studies evaluated fixed process conditions rather than considering a range of values, in a measure to optimise the process. Additionally, these studies had not evaluated the effect of the co-adsorbed water on the economics of the process.

In this study, a process model was proposed for a DAC process, and validated with the laboratory experimental results. Following this, the model was subjected to a multi-objective optimisation (MOO) with the process conditions as the variables, and minimising the cost of capture and maximising the amount of CO_2 captured as the objectives. The optimisation compared a 'dry case' and a 'humid case' to determine the effect of moisture inherent in air. The MOO identified the minimum cost of capture to be 612 USD/tonne for a process with air entering at 25°C under dry conditions, and 657 USD/tonne for air entering at 22 °C and 39% RH. In both of the cases, the incoming air to the process was heated to 27 °C, before passing through the air-sorbent contactors, to benefit from the reduced mass transfer limitations achieved at higher temperatures, as described earlier. While 46 °C had previously been identified to yield the highest uptake of CO_2, a milder adsorption temperature of 27 °C was considered for this study. This was done as an average ambient temperature of 46 °C corresponds to unrealistically warm climates and heating the air to this temperature would require a significant amount of energy. The largest contributors to the cost of capture were identified to be the cost of the air-sorbent contactors, and the cost of providing the thermal energy required for the desorption.

The costs calculated here were higher than that reported in most of the previous studies in the literature. This was identified to be partially due to differences in assumptions and scopes used in the respective studies. Another reason was the slow CO_2 mass transfer kinetics of the sorbent in the current work, which resulted in longer cycle times, and hence higher costs of capture. As mentioned earlier, this can be attributed to the large PEI loading in the sorbent. The study quantified that the cost could be cut down by as much as 27% if the kinetics of the sorbent were enhanced by a factor of two. Furthermore, as mentioned earlier, the adsorption temperature considered for this study was not that which yielded the highest CO_2 uptake. It may be that further improvements in the process economics could be achieved by tailoring the design of sorbent material so that its highest CO_2 uptake occurs at the intended adsorption temperature.

The higher cost for adsorption under humid conditions was identified to be an effect of the additional energy requirement for desorbing the co-adsorbed water. Although the humid case yielded a higher cost of capture, it was noted that it would be unrealistic to expect perfectly dry climates anywhere in the world. In contrast, the inlet air conditions for the humid case can be expected from locations such as Las Vegas, Phoenix, Sonora, Rajasthan, Namibia and Botswana. However, this highlighted that development of sorbents with a reduced affinity for water could improve the economics of the

process. The study quantified an 8% reduction in the cost of capture for a hypothetical sorbent with half the water uptake of the current sorbent.

In conclusion, the process evaluated in this thesis does not appear to be economically feasible in the current state. However, the research identified several avenues which could lead to improvements. Of these, the improvements in sorbents design suggested here could realistically be achieved even with the current state of the technology. However, further research is needed for areas such as the development of low-cost contactors. If a combination of these improvements is achieved, this DAC process has the potential to be economically feasible and a valuable tool for combatting climate change in the future.

Recommendations and opportunities for future work identified from the work in this thesis are as follows

1. **Sorbent development**: One of the main reasons for the higher cost of capture in this DAC process was identified to be the slow mass transfer kinetics of the sorbent. Therefore, for the development of economically feasible DAC processes, it is essential that future research on sorbent design had a focus on producing materials with reduced mass transfer limitations. It would also be critical to carry out research on how sorbent design can be tailored to best suit the ambient conditions of the location of their intended use. Furthermore, the work in this thesis also suggested that sorbents with a reduced affinity to water could be beneficial for the economics of the process.

2. **Sorbent stability**: The research identified that the sorbent displayed a small but noticeable (8%) loss in CO_2 uptake capacity after 1500 h of adsorption/desorption cycles. It was suspected that this was caused by the leaching of the PEI phase from the internal pores. It would be of interest to carry out a detailed investigation to determine the exact nature of this degradation and how the sorbent can be safeguarded against it.

3. **Cyclic Testing**: The cyclic testing done in Chapter 3 demonstrated that the sorbent stability is largely preserved after 50 cycles of adsorption/desorption under varying process conditions. However, it would also be of interest to test the cyclic stability of the sorbent under the preferred process conditions identified in the technoeconomic evaluation in Chapter 4. This would give a more realistic representation of how the sorbent will behave in practical DAC processes.

4. **Air-sorbent contactor design:** The air-sorbent contactor was reported to be the largest contributor to the cost of the DAC process. This is mainly owing to the special qualities desired for good air-sorbent contactors. These include large heat transfer areas to rapidly heat and cool the sorbent during the cycles, low pressure-drop structures to minimise the energy required for pushing air/steam through them, and minimised void volumes to reduce the energy needed for evacuation during desorption. It would be of interest to research how the configuration of the contactor could be designed such that these qualities can be incorporated while minimising the cost of construction. Monolithic contactors as have been evaluated in some studies [73,94,96], may be a promising option for this.

5. **Detailed transport model:** The process model described in this thesis uses a simplified mass transfer model which was demonstrated to be sufficient for predicting the adsorption/desorption of CO_2 by the sorbent in the laboratory process. It is recommended to develop a more rigorous transport model, which could provide a more detailed understanding of the behaviour of this sorbent. A more rigorous model would also be highly beneficial for designing alternative contactors.

6. **Effect of oxygen on the performance of the sorbent**: The experiments described in this thesis evaluated the adsorption/desorption performance of the sorbent from a feed gas of 420 ppm CO_2 in N_2 which was used to simulate the concentration of CO_2 in air. It would be important to determine how the presence of oxygen affects the performance of the sorbent under the process conditions of interest. Some preliminary work on this has been carried out and is included in **Appendix D** of this thesis. The early results (10 cycles) indicate that oxygen in the bottled air is not affecting the adsorbent; however further testing over many more cycles is required.

References

[1] IPCC, Summary for Policymakers, In *Global Warming of 1.5°C. An IPCC Special Report on the impacts of global warming of 1.5°C above pre-industrial levels and related global greenhouse gas emission pathways, in the context of strengthening the global response to the threat of climate change, sustainable development, and efforts to eradicate poverty*V. Masson-Delmotte, et al., Editors.,Eds.; World Meteorological Organization: Geneva, Switzerland,2018.

[2] Koytsoumpa, E.I.; Bergins, C.; Kakaras, E. The CO2 economy: Review of CO2 capture and reuse technologies. *The Journal of Supercritical Fluids*. **2018**, *132*, 3-16.

[3] IPCC, *IPCC Special Report on Carbon Dioxide Capture and Storage. Prepared by Working Group III of the Intergovernmental Panel on Climate Change*, B. Metz, et al., Editors. 2005: New York, USA. p. 442.

[4] Sanz-Pérez, E.S.; Murdock, C.R.; Didas, S.A.; Jones, C.W. Direct Capture of CO2 from Ambient Air. *Chemical Reviews*. **2016**, *116*(19), 11840-11876.

[5] Goeppert, A.; Czaun, M.; Prakash, G.K.S.; Olah, G. Air as the renewable carbon source of the future: an overview of CO2 capture from the atmosphere. *Energy and Environmental Science*. **2012**, *5*, 7833-7853.

[6] Stolaroff, J.K.; Keith, D.W.; Lowry, G.V. Carbon Dioxide Capture from Atmospheric Air Using Sodium Hydroxide Spray. *Environmental Science & Technology*. **2008**, *42*(8), 2728-2735.

[7] Zeman, F. Experimental results for capturing CO2 from the atmosphere. *AIChE Journal*. **2008**, *54*(5), 1396-1399.

[8] Baciocchi, R.; Storti, G.; Mazzotti, M. Process design and energy requirements for the capture of carbon dioxide from air. *Chemical Engineering and Processing: Process Intensification*. **2006**, *45*(12), 1047-1058.

[9] Zeman, F. Energy and Material Balance of CO2 Capture from Ambient Air. *Environmental Science & Technology*. **2007**, *41*(21), 7558-7563.

[10] Dubey, M.K.; Ziock, H.; Rueff, G.; Elliott, S.; Smith, W.S. Extraction of carbon dioxide from the atmosphere through engineered chemical sinkage. *Fuel Chemistry Division Preprints*. **2002**, *47*(1), 81-84.

[11] Lackner, K.S.; Grimes, P.; Ziock, H.-J. Capturing Carbon Dioxide from the Air. Presented at National Conference on Carbon Sequestration. Washington DC, USA.**2001**.

[12] Bandi, A.; Specht, M.; Weimer, T.; Schaber, K. CO2 recycling for hydrogen storage and transportation —Electrochemical CO2 removal and fixation. *Energy Conversion and Management*. **1995**, *36*(6–9), 899-902.

[13] Keith, D.W.; Holmes, G.; St. Angelo, D.; Heidel, K. A Process for Capturing CO2 from the Atmosphere. *Joule*. **2018**, *2*(8), 1573-1594.

[14] Ngu, L.-H.; Song, J.W.; Hashim, S.S.; Ong, D.E. Lab-scale atmospheric CO2 absorption for calcium carbonate precipitation in sand. *Greenhouse Gases: Science and Technology*. **2019**, *9*(3), 519-528.

[15] Nikulshina, V.; Steinfeld, A. CO2 capture from air via CaO-carbonation using a solar-driven fluidized bed reactor—Effect of temperature and water vapor concentration. *Chemical Engineering Journal*. **2009**, *155*(3), 867-873.

[16] Nikulshina, V.; Gebald, C.; Steinfeld, A. CO2 capture from atmospheric air via consecutive CaO-carbonation and CaCO3-calcination cycles in a fluidized-bed solar reactor. *Chemical Engineering Journal*. **2009**, *146*(2), 244-248.

[17] Nikulshina, V.; Gálvez, M.E.; Steinfeld, A. Kinetic analysis of the carbonation reactions for the capture of CO2 from air via the Ca(OH)2–CaCO3–CaO solar thermochemical cycle. *Chemical Engineering Journal*. **2007**, *129*(1–3), 75-83.

[18] Samari, M.; Ridha, F.; Manovic, V.; Macchi, A.; Anthony, E.J. Direct capture of carbon dioxide from air via lime-based sorbents. *Mitigation and Adaptation Strategies for Global Change*. **2019**.

[19] Nikulshina, V.; Hirsch, D.; Mazzotti, M.; Steinfeld, A. CO2 capture from air and co-production of H2 via the Ca(OH)2–CaCO3 cycle using concentrated solar power–Thermodynamic analysis. *Energy*. **2006**, *31*(12), 1715-1725.

[20] Przepiórski, J.; Czyżewski, A.; Pietrzak, R.; Morawski, A.W. MgO/CaO-Loaded Activated Carbon for Carbon Dioxide Capture: Practical Aspects of Use. *Industrial & Engineering Chemistry Research*. **2013**, *52*(20), 6669-6677.

[21] Veselovskaya, J.V.; Derevschikov, V.S.; Kardash, T.Y.; Stonkus, O.A.; Trubitsina, T.A.; Okunev, A.G. Direct CO2 capture from ambient air using K2CO3/Al2O3 composite sorbent. *International Journal of Greenhouse Gas Control*. **2013**, *17*, 332-340.

[22] Derevschikov, V.S.; Veselovskaya, J.V.; Kardash, T.Y.; Trubitsyn, D.A.; Okunev, A.G. Direct CO2 capture from ambient air using K2CO3/Y2O3 composite sorbent. *Fuel*. **2014**, *127*, 212-218.

[23] Bali, S.; Sakwa-Novak, M.A.; Jones, C.W. Potassium incorporated alumina based CO2 capture sorbents: Comparison with supported amine sorbents under ultra-dilute capture conditions. *Colloids and Surfaces A: Physicochemical and Engineering Aspects*. **2015**, *486*, 78-85.

[24] Rodríguez-Mosqueda, R.; Bramer, E.A.; Brem, G. CO2 capture from ambient air using hydrated Na2CO3 supported on activated carbon honeycombs with application to CO2 enrichment in greenhouses. *Chemical Engineering Science*. **2018**, *189*, 114-122.

[25] Stuckert, N.R.; Yang, R.T. CO2 Capture from the Atmosphere and Simultaneous Concentration Using Zeolites and Amine-Grafted SBA-15. *Environmental Science & Technology*. **2011**, *45*(23), 10257-10264.

[26] Kumar, A.; Madden, D.G.; Lusi, M.; Chen, K.-J.; Daniels, E.A.; Curtin, T.; Perry, J.J.; Zaworotko, M.J. Direct Air Capture of CO2 by Physisorbent Materials. *Angewandte Chemie*. **2015**, *127*(48), 14580-14585.

[27] Petukhov, S.S.; Tumanov, A.I.; Trokhina, G.A. The use of synthetic zeolites in the complete removal of impurities from air. *Chemical and Petroleum Engineering*. **1970**, *6*(1), 23-26.

[28] Madden, D.G.; Scott, H.S.; Kumar, A.; Chen, K.J.; Sanii, R.; Bajpai, A.; Lusi, M.; Curtin, T.; Perry, J.J.; Zaworotko, M.J. Flue-gas and direct-air capture of CO2 by porous metal-organic materials. *Philos Trans A Math Phys Eng Sci*. **2017**, *375*(2084).

[29] Choi, S.; Watanabe, T.; Bae, T.-H.; Sholl, D.S.; Jones, C.W. Modification of the Mg/DOBDC MOF with Amines to Enhance CO2 Adsorption from Ultradilute Gases. *The Journal of Physical Chemistry Letters*. **2012**, *3*(9), 1136-1141.

[30] Lackner, K.S. Capture of carbon dioxide from ambient air. *The European Physical Journal*. **2009**, *176*, 93-106.

[31] Wang, T.; Liu, J.; Lackner, K.S.; Shi, X.; Fang, M.; Luo, Z. Characterization of kinetic limitations to atmospheric CO2 capture by solid sorbent. *Greenhouse Gases: Science and Technology*. **2016**, *6*(1), 138-149.

[32] Wang, T.; Lackner, K.S.; Wright, A. Moisture Swing Sorbent for Carbon Dioxide Capture from Ambient Air. *Environmental Science & Technology*. **2011**, *45*(15), 6670-6675.

[33] Song, J.; Liu, J.; Zhao, W.; Chen, Y.; Xiao, H.; Shi, X.; Liu, Y.; Chen, X. Quaternized Chitosan/PVA Aerogels for Reversible CO2 Capture from Ambient Air. *Industrial & Engineering Chemistry Research*. **2018**, *57*(14), 4941-4948.

[34] Shi, X.; Li, Q.; Wang, T.; Lackner, K.S. Kinetic analysis of an anion exchange absorbent for CO2 capture from ambient air. *PLOS ONE*. **2017**, *12*(6), e0179828.

[35] He, H.; Li, W.; Zhong, M.; Konkolewicz, D.; Wu, D.; Yaccato, K.; Rappold, T.; Sugar, G.; David, N.E.; Matyjaszewski, K. Reversible CO2 capture with porous polymers using the humidity swing. *Energy & Environmental Science*. **2013**, *6*(2), 488-493.

[36] Chaikittisilp, W.; Kim, H.-J.; Jones, C.W. Mesoporous Alumina-Supported Amines as Potential Steam-Stable Adsorbents for Capturing CO2 from Simulated Flue Gas and Ambient Air. *Energy & Fuels*. **2011**, *25*(11), 5528-5537.

[37] Chaikittisilp, W.; Khunsupat, R.; Chen, T.T.; Jones, C.W. Poly(allylamine)–Mesoporous Silica Composite Materials for CO2 Capture from Simulated Flue Gas or Ambient Air. *Industrial & Engineering Chemistry Research*. **2011**, *50*(24), 14203-14210.

[38] Choi, S.; Gray, M.L.; Jones, C.W. Amine-Tethered Solid Adsorbents Coupling High Adsorption Capacity and Regenerability for CO2 Capture From Ambient Air. *ChemSusChem*. **2011**, *4*(5), 628-635.

[39] Chen, Z.; Deng, S.; Wei, H.; Wang, B.; Huang, J.; Yu, G. Polyethylenimine-Impregnated Resin for High CO2 Adsorption: An Efficient Adsorbent for CO2 Capture from Simulated Flue Gas and Ambient Air. *ACS Applied Materials & Interfaces*. **2013**, *5*(15), 6937-6945.

[40] Darunte, L.A.; Oetomo, A.D.; Walton, K.S.; Sholl, D.S.; Jones, C.W. Direct Air Capture of CO2 Using Amine Functionalized MIL-101(Cr). *ACS Sustainable Chemistry & Engineering*. **2016**, *4*(10), 5761-5768.

[41] Goeppert, A.; Czaun, M.; May, R.B.; Prakash, G.K.S.; Olah, G.A.; Narayanan, S.R. Carbon Dioxide Capture from the Air Using a Polyamine Based Regenerable Solid Adsorbent. *Journal of the American Chemical Society*. **2011**, *133*(50), 20164-20167.

[42] Goeppert, A.; Zhang, H.; Czaun, M.; May, R.B.; Prakash, G.K.S.; Olah, G.A.; Narayanan, S.R. Easily Regenerable Solid Adsorbents Based on Polyamines for Carbon Dioxide Capture from the Air. *ChemSusChem*. **2014**, *7*(5), 1386-1397.

[43] Wang, J.; Wang, M.; Li, W.; Qiao, W.; Long, D.; Ling, L. Application of polyethylenimine-impregnated solid adsorbents for direct capture of low-concentration CO2. *AIChE Journal*. **2015**, *61*(3), 972-980.

[44] Wang, J.; Huang, H.; Wang, M.; Yao, L.; Qiao, W.; Long, D.; Ling, L. Direct Capture of Low-Concentration CO2 on Mesoporous Carbon-Supported Solid Amine Adsorbents at Ambient Temperature. *Industrial & Engineering Chemistry Research*. **2015**, *54*(19), 5319-5327.

[45] Wang, X.; Ma, X.; Schwartz, V.; Clark, J.C.; Overbury, S.H.; Zhao, S.; Xu, X.; Song, C. A solid molecular basket sorbent for CO2 capture from gas streams with low CO2 concentration under ambient conditions. *Physical Chemistry Chemical Physics*. **2012**, *14*(4), 1485-1492.

[46] Zerze, H.; Tipirneni, A.; McHugh, A.J. Reusable poly(allylamine)-based solid materials for carbon dioxide capture under continuous flow of ambient air. *Separation Science and Technology*. **2017**, *52*(16), 2513-2522.

[47] Sujan, A.R.; Pang, S.H.; Zhu, G.; Jones, C.W.; Lively, R.P. Direct CO2 Capture from Air using Poly(ethylenimine)-Loaded Polymer/Silica Fiber Sorbents. *ACS Sustainable Chemistry & Engineering*. **2019**, *7*(5), 5264-5273.

[48] Sehaqui, H.; Gálvez, M.E.; Becatinni, V.; cheng Ng, Y.; Steinfeld, A.; Zimmermann, T.; Tingaut, P. Fast and Reversible Direct CO2 Capture from Air onto All-Polymer Nanofibrillated Cellulose—Polyethylenimine Foams. *Environmental Science & Technology*. **2015**, *49*(5), 3167-3174.

[49] Sayari, A.; Liu, Q.; Mishra, P. Enhanced Adsorption Efficiency through Materials Design for Direct Air Capture over Supported Polyethylenimine. *ChemSusChem*. **2016**, *9*(19), 2796-2803.

[50] Sakwa-Novak, M.A.; Tan, S.; Jones, C.W. Role of Additives in Composite PEI/Oxide CO2 Adsorbents: Enhancement in the Amine Efficiency of Supported PEI by PEG in CO2 Capture from Simulated Ambient Air. *ACS Applied Materials & Interfaces*. **2015**, *7*(44), 24748-24759.

[51] Pang, S.H.; Lee, L.-C.; Sakwa-Novak, M.A.; Lively, R.P.; Jones, C.W. Design of Aminopolymer Structure to Enhance Performance and Stability of CO2 Sorbents: Poly(propylenimine) vs Poly(ethylenimine). *Journal of the American Chemical Society*. **2017**, *139*(10), 3627-3630.

[52] Kwon, H.T.; Sakwa-Novak, M.A.; Pang, S.H.; Sujan, A.R.; Ping, E.W.; Jones, C.W. Aminopolymer-Impregnated Hierarchical Silica Structures: Unexpected Equivalent CO2 Uptake under Simulated Air Capture and Flue Gas Capture Conditions. *Chemistry of Materials*. **2019**.

[53] Choi, S.; Drese, J.H.; Eisenberger, P.M.; Jones, C.W. Application of Amine-Tethered Solid Sorbents for Direct CO2 Capture from the Ambient Air. *Environmental Science & Technology*. **2011**, *45*(6), 2420-2427.

[54] Abhilash, K.A.S.; Deepthi, T.; Sadhana, R.A.; Benny, K.G. Functionalized Polysilsesquioxane-Based Hybrid Silica Solid Amine Sorbents for the Regenerative Removal of CO2 from Air. *ACS Applied Materials & Interfaces*. **2015**, *7*(32), 17969-17976.

[55] Chaikittisilp, W.; Lunn, J.D.; Shantz, D.F.; Jones, C.W. Poly(L-lysine) Brush–Mesoporous Silica Hybrid Material as a Biomolecule-Based Adsorbent for CO2 Capture from Simulated Flue Gas and Air. *Chemistry – A European Journal*. **2011**, *17*(38), 10556-10561.

[56] Belmabkhout, Y.; Serna-Guerrero, R.; Sayari, A. Amine-bearing mesoporous silica for CO2 removal from dry and humid air. *Chemical Engineering Science*. **2010**, *65*(11), 3695-3698.

[57] Gebald, C.; Wurzbacher, J.A.; Tingaut, P.; Zimmermann, T.; Steinfeld, A. Amine-Based Nanofibrillated Cellulose As Adsorbent for CO2 Capture from Air. *Environmental Science & Technology*. **2011**, *45*(20), 9101-9108.

[58] Gebald, C.; Wurzbacher, J.A.; Tingaut, P.; Steinfeld, A. Stability of Amine-Functionalized Cellulose during Temperature-Vacuum-Swing Cycling for CO2 Capture from Air. *Environmental Science & Technology*. **2013**, *47*(17), 10063-10070.

[59] Gebald, C.; Wurzbacher, J.A.; Borgschulte, A.; Zimmermann, T.; Steinfeld, A. Single-Component and Binary CO2 and H2O Adsorption of Amine-Functionalized Cellulose. *Environmental Science & Technology*. **2014**, *48*(4), 2497-2504.

[60] Wurzbacher, J.A.; Gebald, C.; Piatkowski, N.; Steinfeld, A. Concurrent Separation of CO_2 and H_2O from Air by a Temperature-Vacuum Swing Adsorption/Desorption Cycle. *Environmental Science & Technology*. **2012**, *46*(16), 9191-9198.

[61] Didas, S.A.; Kulkarni, A.R.; Sholl, D.S.; Jones, C.W. Role of Amine Structure on Carbon Dioxide Adsorption from Ultradilute Gas Streams such as Ambient Air. *ChemSusChem*. **2012**, *5*(10), 2058-2064.

[62] Wagner, A.; Steen, B.; Johansson, G.; Zanghellini, E.; Jacobsson, P.; Johansson, P. Carbon dioxide capture from ambient air using amine-grafted mesoporous adsorbents. *International Journal of Spectroscopy*. **2013**, 75+.

[63] Wurzbacher, J.A.; Gebald, C.; Steinfeld, A. Separation of CO2 from air by temperature-vacuum swing adsorption using diamine-functionalized silica gel. *Energy & Environmental Science*. **2011**, *4*(9), 3584-3592.

[64] McDonald, T.M.; Lee, W.R.; Mason, J.A.; Wiers, B.M.; Hong, C.S.; Long, J.R. Capture of Carbon Dioxide from Air and Flue Gas in the Alkylamine-Appended Metal–Organic Framework mmen-Mg2(dobpdc). *Journal of the American Chemical Society*. **2012**, *134*(16), 7056-7065.

[65] Lu, W.; Sculley, J.P.; Yuan, D.; Krishna, R.; Zhou, H.-C. Carbon Dioxide Capture from Air Using Amine-Grafted Porous Polymer Networks. *The Journal of Physical Chemistry C*. **2013**, *117*(8), 4057-4061.

[66] Thakkar, H.; Issa, A.; Rownaghi, A.A.; Rezaei, F. CO2 Capture from Air Using Amine-Functionalized Kaolin-Based Zeolites. *Chemical Engineering & Technology*. **2017**, *40*(11), 1999-2007.

[67] Goeppert, A.; Zhang, H.; Sen, R.; Dang, H.; Prakash, G.K.S. Oxidation-Resistant, Cost-Effective Epoxide-Modified Polyamine Adsorbents for CO2 Capture from Various Sources Including Air. *ChemSusChem*. **2019**, *12*(8), 1712-1723.

[68] Smal, I.M.; Yu, Q.; Veneman, R.; Fränzel-Luiten, B.; Brilman, D.W.F. TG-FTIR Measurement of CO2-H2O co-adsorption for CO2 air capture sorbent screening. *Energy Procedia*. **2014**, *63*, 6834-6841.

[69] Yu, Q.; Delgado, J.d.l.P.; Veneman, R.; Brilman, D.W.F. Stability of a Benzyl Amine Based CO2 Capture Adsorbent in View of Regeneration Strategies. *Industrial & Engineering Chemistry Research*. **2017**, *56*(12), 3259-3269.

[70] Bos, M.J.; Pietersen, S.; Brilman, D.W.F. Production of high purity CO2 from air using solid amine sorbents. *Chemical Engineering Science: X*. **2019**, *2*, 100020.

[71] Zhang, W.; Liu, H.; Sun, C.; Drage, T.C.; Snape, C.E. Capturing CO2 from ambient air using a polyethyleneimine–silica adsorbent in fluidized beds. *Chemical Engineering Science*. **2014**, *116*, 306-316.

[72] Elfving, J.; Bajamundi, C.; Kauppinen, J.; Sainio, T. Modelling of equilibrium working capacity of PSA, TSA and TVSA processes for CO2 adsorption under direct air capture conditions. *Journal of CO2 Utilization*. **2017**, *22*, 270-277.

[73] Sakwa-Novak, M.A.; Yoo, C.-J.; Tan, S.; Rashidi, F.; Jones, C.W. Poly(ethylenimine)-Functionalized Monolithic Alumina Honeycomb Adsorbents for CO2 Capture from Air. *ChemSusChem*. **2016**, *9*(14), 1859-1868.

[74] Goeppert, A.; Meth, S.; Prakash, G.K.S.; Olah, G.A. Nanostructured silica as a support for regenerable high-capacity organoamine-based CO2 sorbents. *Energy & Environmental Science*. **2010**, *3*(12), 1949-1960.

[75] Wang, X.; Song, C. Temperature-programmed desorption of CO2 from polyethylenimine-loaded SBA-15 as molecular basket sorbents. *Catalysis Today*. **2012**, *194*(1), 44-52.

[76] Chang, A.C.C.; Chuang, S.S.C.; Gray, M.; Soong, Y. In-Situ Infrared Study of CO2 Adsorption on SBA-15 Grafted with γ-(Aminopropyl)triethoxysilane. *Energy & Fuels*. **2003**, *17*(2), 468-473.

[77] Knöfel, C.; Martin, C.; Hornebecq, V.; Llewellyn, P.L. Study of Carbon Dioxide Adsorption on Mesoporous Aminopropylsilane-Functionalized Silica and Titania Combining Microcalorimetry and in Situ Infrared Spectroscopy. *The Journal of Physical Chemistry C*. **2009**, *113*(52), 21726-21734.

[78] Mebane, D.S.; Kress, J.D.; Storlie, C.B.; Fauth, D.J.; Gray, M.L.; Li, K. Transport, Zwitterions, and the Role of Water for CO2 Adsorption in Mesoporous Silica-Supported Amine Sorbents. *The Journal of Physical Chemistry C*. **2013**, *117*(50), 26617-26627.

[79] Liu, Q.; Xiong, B.; Shi, J.; Tao, M.; He, Y.; Shi, Y. Enhanced Tolerance to Flue Gas Contaminants on Carbon Dioxide Capture Using Amine-Functionalized Multiwalled Carbon Nanotubes. *Energy & Fuels*. **2014**, *28*(10), 6494-6501.

[80] Hoffman, J.S.; Hammache, S.; Gray, M.L.; Fauth, D.J.; Pennline, H.W. Parametric study for an immobilized amine sorbent in a regenerative carbon dioxide capture process. *Fuel Processing Technology*. **2014**, *126*, 173-187.

[81] Bos, M.J.; Kroeze, V.; Sutanto, S.; Brilman, D.W.F. Evaluating Regeneration Options of Solid Amine Sorbent for CO2 Removal. *Industrial & Engineering Chemistry Research*. **2018**, *57*(32), 11141-11153.

[82] Serna-Guerrero, R.; Belmabkhout, Y.; Sayari, A. Influence of regeneration conditions on the cyclic performance of amine-grafted mesoporous silica for CO2 capture: An experimental and statistical study. *Chemical Engineering Science*. **2010**, *65*(14), 4166-4172.

[83] Drage, T.C.; Arenillas, A.; Smith, K.M.; Snape, C.E. Thermal stability of polyethylenimine based carbon dioxide adsorbents and its influence on selection of regeneration strategies. *Microporous and Mesoporous Materials*. **2008**, *116*(1–3), 504-512.

[84] Sayari, A.; Belmabkhout, Y. Stabilization of Amine-Containing CO2 Adsorbents: Dramatic Effect of Water Vapor. *Journal of the American Chemical Society*. **2010**, *132*(18), 6312-6314.

[85] Knowles, G.P.; Liang, Z.; Chaffee, A.L. Shaped polyethyleneimine sorbents for CO_2 capture. *Microporous and Mesoporous Materials*. **2017**, *238*, 14-18.

[86] Knowles, G.P.; Sher, J.L.; Xiao, P.; Webley, P.A.; Chaffee, A.L., *Novel adsorption process technologies for CO2 post combustion capture via amine type adsorbents*, in *14th International Conference on Greenhouse Gas Control Technologies*. 2018: Melbourne, Australia.

[87] Subagyono, D.J.N.; Marshall, M.; Knowles, G.P.; Chaffee, A.L. CO2 adsorption by amine modified siliceous mesostructured cellular foam (MCF) in humidified gas. *Microporous and Mesoporous Materials*. **2014**, *186*, 84-93.

[88] Heydari-Gorji, A.; Sayari, A. Thermal, Oxidative, and CO2-Induced Degradation of Supported Polyethylenimine Adsorbents. *Industrial & Engineering Chemistry Research*. **2012**, *51*(19), 6887-6894.

[89] Gebald, C.; Repond, N.; Wurzbacher, J.A. *Steam assisted vacuum desorption process for carbon dioxide capture*, US20170203249A1, 2017

[90] Sandhu, N.K.; Pudasainee, D.; Sarkar, P.; Gupta, R. Steam Regeneration of Polyethylenimine-Impregnated Silica Sorbent for Postcombustion CO2 Capture: A Multicyclic Study. *Industrial & Engineering Chemistry Research*. **2016**, *55*(7), 2210-2220.

[91] Li, W.; Choi, S.; Drese, J.H.; Hornbostel, M.; Krishnan, G.; Eisenberger, P.M.; Jones, C.W. Steam-Stripping for Regeneration of Supported Amine-Based CO2 Adsorbents. *ChemSusChem*. **2010**, *3*(8), 899-903.

[92] Hammache, S.; Hoffman, J.S.; Gray, M.L.; Fauth, D.J.; Howard, B.H.; Pennline, H.W. Comprehensive Study of the Impact of Steam on Polyethyleneimine on Silica for CO2 Capture. *Energy & Fuels*. **2013**, *27*(11), 6899-6905.

[93] Fujiki, J.; Chowdhury, F.A.; Yamada, H.; Yogo, K. Highly efficient post-combustion CO2 capture by low-temperature steam-aided vacuum swing adsorption using a novel polyamine-based solid sorbent. *Chemical Engineering Journal*. **2017**, *307*, 273-282.

[94] Sinha, A.; Darunte, L.A.; Jones, C.W.; Realff, M.J.; Kawajiri, Y. Systems Design and Economic Analysis of Direct Air Capture of CO2 through Temperature Vacuum Swing Adsorption Using MIL-101(Cr)-PEI-800 and mmen-Mg2(dobpdc) MOF Adsorbents. *Industrial & Engineering Chemistry Research*. **2017**, *56*(3), 750-764.

[95] Krekel, D.; Samsun, R.C.; Peters, R.; Stolten, D. The separation of CO2 from ambient air – A techno-economic assessment. *Applied Energy*. **2018**, *218*, 361-381.

[96] Kulkarni, A.R.; Sholl, D.S. Analysis of Equilibrium-Based TSA Processes for Direct Capture of CO2 from Air. *Industrial & Engineering Chemistry Research*. **2012**, *51*(25), 8631-8645.

[97] E. Bajamundi, C.J.; Koponen, J.; Ruuskanen, V.; Elfving, J.; Kosonen, A.; Kauppinen, J.; Ahola, J. Capturing CO2 from air: Technical performance and process control improvement. *Journal of CO2 Utilization*. **2019**, *30*, 232-239.

[98] Sinha, A.; Realff, M.J. A parametric study of the techno-economics of direct CO2 air capture systems using solid adsorbents. *AIChE Journal*. **2019**, *65*(7), e16607.

[99] Climeworks. *Our Technology*. 2018 (Accessed on 14 June 2019); Available at: https://www.climeworks.com/our-technology/.

[100] Gobal Thermostat. *A Unique Capture Process*. 2018 (Accessed on 14 June 2019); Available at: https://globalthermostat.com/a-unique-capture-process/.

[101] Carbon Engineering. *Carbon Engineering: CO2 capture and the synthesis of clean transportation fuels*. 2019 (Accessed on 16 July 2019); Available at: https://carbonengineering.com/.

[102] Infinitree LLC. *Technology- Infinitree LLC*. 2017 (Accessed on 31 Dec 2019); Available at: http://www.infinitreellc.com/technology.

[103] Kramer, D. Can carbon capture from air shift the climate change equation? *Physics Today*. **2018**, *71*(9), 26-29.

[104] Jackson, R.B.; Baker, J.S. Opportunities and Constraints for Forest Climate Mitigation. *Bioscience*. **2010**, *60*(9), 698-707.

[105] Knowles, G.P.; Rahman, R.; Veldman, Z.; Wijesiri, R.; Yeasmin, H.; Hoadley, A.; Chaffee., A.L., *Polyethyleneimine-Mesoporous Silica composites for CO2 capture from air*, in *Nanoporous Materials 8*. 2017: Ottawa.

[106] Knowles, G.P.; Rahman, R.; Veldman, Z.; Negi, A.; Chaffee, A.L., *Supported polyethyleneimine sorbents for CO2 capture from air.*, in *The 2nd Australia-Japan Symposium on Carbon Resource Utilisation*. 2018: Brisbane, Australia.

Appendix A(I): Supporting Information for "Desorption Process for Capturing CO_2 from Air with Supported Amine Sorbent"

Supporting Information
for
Desorption Process for Capturing CO_2 from Air with Supported Amine Sorbent

Romesh P. Wijesiri[a,b], Gregory P. Knowles[b], Hasina Yeasmin[a], Andrew F. A. Hoadley[a*] and Alan L. Chaffee[b*]

[a] *Department of Chemical Engineering, Monash University, Wellington Road, Clayton VIC 3800, Australia*
[b] *School of Chemistry, Monash University, Wellington Road, Clayton VIC 3800, Australia*

**Corresponding Authors.*
Andrew. F.A. Hoadley *Tel.: +61 3 9905 3421; Email: Andrew.Hoadley@monash.edu*
Alan L. Chaffee *Tel.: +61 3 9905 4626; Email: Alan.Chaffee@monash.edu*

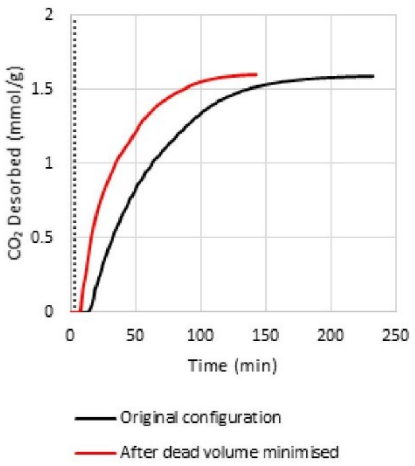

Figure S1. The CO_2 desorption profiles at 26 kPa abs/100 °C at a steam flow rate of 0.5 g/h, under the original condensate trap configuration, and after the dead volume was minimised.

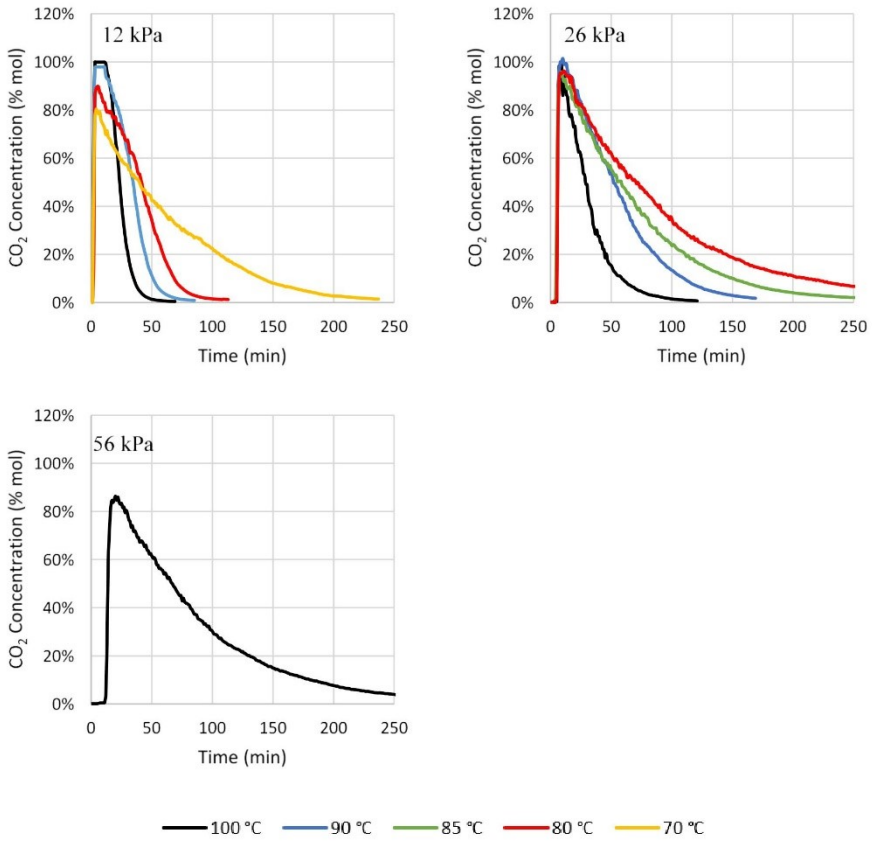

Figure S2. CO_2 concentration profiles for desorption under different temperatures and pressures at a steam flow rate of 6.4 ± 1.2 g/h.

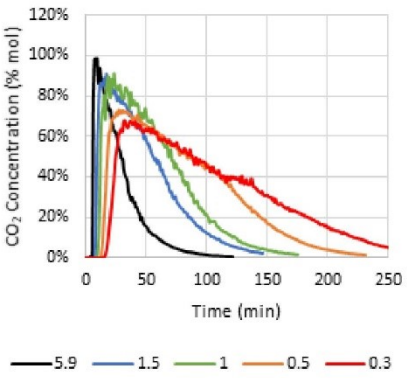

Figure S3. CO_2 concentration profiles for desorption under different steam flow rates at 26 kPa abs/100°C.

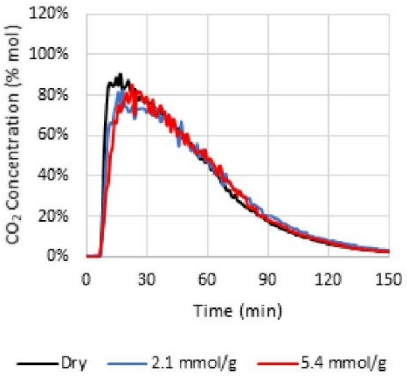

Figure S4. CO_2 concentration profiles for desorption with different amounts of pre-adsorbed water

Appendix A(II): Supporting Information for "Technoeconomic Evaluation of a Process Capturing CO_2 Directly from Air"

Processes **2019**, *7*, 503; doi:10.3390/pr7080503 S1 of S11

Technoeconomic Evaluation of a Process Capturing CO_2 Directly from Air

Romesh Pramodya Wijesiri [1,2], Gregory Paul Knowles [2], Hasina Yeasmin [1], Andrew Forbes Alexander Hoadley [1,*] and Alan Loyd Chaffee [2,*]

[1] Department of Chemical Engineering, 16 Alliance Lane, Clayton Campus, Monash University, VIC 3800, Australia
[2] School of Chemistry, 17 Rainforest Walk, Clayton Campus, Monash University, VIC 3800, Australia
* Correspondence: Andrew.Hoadley@monash.edu (A.F.A.H.); Alan.Chaffee@monash.edu (A.L.C.); Tel.: +61-3-9905-3421 (A.F.A.H.); Tel.: +61-3-9905-4626 (A.L.C.)

Received: 30 June 2019; Accepted: 28 July 2019; Published: 2 August 2019

S1. Calculations for the unit operations in the process

S1.1. Adsorption stage

S1.1.1. Pressure drop across bed

Pressure drop across a sorbent bed was calculated by the Ergun equation [1] (Equation (S1)).

$$\frac{\Delta P_{bed,ads}}{H_{bed}} = 150\frac{\mu_{air}V_{air}(1-\epsilon)^2}{d_{pellet}^2\epsilon^3} + 1.75\frac{\rho_{air}V_{air}^2(1-\epsilon)}{d_{pellet}\epsilon^3}, \quad \text{(S1)}$$

Where $\Delta P_{bed,ads}$ is the pressure drop (Pa), H_{bed} is the bed height (m), μ_{air} is the dynamic viscosity of air (pa s), V_{air} is the superficial velocity of air (m s^{-1}), ε is the void fraction of the bed, and d_{pellet} is the diameter of the sorbent pellets (m).

S1.1.2. Fan power calculation

The power requirement of the fan (W), W_{fan}, was calculated as the total of the energy required to push the air through the contactor (W), ($W_{fan,contactor}$), and the energy required to push the air through the heater/steam condenser (W), ($W_{fan,heater}$), according to Equations (S2) and (S3).

$$W_{fan} = W_{fan,contactor} + W_{fan,heater} \quad \text{(S2)}$$

$$W_{fan,contactor} = \frac{1}{\eta_{fan}} \Delta P \times V \times N_{beds} \times (N_{contactors} - 1) \quad \text{(S3)}$$

Where η_{fan} is the efficiency of the fan (80%), $\dot{V}$ is the volumetric flow rate of air (m^3 s^{-1}) through one bed, N_{beds} is the number of beds in a contactor and $N_{contactors}$ is the number of contactors in parallel in the system.

The energy needed to push the air through the fan cooler, $W_{fan,heater}$, was estimated as 0.005 W per 1 W of cooling [2]. The calculation of the cooling duty of the fan is done in Section S1.2.6.

S1.2. Desorption stage

S1.2.1. Pressure drops though heat exchangers

For the desorption stage, each heat exchanger was assumed to have a pressure drop of 5 kPa.

S1.2.2. Boiler

The boiler duty was calculated according to Equation (S4), where Q_{boiler} is the boiler duty (W), $\dot{m}_{H_2O}$ is the mass flow rate of steam (kg s^{-1}), $C_{p,water}$ is the specific heat capacity of water (J kg^{-1} $°C^{-1}$), and $H_{latent,H2O}$ is the latent heat of vaporization (J kg^{-1}). T_{boil} and T_{amb} are the bubble point temperature (°C) of water at the respective pressure and the inlet temperature (°C) of water, respectively.

$$Q_{boiler} = m_{H_2O}\,(C_{p,water}\,(T_{boil} - T_{amb}) + H_{latent,H_2O}) \quad \text{(S4)}$$

T_{boil} was calculated according to the Antoine correlation for water (Equation (S5)), where P_{boiler} is the pressure in the boiler (mm Hg).

$$T_{boil} = \frac{1730.63}{8.07131 - \log_{10}(P_{boiler})} - 233.426 \quad \text{(S5)}$$

S1.2.3. Superheater

The superheater duty was calculated according to Equation (S6), where $Q_{superheater}$ is the superheater duty (W), $\dot{m}_{H_2O}$ is the mass flow rate of steam (kg s^{-1}) and $C_{p,steam}$ is the specific heat capacity of steam (J kg^{-1} °C^{-1}). T_{boil} and T_d are the boiling point temperature (°C) of water and the desorption temperature (°C), respectively.

$$Q_{boiler} = \dot{m}_{H_2O}\,C_{p,steam}\,(T_d - T_{boil}) \quad \text{(S6)}$$

S1.2.4. Contactor

The mass flow of CO_2 and H_2O out from the contactor were calculated according to Equations (S7), where $\dot{m}_{i,in}$ is the mass flow rate in to the contactor (kg s^{-1}), $m_{sorbent}$ is the mass of the sorbent in the contactor (kg) and MW_i is the molar mass (kg mol^{-1}). $\frac{dq_i}{dt}$ is the mass transfer rate of CO_2 and H_2O to/from the sorbent (mol $kg^{-1}s^{-1}$) calculated according to Equation (1).

$$\dot{m}_{i,out} = \dot{m}_{i,in} - \frac{dq_i}{dt} \times m_{sorbent} \times MW_i \quad \text{(S7)}$$

where the component i refers to either CO_2 or H_2O.

The heat supplied to the bed from the heat transfer fluid was calculated according to Equation (S8).

$$Q_{bed} = U_{contactor} A_{contactor} (T_{heat} - T_{bed}) \quad \text{(S8)}$$

Where Q_{bed} is the heat supplied to the bed (W), $U_{contactor}$ is the overall heat transfer coefficient for the contactor (W m^{-2} °C^{-1}), $A_{contactor}$ is the heat transfer area (m^2) in the contactor and T_{bed} is the temperature (°C) of the bed. T_{heat} is the temperature (°C) of the heat transfer fluid, which is assumed to be 10 °C higher than the target desorption temperature. $U_{contactor}$ was assumed to be 150 W m^{-2} °C^{-1} [3].

S1.2.5. Desuperheater

$\dot{m}_{water,desuperheat}$, the flow rate of water (kg s^{-1}) which needs to be added to desuperheat the steam was calculated according to Equation (S9). The CO_2 and steam entering the desuperheater were assumed to be at the same temperature as the contactor temperature, T_{bed}, as calculated according to Equation (7).

$$\dot{m}_{water,desuperheat} = \frac{\dot{m}_{steam} C_{p,steam} (T_{bed} - T_{boil}) + \dot{m}_{CO2} C_{p,CO2} (T_{bed} - T_{boil})}{C_{p,water} (T_{boil} - T_{amb}) + H_{lat,water}} \quad \text{(S9)}$$

S1.2.6. Condenser

The concentration of H_2O exiting the condenser was calculated according to Equations (S10), where y_{H2O} is the concentration of H_2O (mol-H_2O mol^{-1}), $P_{sat,H2O}$ is the saturation vapour pressure of water (Pa), and $P_{condenser}$ is the pressure inside the condenser (Pa). $P_{sat,H2O}$ was calculated according to the Antoine correlation (Equation (S11)), where $T_{condenser}$ is the condensation temperature (°C).

$$y_{H2O,out} = \frac{P_{sat,H2O}}{P_{condender}} \quad \text{(S10)}$$

$$p_{sat,H_2O} = 10^{8.07131 - \frac{1730.63}{233.426 + T_{condenser}}} \quad \text{(S11)}$$

The mass flow rates (kg s^{-1}) of the water vapor exiting the condenser, $\dot{m}_{vap,out}$, and that of the condensate, $\dot{m}_{water,out}$, were calculated according to Equations (S12) and (S13), where $\dot{m}_{CO_2,in}$ and $\dot{m}_{H_2O,in}$ are the CO_2 and H_2O mass flow rates (kg s^{-1}) in to the condenser.

$$\dot{m}_{vap,out} = \dot{m}_{CO_2,in} \times \frac{y_{H_2O,out}}{1 - y_{H_2O,out}} \quad \text{(S12)}$$

$$\dot{m}_{water,out} = \dot{m}_{H_2O,in} - \dot{m}_{vap,out} \quad \text{(S13)}$$

The cooling duty of the condenser was calculated according to Equation (S14).

$$\begin{aligned} Q_{condenser} = {} & \dot{m}_{water,out}\left(C_{p,water}\left(T_{condenser,out} - T_{condenser,in}\right) + H_{lat,H_2O}\right) \\ & + \dot{m}_{vap,out} C_{p,steam}\left(T_{condenser,out} - T_{condenser,in}\right) \\ & + \dot{m}_{CO_2,in} C_{p,CO_2}\left(T_{condenser,out} - T_{condenser,in}\right) \end{aligned} \quad \text{(S14)}$$

S1.2.7. Vacuum Pump

The energy required for operating the vacuum pumps to pump the desorbed product out (W), $W_{vacuum\ pump}$, was calculated according to Equations (S15)–(S18) [3], where the η_{vacuum} is the efficiency of the vacuum pump (70%), $\dot{n}_i$ is the molar flow rate (mol s^{-1}) in of CO_2 or H_2O, R is the gas constant (J mol^{-1} K^{-1}), and T_{in} is the temperature (°C) of the gas entering the vacuum pump. P_{in} and P_{out} are the pressures (Pa) of the gas entering and exiting the vacuum pump.

$$W_{vacuum,pump} = \sum_{i=CO_2,H_2O} \frac{1}{\eta_{vacuum}} \dot{n}_i R (T_{in} + 273) \left(\frac{n_{p,i}}{n_{p,i} - 1}\right) \left(\left(\frac{P_{out}}{P_{in}}\right)^{\frac{n_{p,i} - 1}{n_{p,i}}} - 1\right) \quad \text{(S15)}$$

$$m_{p,i} = \frac{\gamma_i - 1}{\gamma_i} \frac{1}{\eta_{vacuum}} \quad \text{(S16)}$$

$$\gamma_i = \frac{C_{p,i}}{C_{p,i} - R} \quad \text{(S17)}$$

$$\gamma_i = \frac{C_{p,i}}{C_{p,i} - R} \quad \text{(S18)}$$

where the component i refers to either CO_2 or H_2O.

S2. Calculation of the Energy consumption

The energy consumptions were calculated on a basis of GJ $tonne^{-1}$ of CO_2 captured according to Equations (S19)–(S25).

S2.1. Electrical Energy

$$E_{fan} = \frac{\int_0^{t_{ads}} W_{fan}\, dt}{mass\ of\ CO_2\ captured\ per\ cycle\ (kg)} \times \frac{1}{1 \times 10^6} GJ\ kg\ J^{-1}\ tonne^{-1} \quad \text{(S19)}$$

Where t_{ads} is the total adsorption time (s).

$$E_{vacuum} = \frac{\int_0^{t_{des}} W_{vacuum}\, dt + E_{evacuation}}{mass\ of\ CO_2\ captured\ per\ cycle\ (kg)} \times \frac{1}{1 \times 10^6} GJ\ kg\ J^{-1}\ tonne^{-1} \quad \text{(S20)}$$

Where $E_{evacuation}$ is the energy needed (J) to evacuate the contactor to the desorption pressure according to Equation (S21) [3], where V is the void volume inside the contactor (m^3), m_{air} is the mass of air being evacuated (kg), and $P_{initial}$ and P_{final} are the pressures (kPa abs) at the beginning and end of the evacuation respectively. n_{air} is calculated according to Equations (S16)–(S18).

$$E_{evacutation} = -\frac{1}{\eta_{vacuum}} P_{initial} V_{contactor} \frac{n_{p,air}}{n_{p,air} - 1} \left(\left(\frac{P_{final}}{P_{initial}} \right)^{\frac{n_{p,air} - 1}{n_{p,air}}} - 1 \right) m_{air} \quad \text{(S21)}$$

The total electrical energy requirement was calculated according to Equation (S22).

$$E_{electrical} = E_{fan} + E_{vacuum} \quad \text{(S22)}$$

S2.2. Thermal Energy

$$E_{steam} = \frac{\int_0^{t_{des}} (Q_{boiler} + Q_{superheater})\, dt}{mass\ of\ CO_2\ captured\ per\ cycle\ (kg)} \times \frac{1}{1 \times 10^6} GJ\ kg\ J^{-1}\ tonne^{-1} \quad \text{(S23)}$$

Where t_{des} is the desorption time (s)

$$E_{bed} = \frac{\int_0^{t_{des}} Q_{bed}\ dt}{mass\ of\ CO_2\ captured\ per\ cycle\ (kg)} \times \frac{1}{1 \times 10^6} GJ\ kg\ J^{-1}\ tonne^{-1} \quad \text{(S24)}$$

The total electrical energy requirement was calculated according to Equation (S25).

$$E_{electrical} = E_{steam} + E_{bed} \quad \text{(S25)}$$

S3. Capital cost estimation

S3.1. Contactor

The air contactor was costed as a shell and tube heat exchanger due to its unique configuration, according to the cost correlation (Equations (S26)) found in Sinnott [3].

$$C_{contactor} = 28000 + 54A_{contactor}^{1.2} \quad 10 < A_{contactor} < 1000 \quad \text{(S26)}$$

Where $C_{contactor}$ is the cost of a contactor (USD) and $A_{contactor}$ is the heat transfer area (m^2).

In scaling up the contactor, it was assumed that the $\frac{UA}{m_{sorbent}}$ ratio would be kept constant. So the UA of the scaled up contactor was calculated according to Equation (S27).

$$C_{contactor} = 28000 + 54A_{contactor}^{1.2} \quad 10 < A_{contactor} < 1000 \quad \text{(S27)}$$

$A_{contactor}$ was calculated by assuming $U_{contactor}$ to be 150 W m^{-2} C [3].

S3.2. Fan

Costed according to correlation (Equation (S28)) in Couper [2], where C_{fan} is the cost of the fan (USD) and $\dot{V}_{air}$ is the air flow rate in SCFM.

$$C_{fan} = 2680e^{0.4692 + 0.1203 \ln(\dot{V}_{air}) + 0.0931 (\ln(\dot{V}_{air}))^2} \quad for\ 2000 < \dot{V}_{air} < 500000 \quad \text{(S28)}$$

S3.3. Boiler

Costed according to correlation (Equation (S29)) in Sinnott [3], where C_{boiler} is the cost of the boiler (USD) and A_{boiler} is the heat transfer area (m^2) of the boiler.

$$C_{boiler} = 29000 + 400A_{boiler}^{0.9} \quad 10 < A_{boiler} < 500 \quad \text{(S29)}$$

A_{boiler} was calculated using Equation (S30), by assuming a log mean temperature difference (ΔT_{LM}) of 15 °C, and a U_{boiler} of 1000 W m^{-2} °C^{-1} [3].

$$A_{boiler} = \frac{Q_{boiler}}{U_{boiler}\Delta T_{LM}} \quad \text{(S30)}$$

S3.4. Superheater

Costed according to correlation (Equation (S31)) in Sinnott [3], where $C_{superheater}$ is the cost of the superheater (USD) and $A_{superheater}$ is the heat transfer area of the superheater (m^2).

$$C_{superheater} = 28000 + 54A_{superheater}^{0.9} \quad 10 < A_{superheater} < 1000 \quad \text{(S31)}$$

$A_{superheater}$ was calculated using Equation (S32), by assuming a log mean temperature difference (ΔT_{LM}) of 15 °C, and a $U_{superheater}$ of 30 W m^{-2} °C^{-1} [3].

$$A_{superheater} = \frac{Q_{superheater}}{U_{superheater}\Delta T_{LM}} \quad \text{(S32)}$$

S3.5 Condenser

Costed according to correlation (Equations (S33)) in Couper [2], where $C_{condenser}$ is the cost of the condenser (USD) and $A_{condenser}$ is the heat transfer area (ft^2) of the condenser.

$$C_{condenser} = 475000A_{condenser}^{0.4} \quad 50 < A_{condenser} < 200000 \quad \text{(S33)}$$

$A_{superheater}$ was calculated using Equation (S34), by assuming a $U_{condenser}$ of 500 W m^{-2} °C^{-1} [2].

$$A_{condenser} = \frac{Q_{condenser}}{U_{condenser}\Delta T_{LM}} \quad \text{(S34)}$$

S3.6. Vacuum pump

Costed according to correlation (Equation (S35)) in Couper [2], where C_{vacuum} is the cost of the vacuum pump (USD), $\dot{m}_{gas}$ is the mass of gas being pumped (lbs h^{-1}) and P_1 is the suction side pressure (torr). The average mass flow rate through the vacuum pump during the desorption was taken as $\dot{m}_{gas}$.

$$C_{vac} = 9930\left(\frac{\dot{m_{gas}}}{P_d}\right)^{1.03} \quad 0.3 < \frac{\dot{m_{gas}}}{P_1} < 15 \quad \text{(S35)}$$

S3.7. Adjustment for inflation

As the cost data was based on data from 2003 (Couper [2]) and 2010 (Sinnott [3]) All the equipment capital costs were adjusted for inflation using Equation (S36) and the CEPCI data in Table S1.

$$\frac{C_{year\,x}}{C_{year\,y}} = \frac{CEPCI_{year\,x}}{CEPCI_{year\,y}} \quad \text{(S36)}$$

Table S1. CEPCI data for the relevant years.

Year	2003	2010	2017
CEPCI	402	550	567

S3.8. Total plant cost

The total plant cost (USD) ,C_{plant}, was calculated according to Equation (S37), where the cost of insulation, piping, instrumentation, electrical work, civil and structures, and lagging are accounted for by multiplying the total equipment cost by a factor, f_i, from Table S2 [4].

$$C_{plant} = \Sigma f_i \times (C_{fan} + C_{bed} + C_{boiler} + C_{superheater} + C_{condenser} + C_{vacuum}) \quad \text{(S37)}$$

Table S2. Factors to account for the total plant cost.

	Installation	Piping	Instruments	Electrical	Civil	Structural	Lagging
f_i	0.08	0.2	0.1	0.19	0.1	0.02	0.04

S4. Calculation of the Cost of sorbent

The cost of raw material for the production of the sorbent was assumed based on the prices of generic mesoporous silica and branched PEI, to be 4 USD kg^{-1} [5] and 2 USD kg^{-1} [6], respectively. It was also assumed that the cost of raw material is only 1/3 of the total production cost. For a 65% wt PEI sorbent like the one considered in this study, $C_{sorbent,\ material}$, was calculated according to Equation (S38).

$$C_{sorbent} = (0.35 \times 4 + 0.65 \times 2) \times 3 = \ 8.1\ USD\ kg^{-1} \quad \text{(S38)}$$

S5. NPV analysis

To determine the cost of capture (USD $tonne^{-1}$), C_{CO_2}, a NPV analysis was carried out according to Equations (S39) and (S40) for a breakeven scenario, for 20 years with a discount factor of 10%, where *CR* is the annual capture rate (tonne yr^{-1}) of CO_2.

$$NPV = 0 = -C_{plant} - C_{annual\ opex} \sum_{x=1}^{20} \frac{1}{(1+0.1)^x} + C_{sorbent} \sum_{y=0,4,..,16,20} \frac{1}{(1+0.1)^y} + C_{CO_2} \times CR_{annual} \times \sum_{x=1}^{20} \frac{1}{(1+0.1)^x} \quad \text{(S39)}$$

$$C_{CO_2} = \frac{(C_{plant} + C_{annual\ opex} \sum_{x=1}^{20} \frac{1}{(1+0.1)^x} + C_{sorbent} \sum_{y=0,4,..,16,20} \frac{1}{(1+0.1)^y})}{CR \times \sum_{x=1}^{20} \frac{1}{(1+0.1)^x}} \quad \text{(S40)}$$

S6. Desorption Stage: Model Validation contd.

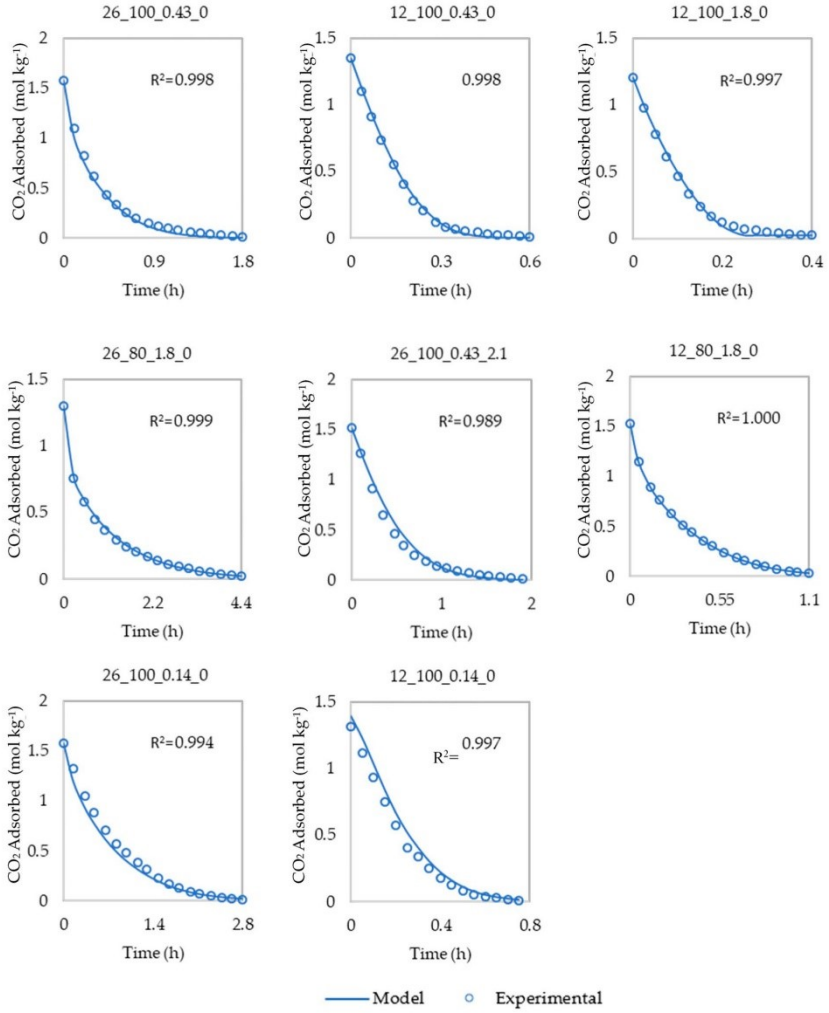

Figure 1. The experimental data and the model predictions for CO_2 mass transfer kinetics in the desorption stage. Legend for titles AA_BBB_CCC_DD (AA- desorption pressure (kPa), BBB- desorption temperature (°C), CCC- desorption steam flow rate (kg h^{-1} kg-sorbent^{-1}), DD- amount of water adsorbed during adsorption stage (mol kg^{-1})).

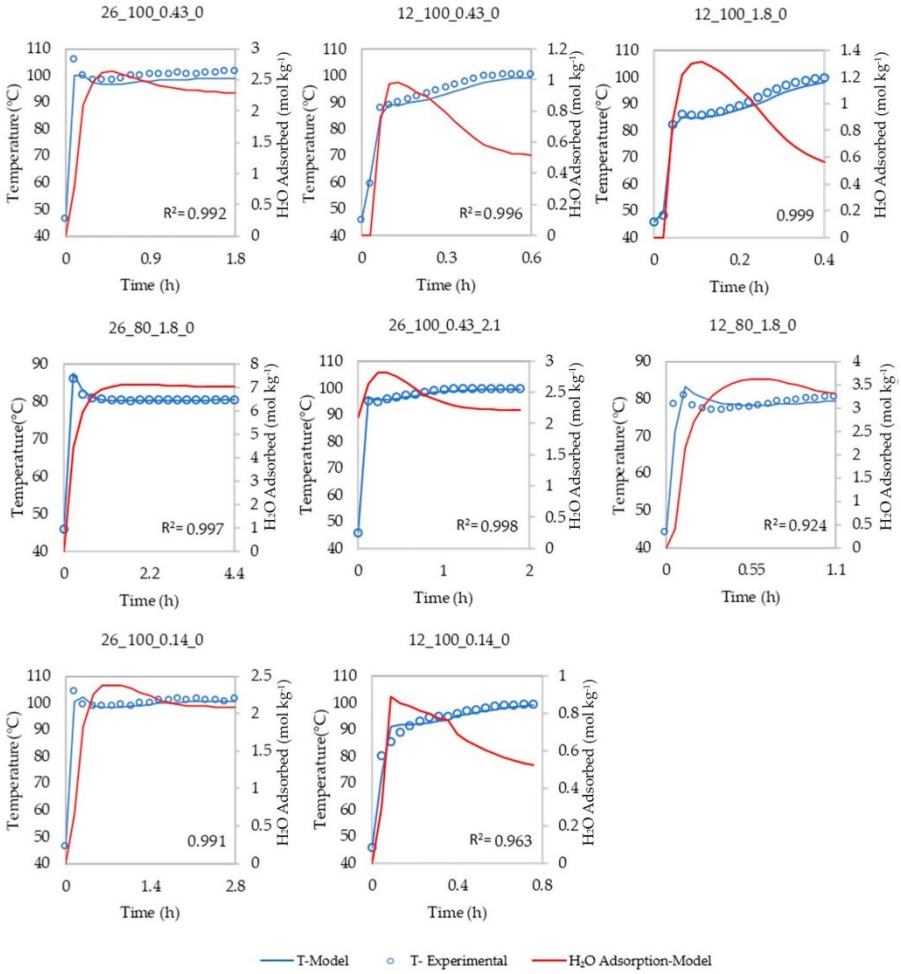

Figure 2. The experimental data and the model predictions for heat transfer and H_2O mass transfer kinetics in the desorption stage. Legend for titles AA_BBB_CCC_DD (AA- desorption pressure(kPa), BBB-desorption temperature (°C), CCC- desorption steam flow rate (kg h^{-1} kg-sorbent^{-1}), DD- amount of water adsorbed during adsorption stage (mol kg^{-1})).

S7. Sensitivity of the results to the MOO options

The results of the sensitivity analysis done on the MOO options is presented in Figure S3. 'base' refers to the default options used for the results discussed in the study. A to E refers to different cases where the MOO options were varied. The MOO options used for these cases are presented in Table S3 and the variations made are highlighted with bold text. The descriptions for each option is given in Table S4 [7].

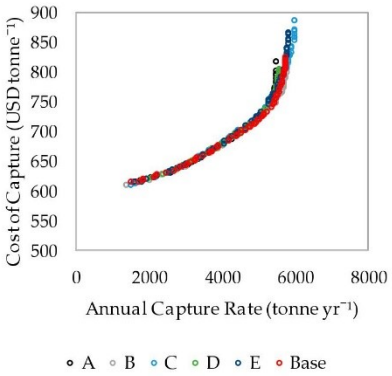

Figure S3. The Pareto plots for MOO carried out with different option. 'base' refers to the default options used for the results discussed in the study. The details on the variations made for A to E are given in Table S3.

Table S3. The details of the MOO options used for the sensitivity analysis.

	Base	A	B	C	D	E
Function Tolerance	1e-3	0.5e-3	1e-3	1e-3	1e-3	1e-3
Crossover fraction	0.8	0.8	0.9	0.8	0.8	0.8
Crossover function	1	1	1	0.9	1	1
Mutation	Adaptive feasible	Adaptive feasible	Adaptive feasible	Adaptive feasible	Uniform (0.01)	Uniform (0.05)

Table S4. The description of the MOO options varied for the sensitivity analysis [7].

Option	Description
Function tolerance	If the weighted average relative change in the spread of the Pareto solutions is less than Function tolerance, then the algorithm stops.
Crossover fraction	The fraction of the next generation that crossover produces. Mutation produces the remaining individuals in the next generation.
Crossover function	Creates children by a random weighted average of the parents. Intermediate crossover is controlled by a single parameter, Ratio $child1 = parent1 + random \times Ratio \times (parent2 - parent1)$
Mutation	Mutation functions make small random changes in the individuals in the population, which provide genetic diversity and enable the genetic algorithm to search a broader space -Adaptive Feasible- Randomly generates directions that are adaptive with respect to the last successful or unsuccessful generation. A step length is chosen along each direction so that linear constraints and bounds are satisfied -Uniform-First, the algorithm selects a fraction of the vector entries of an individual for mutation, where each entry has the same probability as the mutation rate of being mutated. In the second step, the algorithm replaces each selected entry by a random number selected uniformly from the range for that entry

References

1. Ergun, S.; Orning, A.A. Fluid Flow Through Packed Columns. *Chem. Eng. Prog.* **1952**, *48*, 89–94.
2. Couper, J.R. Chemical process equipment: selection and design, Rev. 2nd ed.; Elsevier/Butterworth–Heinemann: Amsterdam, Netherlands, 2010.
3. Sinnott, R.K. Coulson & Richardson's chemical engineering. Chemical engineering design, 4th ed.; Elsevier Butterworth–Heinemann: Oxford, UK, 2005; Volume 6.
4. Brennan, D. Process industry economics: an international perspective; IChemE: Rugby, UK, 1998.
5. Alibaba.com. Mesoporous SiO_2 SiO_2 Hydrophobic Silica Fumed Silica Fusil 215, Fusil 615 Availabe online: https://www.alibaba.com/product-detail/Mesoporous–SiO_2–SiO_2–Hydrophobic–Silica–Fumed_60480295907.html?spm=a2700.7724857.normalList.29.7ed84ba98GxkTx (accessed on 18 June 2019).
6. Alibaba.com. REACH verified producer supply High Quality with competitive price CAS: 9002-98-6 POLYETHYLENEIMINE. Availabe online: https://www.alibaba.com/product-detail/REACH–verified–producer–supply–High–Quality–60755917618.html?spm=a2700.7724857.normalList.13.399e571ei0XjQy (accessed on 18 June 2019).
7. MathWorks. Find Pareto front of multiple fitness functions using genetic algorithm–MATLAB gamultiobj. Availabe online: https://www.mathworks.com/help/gads/gamultiobj.html (accessed on 22 June 2019).

Appendix B(I): Addendum to "CO_2 Capture from Air Using Pelletized Polyethyleneimine Impregnated MCF Silica "

- **Discussion of the breakthrough curves depicted in Figure 2**

At adsorption temperatures below 66 °C, the breakthrough curves can be seen to form drawn-out tails, while still adsorbing approximately 20% of the CO_2 in the feed gas stream. This can also be observed in the CO_2 uptake curves (Figure 2 (b)) which appear to plateau after about 20 h from the start of adsorption. This suggests that the CO_2 faces increasing mass transfer resistances as the sorbent is progressively saturated with CO_2. This may be explained by the results of Knowles et al. [1], which demonstrated that as the amine sites react with the CO_2 forming bicarbonates, the viscosity of the PEI polymer phase increases, effectively solidifying it. This increased viscosity in turn may increase the diffusional resistances that the CO_2 has to overcome to reach the vacant amine sites.

The waves observed in the breakthrough curves (Figure 2(a)) were due to fluctuations in the room temperature in the lab which housed the equipment, due to a faulty air conditioning unit. The oven which the sorbent was contained in was unable to quickly react and compensate for the change in ambient temperature caused by the air conditioning. This resulted in slight changes in adsorption temperatures and caused fluctuations in the rate of adsorption of CO_2 which manifested itself as waves in the breakthrough curves.

- **Error Bars in Figures 2 & 6**

The error bars shown in Figures 2 & 6 were calculated as the standard deviation of the results of replicated experiments. The error bars demonstrate that there is good repeatability in the experiments.

References

[1] Knowles, G.P.; Liang, Z.; Chaffee, A.L. Shaped polyethyleneimine sorbents for CO_2 capture. *Microporous and Mesoporous Materials*. **2017**, *238*, 14-18.

Appendix B(II): Addendum to "Desorption Process for Capturing CO_2 from Air with Supported Amine Sorbent"

- **Error Bars in Figures 4 to 7**

The error bars shown in Figures to 4 to 7 were calculated as the standard deviation of the results of replicated experiments. The error bars demonstrate that there is good repeatability in the experiments.

Appendix B(III): Addendum to "Technoeconomic Evaluation of a Process Capturing CO_2 Directly from Air"

- **Land area requirement for the process**

A preliminary calculation on the minimum land area required for the process under the lowest cost scenarios (refer Table 3), was calculated by assuming the that the air-sorbent contactors would be the only significant contributor. The total area (m^2) ,A_{total}, required by the process was calculated according to **Equation B(III)1,** where $N_{contactors}$ is the number of contactors in the process and $A_{plot\ area,\ contactor}$ is the plot area required for a single contactor (m^2).

$$A_{total} = N_{contactors} \times A_{plot\ area\ ,contactor} \qquad \textbf{(Equation B(III)1)}$$

Each contactor was assumed to be placed in a square plot with sides equal to twice the diameter of the contactor (2.26 m). The additional area was allowed for use during maintenance, etc-.

The land area required for capturing 1 Gigatonne of CO_2 per year, $\bar{A}$ (km^2 $Gtonne^{-1}$ yr), was calculated according to **Equation B(III)2**, where *CR* is the annual capture rate of the process (tonne yr^{-1})

$$\bar{A} = \frac{A_{total}}{CR} \times \frac{10^9\ tonne}{1\ Gtonne} \times \frac{1\ km^2}{10^6\ m^2} \qquad \textbf{(Equation B(III)2)}$$

The results of the calculations are presented in **Table B(III)1**

Table B(III)1. Results of the preliminary calculations on the minimum land area required for the process under the lowest cost scenarios

	$N_{contactors}$	$A_{plot\ area,contactor}$ (m^2)	A_{total} (m^2)	CR (tonne yr^{-1})	$\bar{A}$ (km^2 Gtonne-CO_2^{-1} yr)
Dry Case	14	20.4	286	1521	188
Wet Case	15	20.4	306	1682	182

Appendix C: N_2 sorption isotherms and pore size distribution data for MCFa, MCFb, PEI_80a and PEI_80b

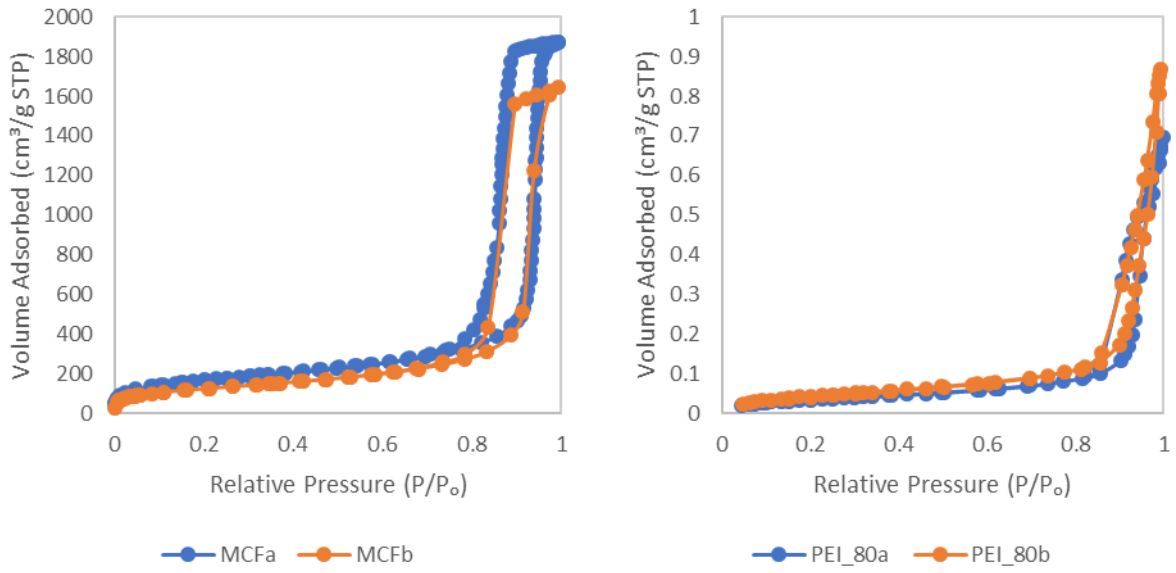

Figure C1. N_2 sorption isotherms for MCFa, MCFb, PEI_80a and PEI_80b

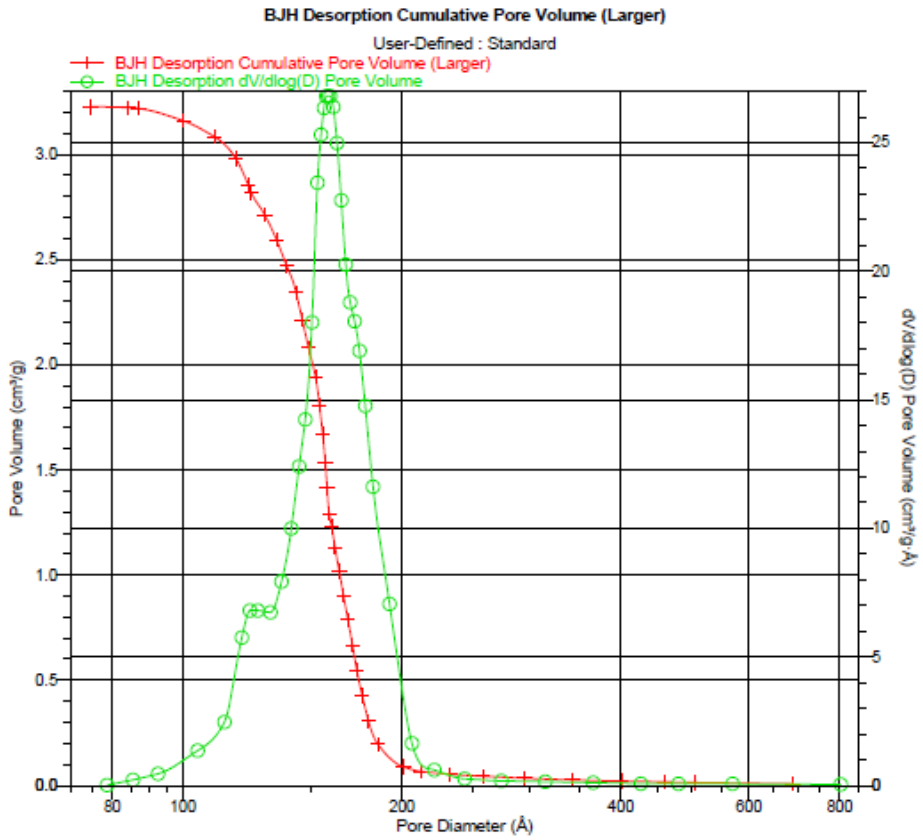

Figure C2. Pore size distribution of MCFa

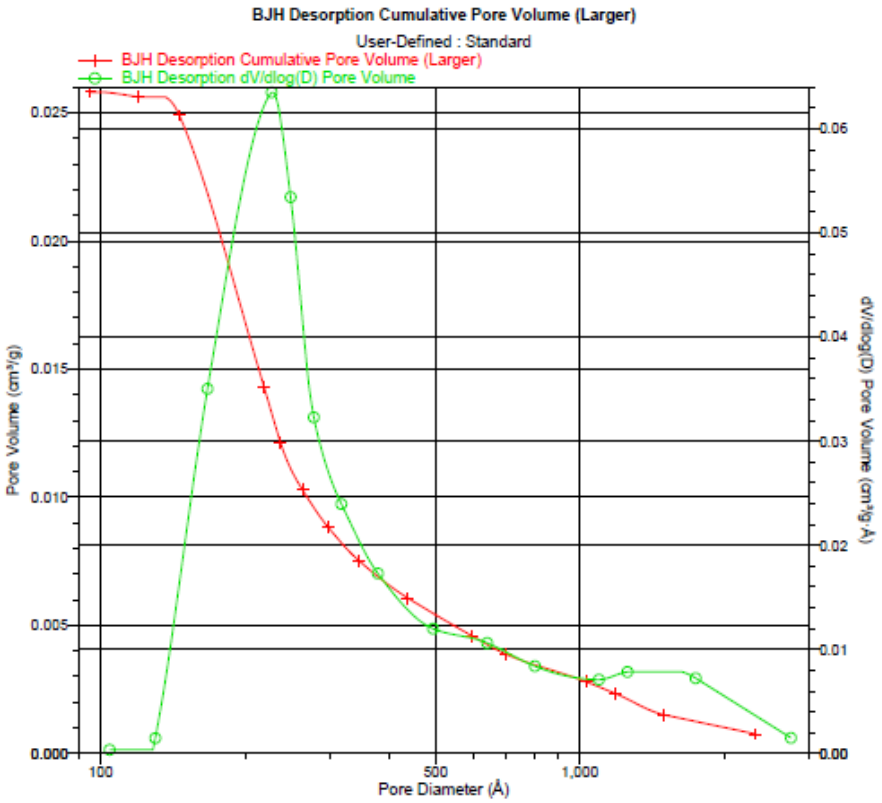

Figure C3. Pore size distribution of PEI_80a

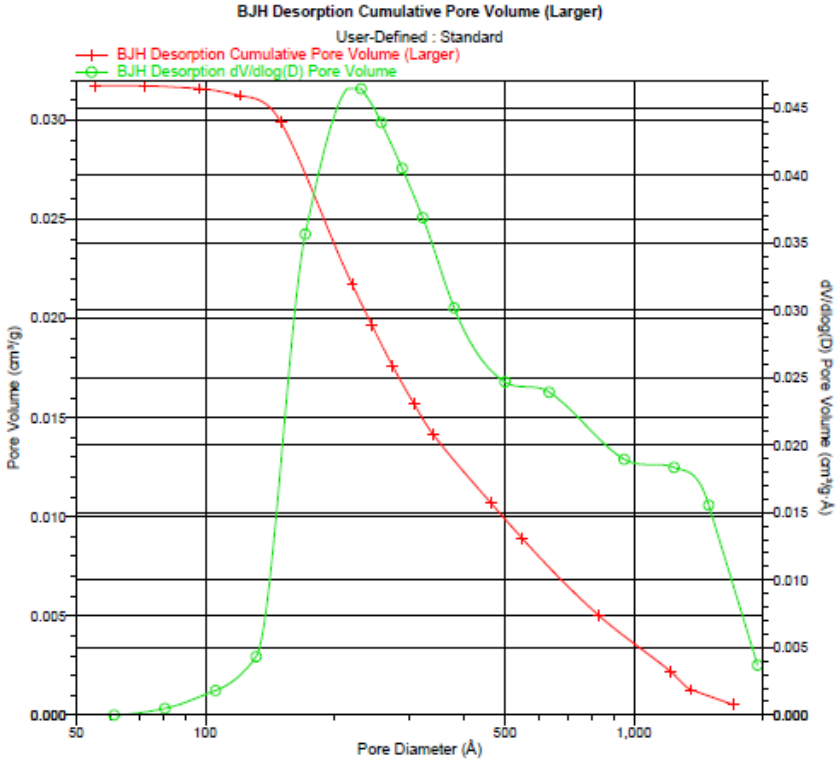

Figure C2. Pore size distribution of PEI_80b

Appendix D: Preliminary Study into the Effect of Oxygen on the Performance of PEI Impregnated MCF Silica for Adsorption of CO_2 from Air.

The work described in this appendix was done with the objective of doing a preliminary evaluation of how the oxygen in air affects the performance of PEI_80b for DAC applications. To achieve this, a new (3.48 g) sample of PEI_80b was exposed to 10 S-TVSA following the method described in **Chapter 3**. The only exception being that compressed air acquired from Air Liquide was used as the adsorption feed gas, instead of 420 ppm CO_2 in N_2. The CO_2 concentration of this gas was measured to be 350 ppm CO_2.

The CO_2 uptake profile when adsorbing from air at a flow rate of 200ml/min at 46 °C is depicted in **Figure B1**, along with that when adsorbing from 420 ppm CO_2 in N_2 and 350 ppm CO_2 in N_2. It is evident that the uptake from the compressed air is slower than that from 420 ppm CO_2 in N_2. This can be attributed to the lower partial pressure of CO_2, which would provide a smaller driving force for adsorption. It can also be seen that the CO_2 uptake profile for adsorption from air is almost identical to that of adsorption from 350 ppm CO_2 in N_2. This suggests that the presence of oxygen has negligible effect on the adsorption kinetics of CO_2 by PEI_80b.

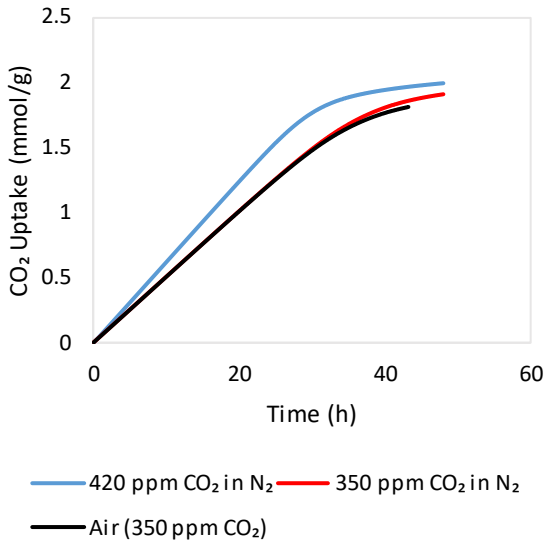

Figure D1. Adsorption of CO_2 by PEI_80b from different feed gases

The CO_2 uptake by the sorbent over 10 S-TVSA cycles is plotted in **Figure B2**. The data presented represents the adsorption at 46 °C, from dry air. The desorption for these cycles was carried out at varying pressures (12-26 kPa abs), temperatures (90-100 °C) and steam flow rates (3.4-9.9 g/h). The

uptake after 29.5 hours of adsorption at the same condition was used for this comparison. As visible in the **Figure B2**, after 10 cycles of adsorption/desorption, which corresponded to a processing time of >300 hours, negligible loss in CO_2 uptake capacity was seen for PEI_80b. This suggests that the stability of the sorbent does not deteriorate significantly in the presence of oxygen.

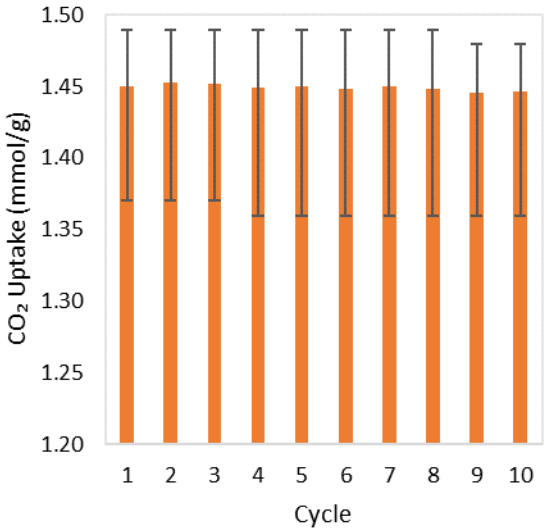

Figure D2. The CO_2 uptake by the sorbent over 10 S-TVSA cycles when adsorbing from air at 46°C. Error bars included are based on the accuracy of the CO_2 sensor.

In summary, these preliminary results indicate that the presence of oxygen air does not have a significant effect on the performance of PEI_80b. This encourages further research in to the application of PEI based sorbent for DAC or other applications where CO_2 is captured from oxygen rich atmospheres.

Appendix E: Calibration of the Instruments in the Experimental Set-up

Bronkhorst F-201C-FAC-11-V Mass Flow Controllers

FC-1

Serial Number: M4205478D

Gas: 1000 ppm CO_2 in N_2

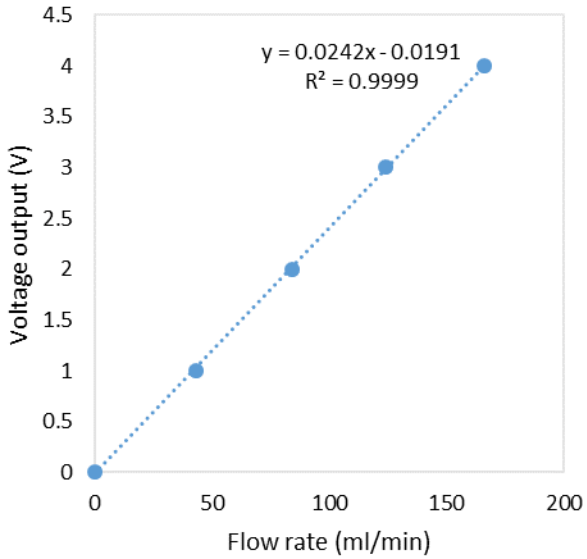

Figure E1. Sample calibration plot for FC-1

FC-2

Serial Number: M4205478B

Gas: N_2

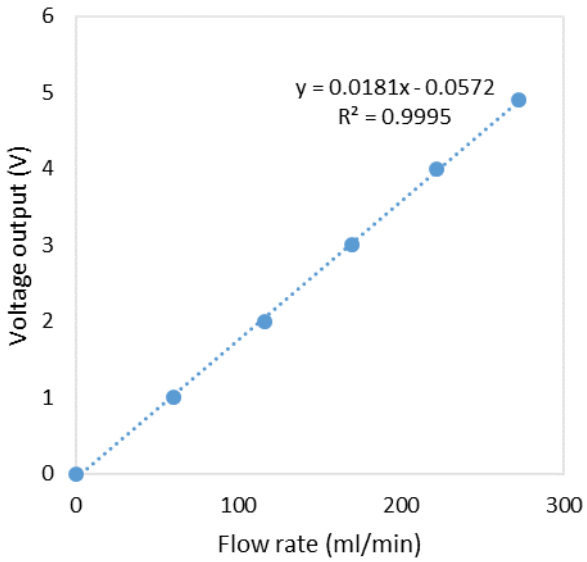

Figure E2. Sample calibration plot for FC-2

FC-3

Serial Number: M4205478A

Gas: 1000 ppm CO_2 in N_2

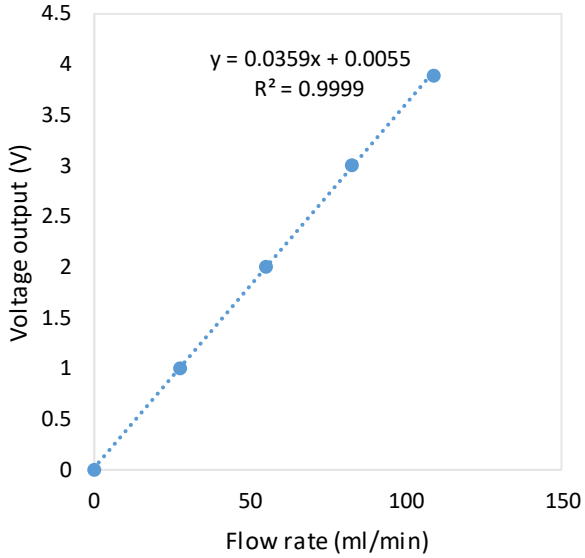

Figure E3. Sample calibration plot for FC-3

FC-4

Serial Number: M4205478C

Gas: N_2

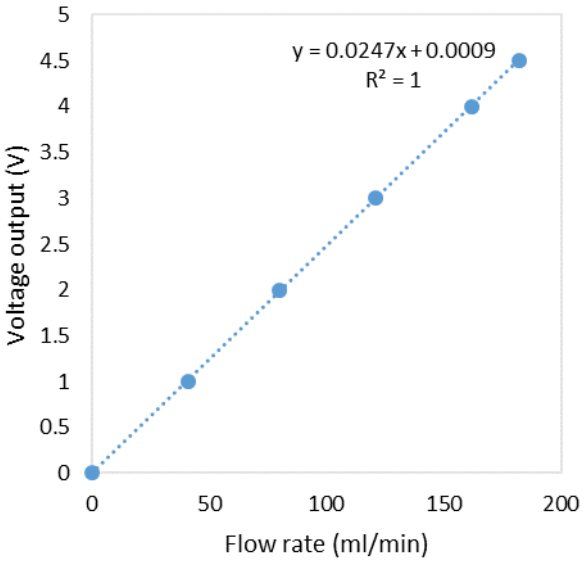

Figure E4. Sample calibration plot for FC-4

Edinburgh Sensors Gascard NG 0-1000 ppm CO_2 sensor

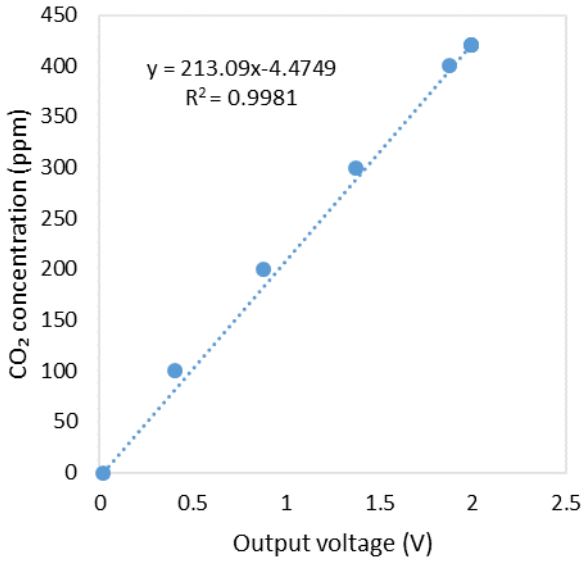

Figure E5. Sample calibration plot for the 0-1000 ppm CO_2 sensor

Gas Sensing Solutions Sprint IR6s 0-100% CO_2 sensor

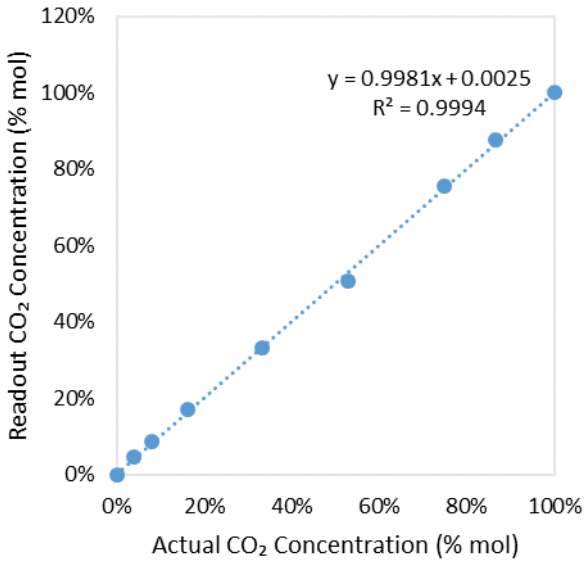

Figure E6. Sample calibration plot for the 0-100% CO_2 sensor

Bioprocess control µFlow 0-800 Nml/h gas flow meter

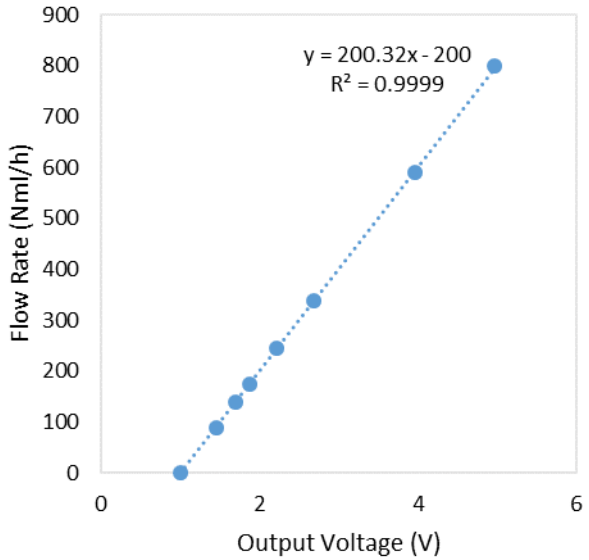

Figure E7. Sample calibration plot for 0-800 Nml/h gas flow meter

New Era-300 syringe pump (water)

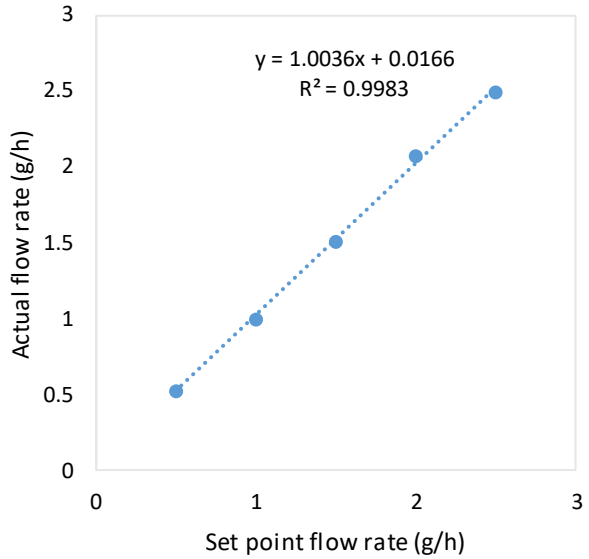

Figure E8. Sample calibration plot for syringe pump used in the steam generator

Appendix F: Labview Program Used for Data Acquisition

Adsorption/Regeneration Stage

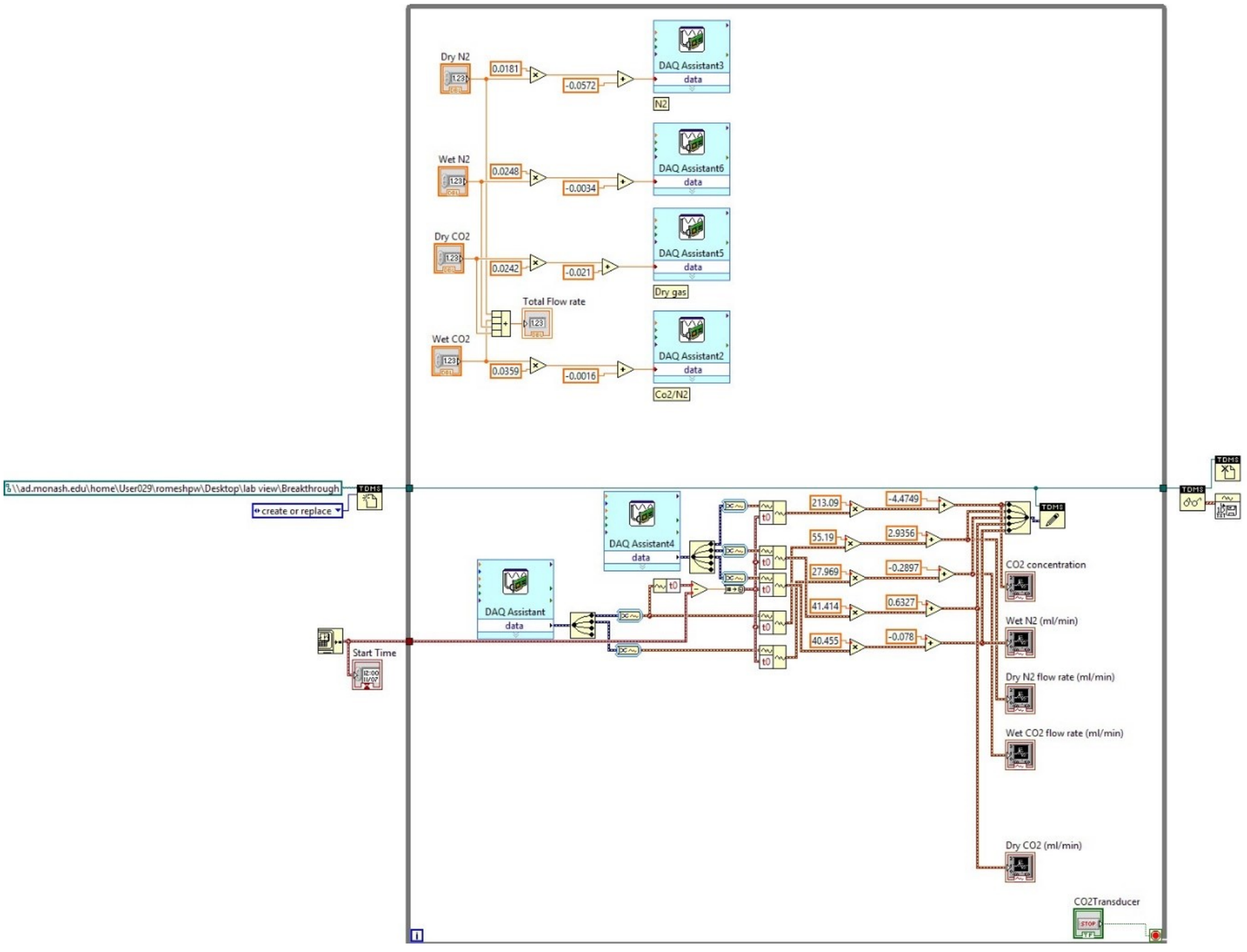

Figure F1. LabVIEW program used for data acquisition in the adsorption/regeneration stage

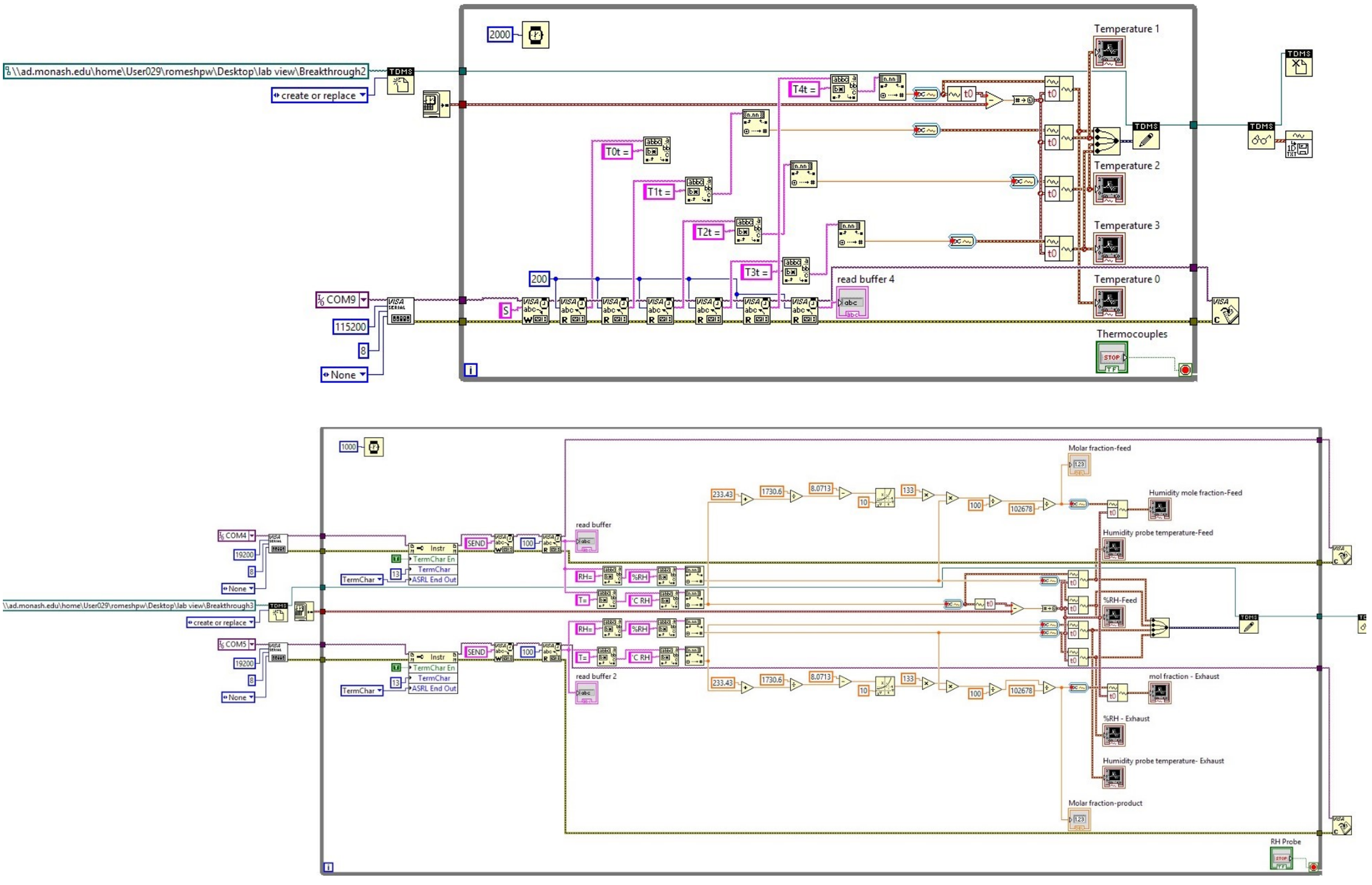

Figure F2. LabVIEW program used for data acquisition in the adsorption/regeneration stage *contd.*

Desorption Stage

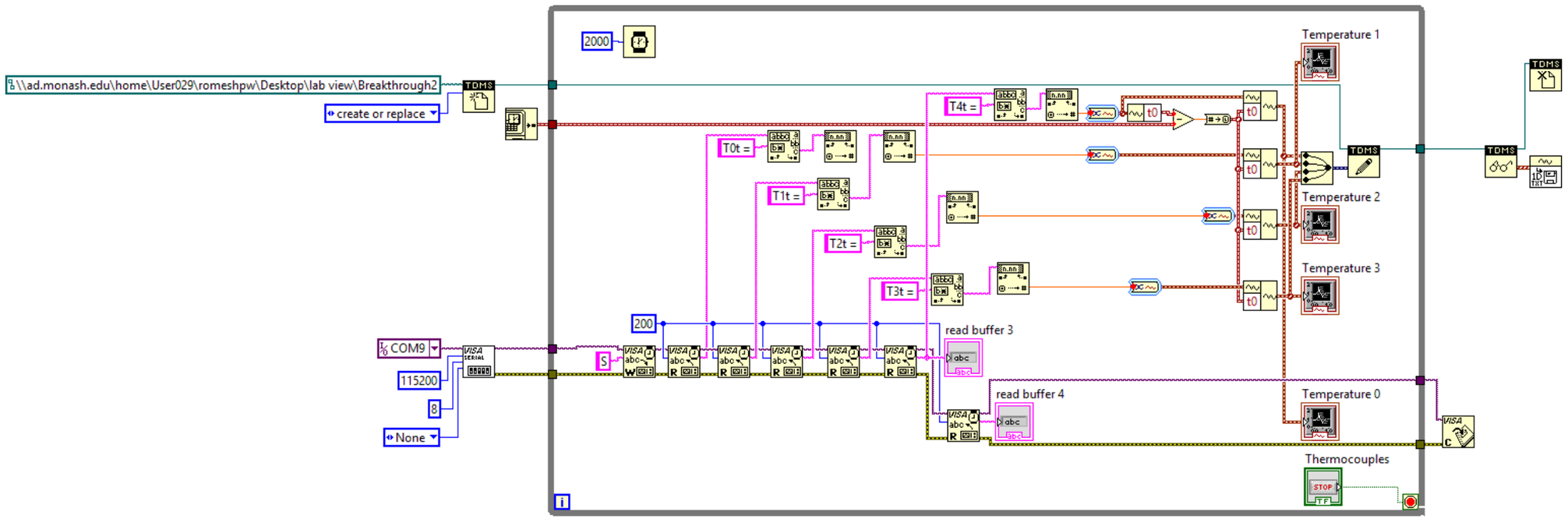

Figure F3. LabVIEW program used for data acquisition in the desorption stage